

3.1 Electromechanical measuring devices

There are several advantages of traditional electromechanical instruments: simplicity, reliability, low price. The most important advantage is that the majority of such instruments can work without any additional power supply. Since people's eyes are sensitive to movement also this psycho-physiological aspect of analogue indicating instruments (with moving pointer) is appreciated.

On the other hand, there are several drawbacks associated with electromechanical analogue indicating instruments. First of all, they do not provide output signal, thus there is a need for operator's activity during the measurement (at least for the reading of an indicated value). Another drawback is that such instruments generally use moving mechanical parts, which are sensitive to shocks, aging or wearing out. Relatively low price of moving pointer instruments today is not as advantageous as earlier, because on the market there are available also very cheap digital measuring devices with virtual pointer.

Regrettably, it can be stated that most of the electromechanical analogue instruments are rather of poor quality. In most cases these instruments are not able to measure with uncertainty better than 0.5%. The accuracy is also affected by so-called parallax error, in which the reading result depends on the position of the user's eye. The measurement is often invasive, because such mechanisms may need relatively large power consumption to cause the movement. Thus, electromechanical voltmeters exhibit insufficiently large resistance, while the resistance of electromechanical ammeters is not sufficiently small.

There is no doubt that the future is for automatic, computer supported measuring systems. But electromechanical instruments are still present in our lives (for example the attempts to substitute such instruments in cars finished with not a success).

The *moving coil* instrument is the most popular indicating electromechanical device. An example of such an instrument is presented in Figure 3.1.

A rectangular coil with the pointer fixed to its axle is used as the moving part in such instruments. The conic ends of axles are pressed against the bearings. The

current is delivered to the coil by two springs – these springs are also used as the mechanisms generating returning torque for the pointer.

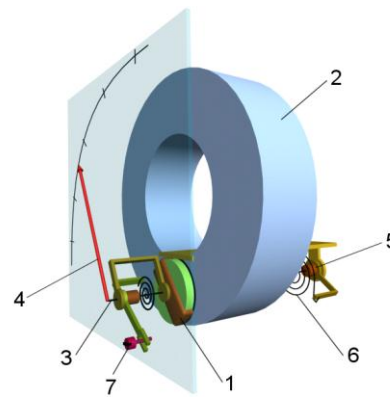


FIGURE 3.1

The example of moving coil indicating instrument (1- moving coil, 2 – permanent magnet, 3 – axle, 4 – pointer, 5 – bearings, 6 – spring, 7 – correction of zero).

The moving coil is placed into the gap between the magnet poles and soft iron core, shaped in such a way as to produce uniform magnetic field. The movement of the coil is caused by the interaction between the magnetic field of the magnet and the magnetic field generated by the coil. The rotation of the coil (and the pointer attached to it) is due to the torque M , which depends on the flux density B of the magnet, on dimensions d and l of the coil, on number of turns z of the coil and of course on the measured current I :

$$M = Bzdl \cdot I \quad (3.1)$$

The angle of rotation α results from the balance between the torque and the returning torque of the springs $M_z = k \alpha$ (k is the constant of the elasticity of the spring). Thus from the condition $M = M_z$ we find that the rotation is

$$\alpha = \frac{Bzdl}{k} \cdot I = c \cdot I \quad (3.2)$$

The angle of rotation is proportional to the measured current I , which is advantageous, because it means that the scale is linear. The larger is the constant c in Equation (3.2) the more sensitive (thus better) is the measuring device, because less current is required to cause the movement of the coil. The best way to improve the sensitivity of the device is to use large magnetic flux density B . The increasing of the number of turns or the dimensions of the coil is not very effective, because at the same time the weight and the resistance of the coils increase. Currently, it is possible to manufacture the moving coil device with the power consumption not larger than several μW (and current not larger than several μA) for the full deflection of the pointer.

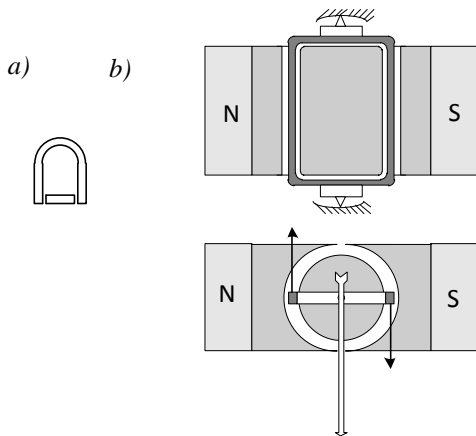


FIGURE 3.2 The moving coil mechanism: a) the symbol of instrument, b) the principle of operation.

The elasticity of the spring plays important role because it influences the character of the pointer movement. It is convenient if this movement is with small oscillation (Figure 3.3). In the case of pure inertial movement without an overshoot the observer is not sure if the pointer reaches final position. It is important to obtain the oscillatory movement with a short period and with reasonable damping of oscillation. Ideally, only one oscillation period should be visible – the next one should be damped.

The parameters of the movement depends on the mass m of the moving part and on the elasticity coefficient, k

$$T = \frac{T_0}{\sqrt{1-b^2}}, \quad T_0 = 2\pi\sqrt{\frac{m}{k}}, \quad b = \frac{P}{2\sqrt{mk}} \quad (3.3)$$

where T is the time constant, T_0 is the period of oscillations of the moving element, b is the degree of damping and P is the damping coefficient.

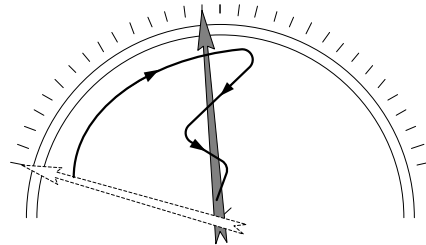


FIGURE 3.3 The movement of the pointer after connection of the device to the measured current.

Thus the character of the movement depends on the ratio between the mass, the elasticity of the springs and the damping. In the case of other instruments a special air damper is used in order to obtain correct damping of the movement. But in the case of a moving coil device the aluminum frame of the coil can work as the damper – the eddy currents induced in this frame interact with the magnetic field of the magnet slowing down the velocity of the movements.

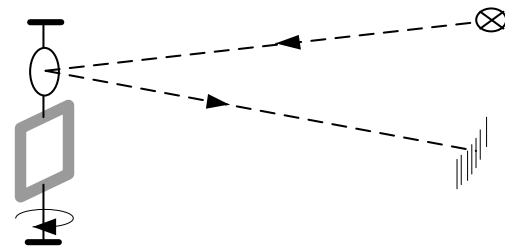


FIGURE 3.4 The enlargement of the length of the pointer – the light indicator.

The sensitivity of the device can be improved by increasing of the length of the pointer. The best solution is to substitute the mechanical pointer by the light indicator (Figure 3.4) – the length can be additionally increased by multiple reflection of the light beam. Sometimes also bearings are substituted by ribbons. This ribbons act as the current supplying wires and also as the springing parts.

The moving coil device can be used directly as the *microammeter* without any additional elements (Fig. 3.5a). If in series with the moving coil device an additional resistor R_d (*series resistor*) is connected, then we obtain the *millivoltmeter* or *voltmeter* (Fig.3.5b) (because the current I in the device is then proportional

to the voltage U). When the millivoltmeter is connected in parallel with another resistor R_b , called a *shunt resistor* we obtain the ammeter (Fig.3.5c), because voltage U_b is proportional to the measured current I_x (the resistance of millivoltmeter is much larger than resistance of the shunt resistor R_b thus we can assume that $U_b \cong I_x R_b$).

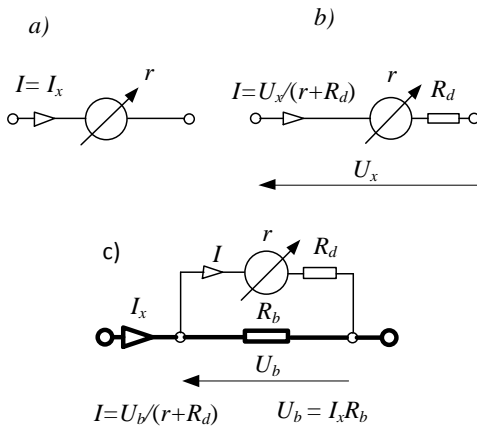


FIGURE 3.5
The design of microammeter (a), voltmeter (b) and ammeter (c)

The temperature influences the flux density B of the permanent magnet and the elasticity of the springs k . Fortunately, both of these influences act in opposite changes of the α . Therefore, their influences are negligible when the device is used as the microammeter (Fig. 3.5a).

The case of the millivoltmeter (Fig. 3.5b), and also indirectly of ammeter (Fig. 3.5c), is more complicated. The change of temperature causes change or the resistance r of the coil (the changes of resistance of the other resistors R_d and R_b are negligible, because they are prepared from *manganin* – special temperature independent alloy). Thus the current I , in the device changes with the temperature for fixed value of the measured voltage U , according to relation $I = U / (r + R_d)$. This change is significant, because copper wire of the coil exhibits change of the resistance of about $4\%/10^\circ\text{C}$. The temperature error of the millivoltmeter circuit presented in Fig. 3.5b we can describe as follows:

$$\delta_T = \frac{\frac{U}{r+R_d} - \frac{U}{r+\Delta r+R_d}}{\frac{U}{r+R_d}} \cong \frac{I}{I + \frac{R_d}{r}} \frac{\Delta r}{r} = \frac{4\%}{1 + \frac{R_d}{r}} \quad (3.4)$$

Thus the error caused by the change in temperature depends on the ratio R_d/r . It is easy to calculate that if the millivoltmeter is designed for measurements with uncertainty better than 0.5% then it is necessary to use the resistors with values $R_d = 7 \cdot r$. This means deterioration of the sensitivity of the millivoltmeter. Let us consider a case of a moving coil device with resistance 10Ω and nominal current 1 mA . Theoretically, such device could be used to design a millivoltmeter with a minimal range $U_{nom} = I \cdot r = 10 \text{ mV}$. But if we are planning to design a millivoltmeter of the class of accuracy 0.5% it is necessary to use additional resistance $R_d = 70 \Omega$, which limits the minimal range of such millivoltmeter to 80 mV . For the voltmeters, the problem of temperature errors correction is usually easy to solve, because it is necessary to use the series resistor. For example, in order to design a 10 V range voltmeter with a device described above it is necessary to connect a resistor of about $10 \text{ k}\Omega$, much larger than is required for the temperature error correction.

The ammeter instrument can be designed similarly to the millivoltmeter – by measuring voltage drop on the shunt resistor R_b (Fig. 3.5c). For example, if we use the moving coil device with the parameters described above and we would like to design an ammeter with a range 1 A and the accuracy class 0.5% then it is necessary to use a shunt resistor which would result in voltage drop larger than 80 mV (thus $R_b = 80 \text{ m}\Omega$).

Of course as better is instrument (more sensitive) as smaller shunt resistor is necessary. In the case of voltmeter we require resistance as large as possible. Reversely is in the case of ammeter – in this case we expect that the resistance should be as small as possible.

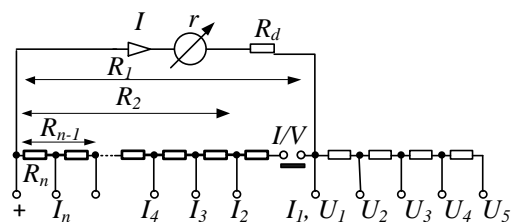


FIGURE 3.6
The design of universal multi-range voltmeter

Figure 3.6 presents the design of universal ammeter and voltmeter (voltammeter) with selectable ranges. To obtain the multi-range ammeter the special design of *universal shunt resistor* is very useful. The universal shunt resistor is designed to obtain the same current I for various input currents. Thus it should be:

$$\begin{cases} (I_n - I)R_n = I[(r + R_d) + (R_1 - R_n)] \\ (I_{n-1} - I)R_{n-1} = I[(r + R_d) + (R_1 - R_{n-1})] \end{cases} \quad (3.5)$$

After simple calculations we obtain the condition of universal shunt resistor in form:

$$\frac{I_n}{I_1} = \frac{R_1}{R_n} \quad (3.6)$$

The moving coils measuring instruments are usually manufactured as the panel meters (with class of uncertainty typically 1, 1.5 or 2.5%) and as the laboratory meters with class of uncertainty typically 0.5%. Fig. 3.7 presents an example of analogue indicating meter.



FIGURE 3.7
The examples of analogue panel meter (permission of EraGost)

The main disadvantage of the moving coil meters is that they indicate only *DC* values of the signals. In the past, these devices were also used for measurements of *AC* values with the aid of rectifiers. Although such devices measure the average value it is possible to scale it in *rms* values, knowing that $X_{rms}/X_{AV} = 1.11$. But this dependence is valid only for pure sinusoidal signals. Thus the rectifying *AC* measuring devices can be used only for the measurements of poor accuracy.

For *AC* measurement can be used the *moving iron meter*. The main advantage of moving iron meter is that such instrument measures the *rms* value of the signal. The design of *moving iron meter* is presented in Figure 3.8.

The measured current is connected to the stationary coil and the magnetic field generated by this coil interacts with the moving iron element. The iron part is simply attracted by the coil acting as electromagnet (Figure 3.8b). The angular deflection α depends on the measured current I and the change of the inductance dL caused by this deflection:

$$\alpha = \frac{1}{2k} \frac{dL}{d\alpha} I^2 \quad (3.7)$$

Although the deflection is a nonlinear function of measured current it is possible to design the device (the component $dL/d\alpha$) in such a way that the expression $(dL/d\alpha) I^2$ is close to linear. Because the response of the device depends on the squared value of the current it is possible to obtain the meter of *rms* value. Due to the error caused by magnetic hysteresis (when *DC* current is measured) these devices are used almost exclusively for *AC* measurements.

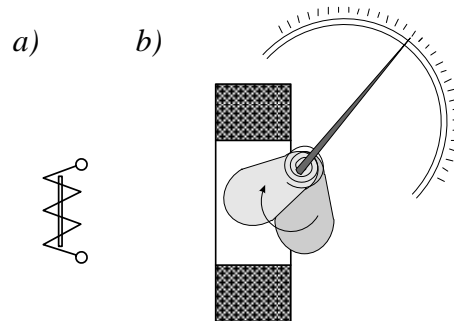


FIGURE 3.8
The moving iron meter: a) the symbol of such instrument, bc) the principle of operation

The moving iron meter exhibits several advantages: simplicity of the design – no need to supply the moving element, easy change of the range by selecting the number of the turns in the coil. The drawbacks of moving iron devices are relatively large power consumption ($0.1 - 1VA$) and small sensitivity (in comparison with moving coil device). The smallest obtainable range of moving iron milliammeter is several *mA*. Also, the frequency bandwidth is limited to about $150 Hz$.

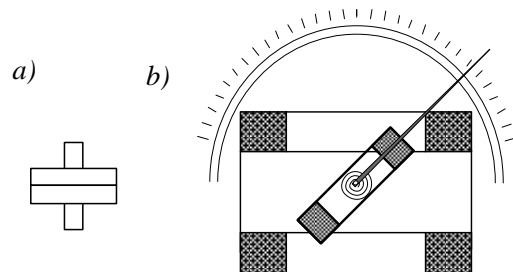


FIGURE 3.9
The electrodynamic meter: a) the symbol of such instrument, b) the principle of operation.

The *electrodynamic meters* (Figure 3.9) operate directly according SI definition of the ampere (see page 30) – attraction between current carrying wires. Therefore these meters were formerly used as the most accurate indicating instrument. Today for accurate measurements these instruments are substituted by the digital devices.

The electrodynamic device design is based on two coils: a stationary and a moving one. The currents flowing through these coils induce a force, which causes rotation of the movable coil. The torque M resulting from the interaction between two coils depends on currents: I_1 in stationary coil, I_2 in movable one and the phase shift φ between these currents:

$$M = cI_1I_2 \cos \varphi \tag{3.8}$$

Thus if one coil is connected to the current and the second to the voltage we can directly measure the power, because $P=UI\cos\varphi$. Fig. 3.10 presents typical connection of electrodynamic meter as the wattmeter. The wattmeter has two pairs of terminals – the current and the voltage terminals. In the voltage circuit there is usually introduced a series resistor R_d . Thus the torque can be calculated from the following equation:

$$M = c \frac{I}{R_d} IU \cos \varphi = k \cdot P \tag{3.9}$$

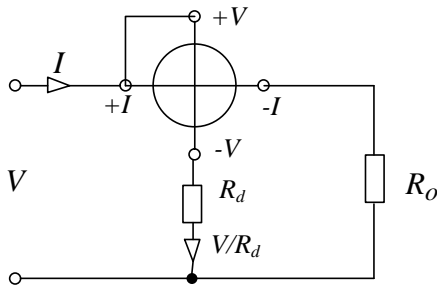


FIGURE 3.10
The connection of the wattmeter for the measurement of electric power.

The electrodynamic meters can be used for current and voltage measurement (in such cases both coils are connected in series). But the main drawback of electrodynamic devices is large power consumption (several VA) and therefore pure sensitivity. Therefore nowadays they are practically used only as wattmeters, where several VA power consumption is negligible.

The induction *watt-hour meters* (energy meters) are still present in our houses, although they exhibit serious drawbacks. First of all the reading must be taken by a

person in order to account the energy used (i.e. there is no output signal which could be read automatically). Moreover, these meters are electromechanical with quite complex system of error correction. Thus, in the future the mechanical energy meters will be substituted by electronic ones. This process is slow due to the range of problems – it is necessary to replace millions of devices.

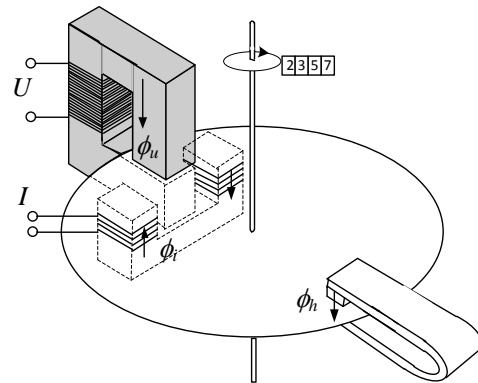


FIGURE 3.11
The principle of operation of the induction watt-hour meter.

Figure 3.11 presents the principle of operation of the induction watt-hour meter (*Ferrari's system*). Two independent cores are supplied by the currents proportional to the current and the voltage. These currents generate magnetic fluxes ϕ_i and ϕ_u , which flow through a rotating aluminum disc, in which eddy currents are induced.

The rotating torque M_r is due to the interaction between the eddy currents and the fluxes. The torque depends on the values of the currents in the cores and the phase angles between them

$$M_r = c\omega I_1I_2 \sin(I_1, I_2) \tag{3.20}$$

The first current is proportional to the measured current $I_1 = I$, while the second current is proportional to the voltage $I_2 = kU$. Due to large inductivity of the voltage core the current I_2 is shifted in phase by almost 90° with respect to the supplied voltage and $\sin(I_1, I_2) \cong \cos(U, I) = \cos\varphi$. Thus the torque is dependent on the measured power

$$M_r \cong ck\omega \cdot IU \cos \varphi \tag{3.21}$$

Additionally, the induction meter is equipped with the braking magnet. Interaction between the magnetic field of the permanent magnet and the eddy currents induced by this field causes a braking torque

proportional to the angular speed of the disk. Under the influence of both torques the watt-hour meter acts as the asynchronous motor with the speed of the disk proportional to the power supplied to the load. As a result, the number of revolutions n in the time period t (angular speed) is the measure of power

$$\frac{n}{t} \cong KUI \cos \phi \quad (3.22)$$

The mechanical register counts the number of revolutions and hence indicates the energy consumed by the load.

The principle of operation described above is significantly simplified. In the real instruments the phase shift in voltage coil is not exactly 90° thus additional phase correction winding is necessary. The braking torque is caused not only by the magnet, but also by the two cores and additional magnetic shunt is necessary for correction of this effect. Also additional correction is necessary to compensate for the effect of friction in the aluminum disc bearings. The total error of the induction meter is various for various measured power and it is described by the error characteristic. All corrections should be precisely set to ensure that the characteristic of errors does not exceed required limits. The main weakness of the induction watt-hour meters is that these corrections, hence generally the performance of the meter, changes with the aging process resulting in the risk that consumer or energy distributor are deceived.

3.2 The bridge circuits

The bridge circuits were used as the most accurate devices for the measurements of resistance (and generally impedance). Nowadays, the bridge circuits are not as important, because now, more effective direct methods of impedance measurement are developed (based on the Ohm's law). But the bridge circuits are commonly used as the resistance (impedance) to voltage converters.

Two main bridge circuits: supplied by the voltage source or the current sources are presented in Figure 3.12.

For the bridge circuits presented in Figure 3.12 the dependence of the output voltage U_{out} on the circuit parameters are as follows:

$$U_{out} = \frac{R_1 R_4 - R_2 R_3}{(R_1 + R_2)(R_3 + R_4)} U_0 \quad (3.23a)$$

$$U_{out} = \frac{R_1 R_4 - R_2 R_3}{R_1 + R_2 + R_3 + R_4} I_0 \quad (3.23b)$$

Thus the condition of the balance $U_{out} = 0$ of the bridge circuit is

$$R_1 R_4 = R_2 R_3 \text{ or } R_1 R_4 - R_2 R_3 = 0 \quad (3.24)$$

The condition (3.24) is a universal condition for all bridge circuits, and can be described as: *the bridge circuit is in the balance state when the products of the opposite impedances are the same.*

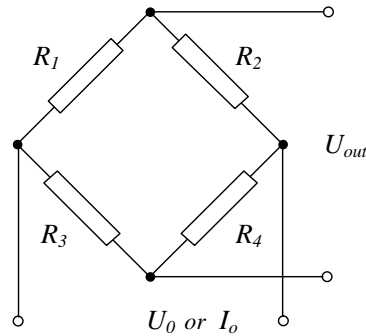


FIGURE 3.12
The Wheatstone bridge circuit.

The bridge circuits are used in two main modes of operation: as *balanced (null type)* circuit (Warsza 2005a) or as *unbalanced (deflection type)* circuit (Warsza 2005b). The *null type bridge circuit* is balanced by the setting of one or more impedances to obtain the state $U_{out} = 0$ and then the measured value of resistance $R_x = R_1$ is determined from the equation

$$R_x = R_2 \frac{R_3}{R_4} \quad (3.25)$$

In the deflection type of bridge circuit we first balance the bridge circuit and then we can determine the change of resistance from the output signal as

$$U_{out} \cong S \frac{\Delta Z_x}{Z_x} U_0 \quad (3.26)$$

Thus the unbalanced bridge circuit operates as the transducer of the change of impedance to the voltage (S is the sensitivity coefficient of the unbalanced bridge circuit).

3.2a Balanced bridge circuits

In the balance mode one or more elements are changed to obtain balance condition. For example in the bridge presented in Figure 3.12 the balance is obtained by changing resistance R_2 (Figure 3.13a). But

such method is inconvenient because such change is usually realized manually. Because bridge circuit is composed from two voltage dividers (see Figure 2.9) instead of changing resistance we can introduce change of voltage in voltage divider. Figure 3.13b presents the method of balancing the bridge by introducing additional voltage drop on resistor R_4 . This way we can remote balance the bridge.

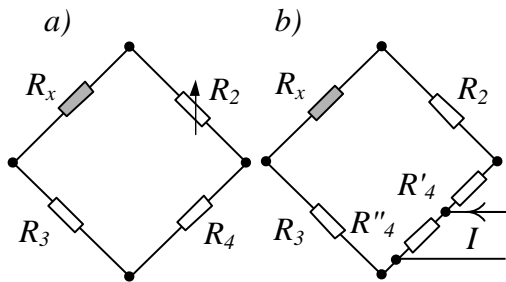


FIGURE 3.13
Balancing the bridge circuit by change of resistance (a) or by change of current (b)

If we are able to balance the bridge by current it is easy to introduce feedback to auto-balance the bridge, as it is presented in Figure 3.14.

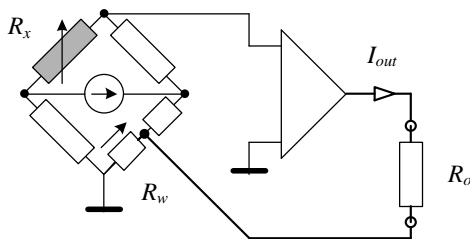


FIGURE 3.14
Auto balanced bridge circuit by internal feedback

Figure 3.15 presents other method of auto-balancing. In the first arm of bridge is connected sensor known as magnetoresistor – resistor changing resistance with magnetic field. If we connect the coil generating magnetic field on opposite direction the sensor is now detector of balance of the magnetic field. The feedback current is changing to obtain balance of the bridge. Some producer of magnetoresistive sensors design special planar coil to introduce feedback magnetic field.

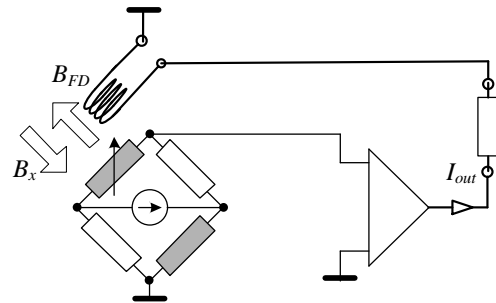


FIGURE 3.15
Auto balanced bridge circuit by external feedback

The bridge circuit with four resistors (as in Figure 3.12) is known as Wheatstone bridge. Instead of resistors it is possible to connect impedance $Z = |Z|e^{j\varphi}$. If we supply the bridge by AC voltage the balance condition 3.24 is now:

$$\begin{cases} |Z_1||Z_4| = |Z_2||Z_3| \\ \varphi_1 + \varphi_4 = \varphi_2 + \varphi_3 \end{cases} \quad (3.27)$$

Thus to obtain the balance of AC bridge circuit two conditions should be fulfilled: magnitude and phase (3.37). This means that in order to balance such bridge circuit two independent adjusting elements are necessary. The process of balancing is therefore more complicated than in the DC bridge circuit.

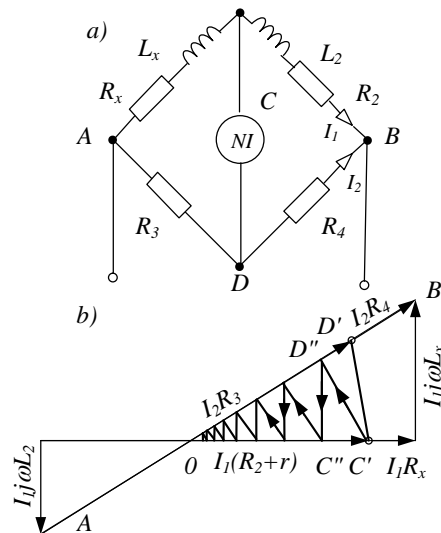


FIGURE 3.16
An example of AC bridge and simplified diagram illustrating the process of balancing

Let us consider the vector diagram presented in Fig. 3.16b. The bridge is balanced by the successive approximation. Assume that for balancing we use the elements R_2 and R_3 and the unbalanced voltage is represented by the line $C'D'$. By changing the R_3 we move the point D' to position D'' . Note that it is not possible to obtain the zero value of the $C - D$ distance because in this step of balancing the $C' - D''$ distance is the local minimum of the output voltage. If we now change the R_2 value we move the point C' to position C'' (this time the distance $C'' - D''$ is the local minimum of the output voltage). We can see that to obtain the balance it is necessary to perform many steps of approximation.

By appropriate design of bridge circuit it is possible to improve the balancing process – even down to two steps. It is also possible to use two null indicating devices with a 90° phase shift between them, which enable practically mutually independent balancing of both components. But generally the time of measurement using the AC bridge circuit is limited due to the complex problem of searching for the balanced state conditions.

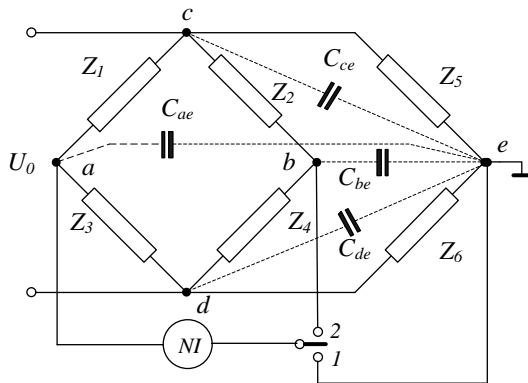


FIGURE 3.17
The methods of reduction of the influence of parasitic capacitances by including the Wagner earth additional elements

In the case of the AC bridge circuits another problem appears – it is difficult to eliminate influence of the stray and to earth capacitances (Figure 3.17). For that reason, it is necessary to shield all the elements in the AC bridge circuits. Shielding does not eliminate the capacitive coupling but enables investigators to establish their level during the balancing. More effective is to use the *Wagner earth* (*Wagner ground*) with additional elements Z_5, Z_6 connected as presented in Fig. 3.17.

The bridge circuit with the Wagner elements consists of two bridges. First, the bridge $Z_1Z_3Z_5Z_6$ is balanced

(the switch of null indicator in position 1), and then the bridge $Z_1Z_2Z_3Z_4$ (the switch of null indicator in position 2). (Sometimes it can be necessary to balance both bridges many times – approaching the equilibrium state in a stepwise manner). In the state of balance of both bridges the potentials of points a, b and e are the same and equal to the potential of earth. Therefore the capacitances C_{ae} and C_{be} do not influence the distribution of currents. The capacitances C_{de} and C_{ce} are connected to the Wagner elements and also do not influence the balance condition of the main bridge circuit.

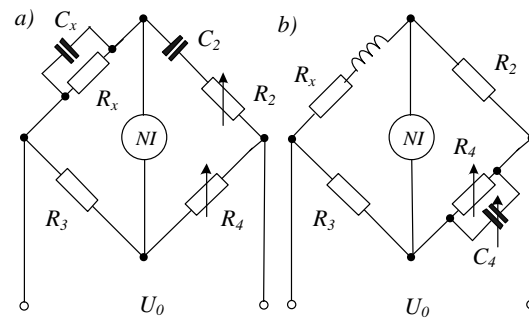


FIGURE 3.18
The Wien bridge circuit (a) and Maxwell-Wien bridge circuit (b)

A huge number of various AC bridge circuits were designed and developed: Maxwell, Wien, Schering, Hay, Owen, Anderson, de Sauty, Heaviside etc. Moreover, all these bridges exist in various mutations and modifications. [Hague 1971,]. Historically the oldest and most known are the Wien bridge (Fig. 3.18a) and Maxwell bridge (Fig. 3.18b) circuits.

The conditions of the balance state of *Wien bridge* circuit are as follows:

$$C_x = \frac{C_2 R_4}{R_3 (1 + \omega^2 C_2^2 R_2^2)}, \quad R_x = \frac{R_3 (1 + \omega^2 C_2^2 R_2^2)}{\omega^2 R_2 R_4 C_2^2} \quad (3.28)$$

The conditions of the balance are frequency dependent. Therefore the Wien bridge is rather seldom used for capacitance measurement, but it is frequently used as the frequency-dependent part of the oscillator, according to the dependence:

$$\omega^2 = \frac{1}{R_x C_x R_2 C_2} \quad (3.29)$$

The conditions of the balance state of the *Maxwell-Wien* bridge (called also often as the *Maxwell bridge*) are as follows:

$$L_x = R_2 R_3 C_4, \quad R_x = R_2 \frac{R_3}{R_4} \quad (3.30)$$

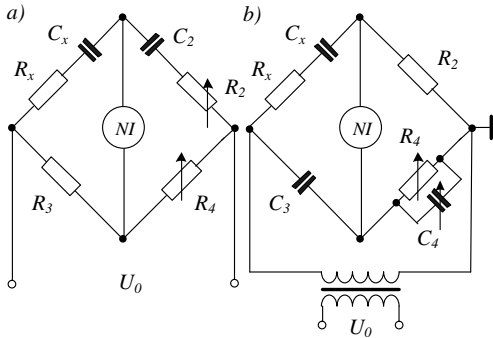


FIGURE 3.19
Two examples of the bridge circuits for capacitance measurements: de Sauty-Wien bridge (a) and Schering bridge (b)

Fig. 3.19a presents the AC bridge circuit for capacitance measurements (the *de Sauty-Wien bridge*). The conditions of the balance state can be described as:

$$C_x = C_2 \frac{R_4}{R_3}, \quad R_x = R_2 \frac{R_3}{R_4} \quad (3.31)$$

The $tg \delta_x = \omega C_x R_x$ can be calculated as:

$$tg \delta_x = \omega C_2 R_2 \quad (3.32)$$

Fig. 3.29b presents special kind of the bridge circuit – the *Schering bridge* designed for high voltage and cable testing. The main part of supply high voltage is on the capacitances C_x and C_3 , and adjustable elements R_4 , C_4 are additionally grounded. The measured parameters can be determined from the equations

$$C_x = C_3 \frac{R_4}{R_2}; \quad R_x = R_2 \frac{C_4}{C_3}, \quad tg \delta_x = \omega C_4 R_4 \quad (3.33)$$

Also simple inductance bridge circuit presented in Figure 3.16 can be used for inductance measurement. Assuming that the impedances of the arms are as follows: $Z_x=R_x+j\omega L_x$, $Z_2=R_2+j\omega L_2$, $Z_3=R_3$, $Z_4=R_4$ after simple calculations we obtain the balance conditions in form

$$L_x = L_2 \frac{R_3}{R_4}, \quad R_x = R_2 \frac{R_3}{R_4} - r \quad (3.34)$$

To obtain the balance of this bridge circuit the Q factor ($Q=\omega L/R$) of the inductances measured L_x and standard one L_2 should be the same. For that reason, an

additional resistor r is used. This resistor is connected to L_x or L_2 element (this connection is chosen experimentally – only in one position is possible to balance the bridge).

The inductance bridge circuit is useful for measurements of inductance $L_x R_x$ as well the Q factor $\omega L_x/R_x$. It is also possible to measure the mutual inductance M_x . For determination of the M_x value the measurements are performed two times – with the coils connected in the same directions of the flux L' and with the coils connected in opposite directions L''

$$L' = L_1 + L_2 + 2M \quad \text{and} \quad L'' = L_1 + L_2 - 2M \quad (3.35)$$

Then, the mutual inductance can be calculated as

$$M = \frac{L' - L''}{4} \quad (3.36)$$

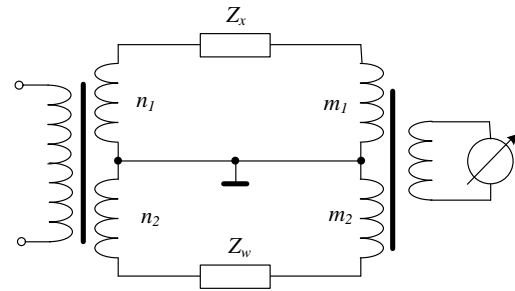


FIGURE 3.20
An example of the transformer bridge

Figure 3.20 presents the example of the *transformer bridge circuit* with two transformers. The output transformer acts in this circuit as the current comparator – the null indicator points to zero, when the resultant flux in the transformer is also equal to zero. The condition of the balance of this circuit is

$$\frac{Z_x}{Z_w} = \frac{n_1}{n_2} \frac{m_1}{m_2} \quad (3.36)$$

Thus the state of balance can be obtained not by changing the values of impedance but by change of number of turns. This is very convenient, because the number of turns can be precisely adjusted. Especially in the case of the digital bridge circuits it is much easier to connect the windings than to change the resistors or capacitors. Figure 3.21 presents the example of transformer bridge designed for capacity measurement.

The conditions of the balance of the circuit presented in Fig. 3.21 are as follows:

$$C_x = C_w \frac{n_2 n_4}{n_1 n_3}; R_x = R_w \frac{n_1 n_3}{n_2 n_5}; tg \delta_x = \frac{n_5}{n_4 \omega R_w C_w} \quad (3.37)$$

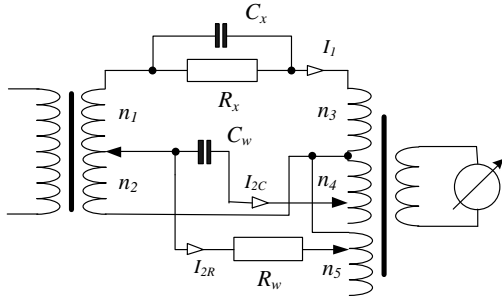


FIGURE 3.21
An example of the transformer bridge circuit designed for capacitance measurement

The transformer bridge circuits exhibit several important advantages in comparison with impedance bridge circuits. As was mentioned earlier, the balancing is possible by the change of the number of turns. In transformer bridges the parasitic capacitances shunt the transformer turns and practically do not influence the conditions of the balance. Also the sensitivity of the transformer bridges is significantly better than in the case of impedance bridges. In order to make use of these advantages it is necessary to construct the transformers very precisely, with minimal stray fields. Therefore the transformer bridges are usually more expensive than classic circuits without transformer coupling.

Returning to the Wheatstone bridge circuit it should be noted that this bridge exhibits limitations when very small resistances are measured. In the case of the measurements of very small (less than 1Ω) the result can be influenced by the contact resistances, thermoelectric voltages and most of all the resistances r of the wires connecting the resistance to the bridge. The influence of the thermoelectric voltages can be reduced by performing the measurement procedure in two steps – for positive and negative polarization of the supply voltage, and then by calculation of the average value from these two measurements.

For very small resistance, very useful is the modification of the Wheatstone bridge in the form presented in Fig. 3.22 (*the Kelvin bridge*). The condition of the balance for this bridge is as follows

$$R_x = R_2 \frac{R_3}{R_4} + r \frac{R_3 R_4' - R_3' R_4}{R_4 (R_3 + R_4 + R_p)} \quad (3.38)$$

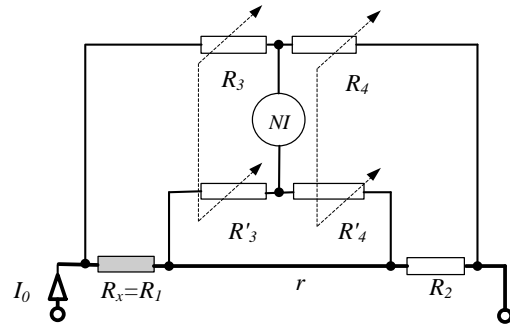


FIGURE 3.22
The methods of reduction of the influence of the connecting wires in the Kelvin bridge circuit

First of all, the resistance of connection wire r should be small – therefore such wire is prepared as a short and large diameter wire. The second term in the equation (3.38) as negligible if the following condition is fulfilled

$$R_3 R_4' = R_3' R_4 \quad \text{or} \quad \frac{R_3}{R_3'} = \frac{R_4}{R_4'} \quad (3.39)$$

The condition (3.39) is relatively easy to achieve by mechanical coupling of the resistors R_3/R_3' and R_4/R_4' . In such case, the condition for balance of the Kelvin bridge is the same as for the Wheatstone bridge. The Kelvin bridge enables measurement of the resistances in the range $0.0001 \Omega - 10 \Omega$.

3.2b Unbalanced bridge circuits

The unbalanced bridge circuits are used as the transducers converting the change of the resistance (and generally impedance) into the output voltage:

$$U_{out} = S U_o \frac{\Delta R_x}{R_{x0}} = S U_o \varepsilon \quad (3.40)$$

where S is the sensitivity of the transducer and ε is the relative change of the resistance

$$R_x = R_{x0} \pm \Delta R_x = R_{x0} \left(1 + \frac{\Delta R_x}{R_{x0}} \right) = R_{x0} (1 \pm \varepsilon) \quad (3.41)$$

where R_{x0} is usually the resistance in the balance state and $\varepsilon = \Delta R_x / R_{x0}$.

Of course described in previous auto-balanced circuit with feedback also operates as transducer of relative change of resistance:

$$I_{out} = S \frac{\Delta R_x}{R_{x0}} = S \varepsilon \quad (3.42)$$

There are a lot of sensors where the output signal is proportional to $\Delta Z/Z$ or $\Delta R/R$, for example the temperature sensor $R_T = R_{T0}(1 + \alpha \Delta T)$. The unbalanced bridge circuits are usually designed with symmetry in respect to the output diagonal (Fig. 3.23a) or to the supply diagonal (Fig. 3.23b).

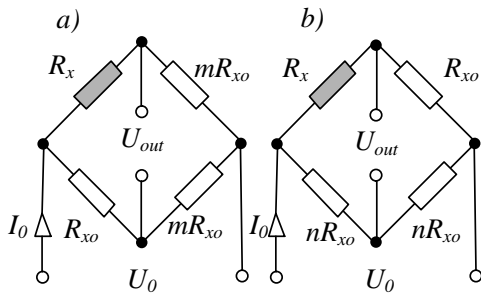


FIGURE 3.23
Two kinds of symmetry of the unbalanced bridge circuit

Substituting the relation (3.41) into the equations (3.23) after simple calculations we can derive the dependencies of the transfer characteristics of unbalanced bridge circuits:
for the circuit a)

$$U_{out} / U_0 = \frac{m}{(1+m)^2 + (1+m)\varepsilon} \varepsilon \quad (3.43)$$

and for the circuit b)

$$U_{out} / U_0 = \frac{1}{2(2+\varepsilon)} \varepsilon \quad (3.44)$$

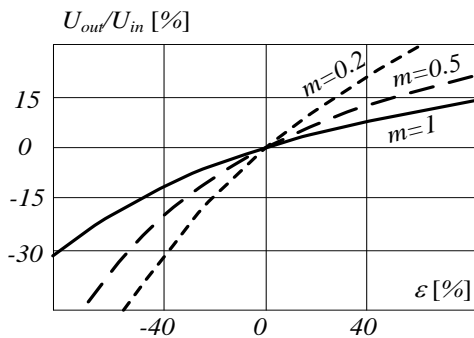


FIGURE 3.24
The example of the transfer characteristics of unbalanced bridge circuit

We can see that these circuits are nonlinear. The nonlinearity depends on the design of the bridge – for circuit b) it does not depend on the n value, but in the circuit a) it depends on the m value. Figure 3.24 presents the example of the dependences $U_{out} = f(\Delta R_x/R_{x0})$.

The nonlinearity of the bridge transducer is not always a drawback – in some circumstances this bridge nonlinearity can be used to correct the nonlinearity of the sensor. Let us consider the example presented in Figure 3.25. We use a thermistor sensor with very nonlinear characteristic $R = f(T)$ in order to measure the temperature. If the bridge characteristic would be linear, then the resultant characteristic of the transducer $U_{out} = f(T)$ would also be nonlinear – curve 1 in Figure 3.25. By appropriate choice of the bridge configuration (bridge nonlinearity), in our case by applying $m = 0.3$ we obtain almost linear processing of the temperature into the output voltage – curve 3 in Figure 3.25.

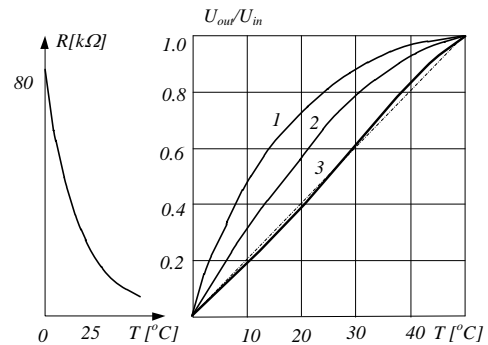


FIGURE 3.25
The transfer characteristic of the typical thermistor sensor and the resultant characteristics of the bridge circuit with thermistor sensor (1 – calculated under assumption that the bridge circuit is linear; 2 – calculated for $m = 1$; 3 – calculated for $m = 0.3$).

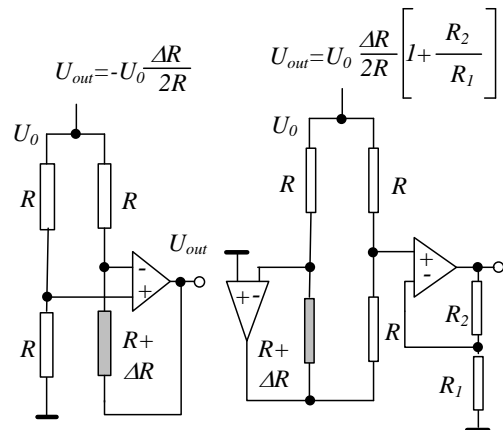


FIGURE 3.26
Two examples of the bridge circuit with feedback (Kester 1999)

There are various methods of linearization of the unbalanced bridge circuit. The best is applying a feedback because in such case only small linear part of transfer characteristic is used (see Figure 2.21). Indeed the transfer characteristic of the circuit presented in Figure 3.14 is practically linear. Figure 3.26 presents similar circuit with feedback [Kester 1999].

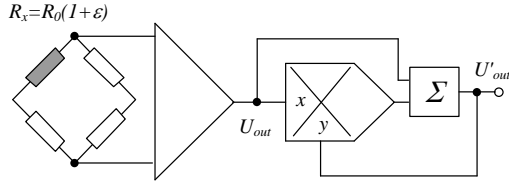


FIGURE 3.27
The linearization of the bridge circuit by applying the multiplier device

Other method of linearization is applying of the multiplier (Figure 3.27) [Tran 1987]. Taking into account Eq. 3.42 we can assume that the change of output signal of the bridge circuit supplied by the voltage $U = 0.5 U_o$ is:

$$U_{out} = \frac{\varepsilon}{(2 + \varepsilon)} U \quad (3.45)$$

After connection of the multiplier circuit as it is presented in Fig. 3.27 the output voltage is:

$$U'_{out} = U_{out} + \frac{U_{out} U'_{out}}{K} = \frac{U_{out}}{1 - U_{out}} = \frac{\frac{\varepsilon}{2 + \varepsilon}}{1 - \frac{\varepsilon}{2 + \varepsilon}} = \frac{1}{2} \varepsilon \quad (3.46)$$

Thus the transfer characteristic of the bridge circuit with multiplier is linear.

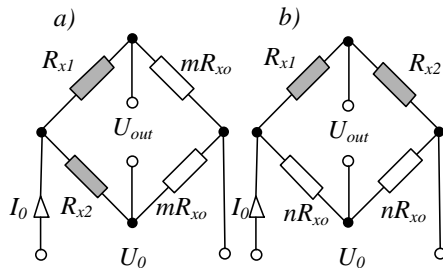


FIGURE 3.28
Two kinds of symmetry of the unbalanced bridge circuit with differential sensor.

It is very convenient to use two *differential sensors* instead of just one sensor. In the differential sensors the changes of the resistances are in the opposite direction:

$$\begin{cases} R_{x1} = R_{x0}(1 + \varepsilon) \\ R_{x2} = R_{x0}(1 - \varepsilon) \end{cases} \quad (3.47)$$

Also in this case we can connect the sensors in two kinds of symmetry as it is shown in Figure 3.28.

Substituting the relation (3.49) into the equations (3.23) after simple calculations we can derive the dependencies of the transfer characteristics of unbalanced bridge circuits: for the circuit a)

$$U_{out} / U_0 = \frac{2m}{(1 + m)^2 - \varepsilon^2} \varepsilon \quad (3.48)$$

and for the circuit b)

$$U_{out} / U_0 = \frac{1}{2} \varepsilon \quad (3.49)$$

Thus the bridge circuit with differential sensors in symmetry b) is linear.

Let us consider the sensitivity of the unbalanced bridge circuit. Neglecting the nonlinearity (calculating the S factor for $\varepsilon = 0$) from Equations (3.43) or (3.48) we obtain:

for the single sensor:

$$S = \frac{m}{(1 + m)^2} \quad (3.50)$$

and for two differential sensors:

$$S = \frac{2m}{(1 + m)^2} \quad (3.51)$$

The bridge circuit with differential sensors is two times more sensitive than the bridge with one sensor. If the bridge circuit is an AC bridge then the sensitivity is a complex value and:

$$m = \frac{Z_2}{Z_1} = \frac{|Z_2| e^{j\varphi_2}}{|Z_1| e^{j\varphi_1}} = \frac{|Z_2|}{|Z_1|} e^{j(\varphi_2 - \varphi_1)} = |m| e^{j\theta} \quad (3.52)$$

Thus the sensitivity S for the differential sensors is

$$S = \frac{2|m|}{1 + 2|m|\cos\theta + m^2} \quad (3.53)$$

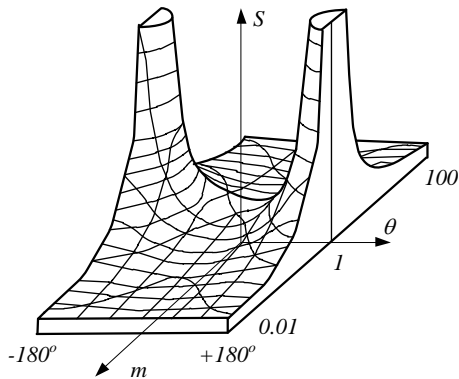


FIGURE 3.29
The dependence of the sensitivity S of the bridge circuit on the circuit configuration.

Fig. 3.29 presents a graphical representation of the dependence (3.53). From this figure we can conclude that:

- the sensitivity is largest when the ratio m is equal to 1,
- the sensitivity can be larger, when the phase difference between impedances Z_1 and Z_2 is larger.

The general dependence $U_{out}=f(\Delta R/R)$ of the unbalanced bridge circuit with four sensors is

$$U_{out} = \frac{I}{4} \left(\frac{\Delta R_1}{R_1} - \frac{\Delta R_2}{R_2} - \frac{\Delta R_3}{R_3} + \frac{\Delta R_4}{R_4} \right) U_o \quad (3.54)$$

Thus for one sensor the sensitivity is $S=1/4$, for two sensors it is $S=1/2$, while for four sensors we obtain four times larger sensitivity in comparison with the one-sensor case

$$U_{out} = \varepsilon U_o \quad (3.55)$$

Unbalanced bridge circuit as the converter $U_{out}=f(\Delta R/R)$ exhibits two *important advantages*:

- the zero component is removed by balancing the bridge and we convert only signal; proportional to the change of resistance $\Delta R/R$. It is important because often we detect only small change of the large resistance;
- according to Equation (3.54) in unbalanced bridge we can realize the differential operation - rejection of common component, for example temperature zero drift (see Figure 2.31).

3.3 The conditioning circuits

Often to the sensor is connected the *conditioning circuit* mediated between sensor and the rest of the

measuring system [Pallas-Areny et al 2001]. It can be simply an amplifier, but sometimes it can fulfill other functions as: linearization of the sensor, error reduction, analog - to digital conversion, saving in memory and even interfacing to net or computer.

The conditioning circuit is indispensable in the case of *parametric sensors* – sensors where the measured value causes change of parameter: resistance, capacity or inductance. We cannot send these output and we should convert it into signal – voltage or current. This is a function of condition circuit.

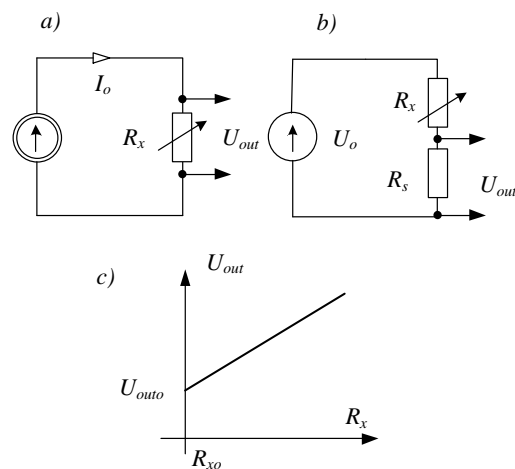


FIGURE 3.30
The typical converters of the resistance into the voltage: voltage drop (a), voltage divider (b) and their transfer characteristic (c)

Figure 3.30 presents two methods of conversion of the resistance to the voltage. The first one seems to be the most obvious – it utilizes the *Ohm's law* – the resistance is supplied by the stabilized current I_o and the voltage drop U_{out} is proportional to the sensed resistance

$$U_{out} = I_o R_x \quad (3.56)$$

Thus we have linear conversion of the resistance into voltage signal. But the dependence (3.56) is valid only if the resistance connected to the output of transducer is infinitively large. Consider finite resistance of the output load R_{out} . In such case we obtain a nonlinear characteristic $U_{out} = f(R_x)$ and this nonlinearity depends on the ratio R_x/R_{out} . The *Ohm's law* is also used in the converter presented in Figure 3.30b. The measured resistance is connected in the circuit of the voltage divider supplied by the voltage source U_o . The output signal U_{out} is described by the equation

$$U_{out} = U_o \frac{R_s}{R_s + R_x} = U_o \frac{I}{I + \frac{R_x}{R_s}} \quad (3.57)$$

The conversion is nonlinear, which is not always a drawback, because in certain cases it can be used for linearization of a non-linear sensor. The main disadvantage of the circuits presented in Figure 3.30 is that the dependence $U_{out} = f(R_x)$ does not start from zero because the resistance of the sensor usually also does not start from the zero value but from the certain R_{x0} value

$$R_x = R_{x0} \pm \Delta R_x = R_{x0} \left(1 \pm \frac{\Delta R_x}{R_{x0}} \right) = R_{x0} (1 \pm \varepsilon) \quad (3.58)$$

Similarly the output signal of the converters presented on the Figure 3.30 includes the constant component U_{out0} , because

$$U_{out} = U_{out0} (1 + \varepsilon) \quad (3.59)$$

This offset component is disadvantageous, because more convenient is the case when the output signal of the transducer is zero for starting point of the range of the sensor. If this condition is fulfilled then we can connect the typical voltmeter as the measuring instrument. Moreover, large offset component can cause the saturation of the amplifier (if any amplifier is used).

Therefore better is to use the circuit with common mode rejection – Figure 3.31. The most frequently is used the unbalanced bridge circuit described in previous Section (deflection type bridge). If this bridge circuit is in the balance state for the starting point of the sensor resistance then the output signal is offset-free, because

$$U_{out} \cong S \frac{\Delta R_x}{R_{x0}} = S \cdot \varepsilon \quad (3.60)$$

The deflection type bridge circuit exhibits several other important advantages. First of all such a circuit is immune to the variation of the external interferences, for example changes of the ambient temperature. If all resistors in the bridge circuit are the same and only one of them is the sensor ($\varepsilon_1 = \delta x$), then with the change of the ambient temperature all resistors change their resistances: $\varepsilon_2 = \varepsilon_3 = \varepsilon_4 = \delta T$ while $\varepsilon_1 = \delta x + \delta T$. Thus according to Eq. (3.54) δT components are eliminated and only useful δx component remains at the output of the bridge

$$U_{out} = \frac{1}{4} (\delta x + \delta T - \delta T - \delta T + \delta T) = \frac{1}{4} \delta x \quad (3.61)$$

It is much better to use the differential type of the sensor ($\varepsilon_1 = +\delta x$, $\varepsilon_2 = -\delta x$ and $R_1 = R_{x0}(1+\varepsilon)$, $R_2 = R_{x0}(1-\varepsilon)$) connected to the adjacent arms of the bridge circuit. In this case we obtain elimination of interference effects with two times larger output signal. And of course the best case is to use four differentially connected sensors, because in such circuits we obtain four times larger output signal.

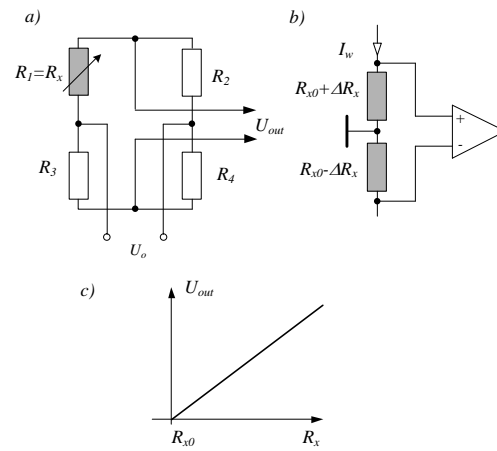


FIGURE 3.31 Converters of the resistance into the voltage with elimination of the offset component: unbalanced bridge (a), with differential amplifier (b) and their transfer characteristic (c)

The unbalanced bridge circuit usually exhibits non-linear transfer characteristic. But as it was described in previous Section it is possible to correct non-linearity – the best recommended method is to use feedback.

Similar performances as the unbalanced bridge circuits exhibits the circuit with differential amplifier (Figure 3.31b). The differential amplifier converts the difference of the input signals ($U_{out} = K_u (U_1 - U_2)$). Thus if one of the input resistors is active (a measuring sensor) and the second one is the same passive resistor we obtain elimination of the offset voltage and also elimination of the interferences. Such principle is used in Anderson loop – described in Chapter 2.3.

If we use four active sensors in a bridge circuit we do not have free resistor to balance the bridge. Theoretically, we can connect parallel balancing resistor to one of the arms. But in this case one of the resistors exhibits different performances than the other three resistors, which can cause incomplete elimination of the external influences, for example temperature error. Figure 3.32 present two examples of the methods enabling to balance such bridge circuits.

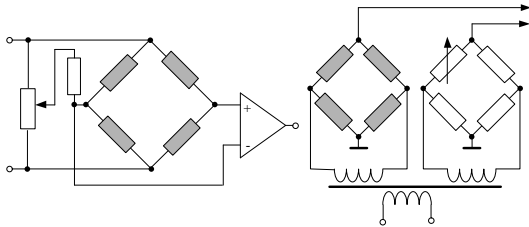


FIGURE 3.32
Methods of balancing of four sensor bridges

The methods of conversion of the resistance to the voltage signal described above are also suitable for the conversion of the capacitance, inductance or generally impedance. In such case the bridge circuit should be supplied by the AC voltage. The Wheatstone bridge can be substituted by the special AC bridge circuit (Maxwell, Wien or other). But in this case we have to eliminate parasitic capacitances and inductances. It is also necessary to consider the influence of the cable's capacitance. The AC circuits require balancing of two components – magnitude and phase.

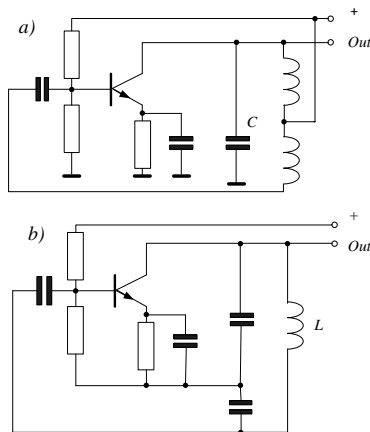


FIGURE 3.33
The conversion of the capacitance C or inductance L to the AC signal with frequency dependent on the measured parameter: a) Hartley oscillator, b) Colpitts oscillator

Even if we balance both components of the unbalanced AC bridge circuit we do not solve all problems. The output signal contains two components – one in phase with the supply voltage, and the other one shifted by 90 degrees. The shifted component can be effectively eliminated by phase-sensitive rectifier (more details will be given in Section 3.6).

Especially in the case of capacitance or inductance sensors instead of voltage converters better is to use converters to frequency. Frequency we can transmit

much easier than voltage and frequency output we can consider as simple and cheap digital output.

For to frequency conversion classical oscillators can be used. Figure 3.33 presents two such circuits – *Hartley* and *Colpitts* oscillators. In these circuits, the nonlinear dependence of the frequency on the measured parameter is inconvenient, because usually frequency f is $f \approx \sqrt{1/X}$, where X is C or L .

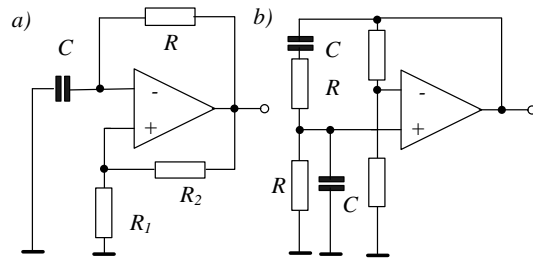


FIGURE 3.34
The conversion of the capacitance C or resistance R to the AC signal with frequency dependent on the measured parameter: a) multivibrator oscillator, b) Wien bridge oscillator

It also is possible to adapt the oscillator utilizing the operational amplifier presented in Figure 3.35a. The frequency depends on the capacitance C (or resistance R) as follows

$$f = \frac{1}{2RC \ln(1 + 2R_1 / R_2)} \quad (3.62)$$

Figure 3.34a present also RC oscillator with classical Wien bridge with the resonance frequency:

$$f = \frac{1}{2\pi RC} \quad (3.63)$$

We can also convert measured value into voltage and use one of voltage to frequency converters. Of course such converters are ready to use in the case of voltage output sensors.

Figure 3.35 presents a typical design of a V/f converter with an integrator circuit charging a capacitor C at a rate proportional to the amplitude of input voltage U_{in} . Each time when the output voltage of integrator circuit reaches certain value equal to the reference voltage U_{ref} the comparator switches into a reset mode and discharges the capacitor (because diode D change its biasing). The frequency of the output signal depends on the amplitude of input voltage

$$f = \frac{U_{in}}{RCU_{ref}} \quad (3.64)$$

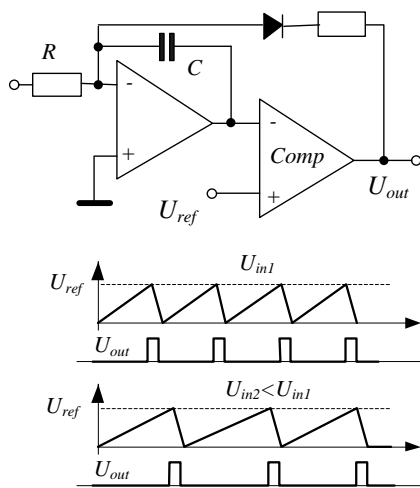


FIGURE 3.35
The voltage to frequency converter [Tran Tien Lang 1987]

Figure 3.36 presents the hybrid voltage to frequency converter of Analog Devices – model AD-537. This converter AD537 enables the conversion of the input voltage to the frequency up to 100 kHz with nonlinearity error less than 0.05%. The conversion factor $K=U_{in}/f$ can be set by connecting appropriate external R and C elements to the device. This figure presents the example of application of this transducer to the temperature conversion with the conversion factor 10 Hz/°C (for chromel-constantan thermocouple sensor).

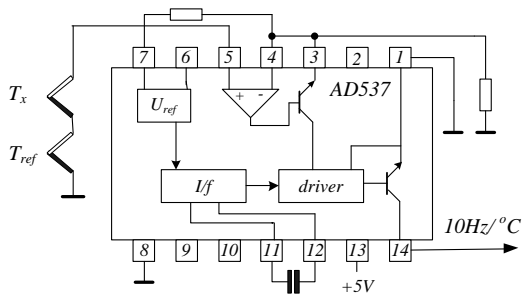


FIGURE 3.36
An example of the temperature transducer utilizing AD537 voltage-to-frequency converter of Analog Devices

In measuring systems very often is used device known as voltage controlled oscillator VCO presented in Figure 3.38. For control the frequency the varicap diode DC can be used. Varicap is a diode with the capacity depending on the voltage.

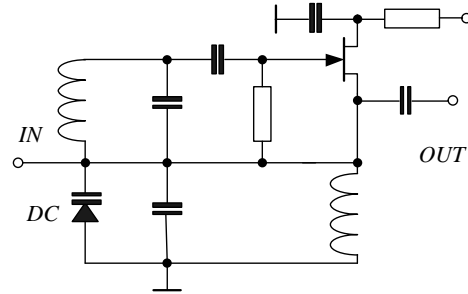


FIGURE 3.37
An example of the temperature VCO device (voltage controlled oscillator)

3.4 The main sensors of physical values

Sometimes we can meet mismatch in usage of such terms as: sensor, transducer and detector. According to VIM *the sensor* is an element of a measuring system that is directly affected by a phenomenon, body, or substance carrying a quantity to be measured. The *transducer* is a device, used in measurement, which provides an output quantity having a specified relation to the input quantity. Thus the sensor is some kind of transducer. But a new generation of the sensors, known as *intelligent sensors*, has included sometimes quite complex electronic circuit - operating as transducers.

The *detector* is some kind of sensor that indicates the presence of a phenomenon, body, or substance when a threshold value of an associated quantity is exceeded. Thus the sensor is a first element of the measuring system directly contacting with investigated value.

The sensors can be used to directly measurement of investigated physical value. But often they can be used as intermediate element. For example the temperature sensor can be used to measure of temperature, but also to measure humidity in psychrometer device, air flow in anemometer device or CO2 contents in thermoconductive analyzer. The Hall sensor of magnetic field is more often used to measure mechanical values and electrical current than to measure the magnetic field intensity.

Recently a huge number of various sensors have been developed [Fraden 2003]. In this Sections only eight selected, most important primary sensors are described to present typical problems of their applications and signal conditioning.

3.4.a. Resistance temperature detector - RTD

One of the most frequently used sensors is the temperature sensor. Various thermal effects can be used to detect the temperature – thermal expansion,

thermoelectric effect, thermoresistive effect, thermal radiation, change in quartz frequency, change of semiconductor junction properties etc. The change of resistance is widely used to measure the temperature because sensor is relatively simply and in case of platinum sensor with high accuracy.

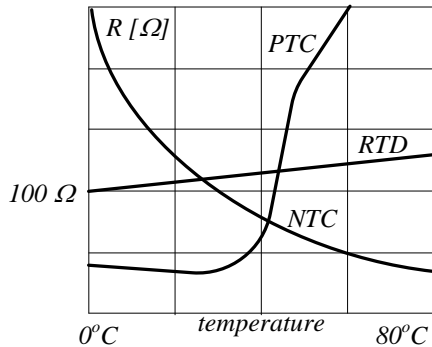


FIGURE 3.38
The example of transfer characteristics of the main thermoresistive sensors (after Fraden 2003)

Figure 3.38 presents transfer characteristics of the main thermoresistive sensors: metal platinum resistor RTD, thermistor NTC and thermistor with positive temperature coefficient PTC. Thermistors have much larger sensitivity but they are rather nonlinear and with modest accuracy. The metal thermoresistors are close to linear and with high accuracy (resistance of platinum sensor are described by international standard IEC 751).

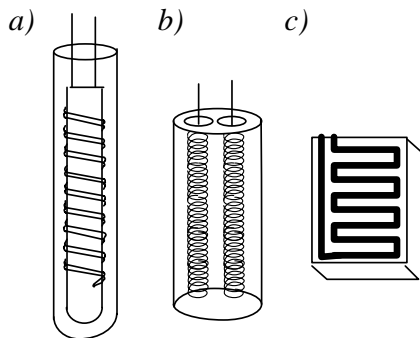


FIGURE 3.39
Typical design of platinum temperature sensors

Among various metal platinum is the best choice because it exhibits: very linear dependence on the temperature, relative large temperature coefficient ($\alpha = 0.385 \text{ \% / } ^\circ\text{C}$), high resistivity and good plasticity enabling preparation of thin wire, wide range of

operating temperature ($-270 - 850 \text{ } ^\circ\text{C}$), immunity to corrosion and very stable (it is estimated that it is better than 0.05°C per year). Figure 3.39 presents typical designs of platinum sensors of temperature.

Usually thin platinum wire is wound on ceramic or insulated metal core, often in bifilar mode to avoid inductivity (see Figure 2.64). Better accuracy exhibits design with helical wire inserted in the bores – this way the influence of thermal stress is eliminated (Figure 3.39b). For cheaper design is also used the thin film technology (Figure 3.39c).

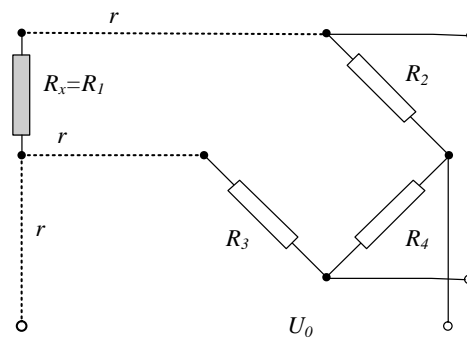


FIGURE 3.40
Three wire connection of the sensor

The platinum sensor is usually connected to the bridge circuit (see Figure 3.12). When the sensor is connected to the bridge circuit with relative long wires, the temperature changes of the resistance of these wires can cause significant error. In such case *three wires* connections is recommended (Figure 3.40).

If all three wires exhibit the same resistance (the same length) we can write that:

$$(R_x + r)R_4 = R_2(R_3 + r) \quad (3.65)$$

and

$$R_x R_4 = R_2 R_3 + r(R_2 - R_4) \quad (3.66)$$

If additionally the condition $R_2 = R_4$ is fulfilled then the influence of the resistance r of the connecting wire is negligible.

Better accuracy is possible to obtain in four wires connection (Figure 3.41). In this connection there are two pairs of terminals – for current delivery and for voltage sensing. The current wires are outside the measuring circuit therefore their resistance r_i does not influence the measuring result (especially if we supply the sensor with current stable source). The resistance of sensing wires r_s also does not influence the result because voltmeter has usually very high resistance thus

the current is very small. Generally the four wires connection is obligatory for very small (less than 1 Ω) measured resistance.

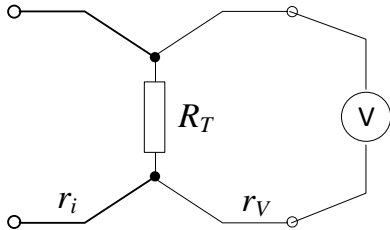


FIGURE 3.41
Four wire connection of the sensor

There are many other measuring circuits for thermoresistive sensors - Figure 3.42 presents simple circuit with operational amplifier. If $R_T = R$ the output signal is equal to zero I other cases is:

$$V_T = -\frac{V_o}{2R}(R_T - R) \tag{3.67}$$

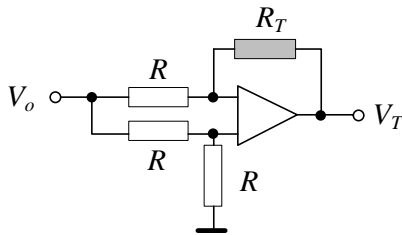


FIGURE 3.42
The measuring device with operational amplifier

Platinum RTDs typically are available in two classes of accuracy - class A and Class B. Sensors of class A have in ice point tolerance of ± 0.06 ohms. Class B is standard accuracy and has an ice point tolerance of ± 0.12 ohms. The error of RTDs increases with temperature – at 600 °C tolerance is ± 0.43 ohms (1.45 °C) for class A and ± 1.06 ohms (3.3 °C) for class B. Specially prepared from 99.999% pure platinum resistors are used as Standard Platinum Resistance Thermometers (SPRT) and exhibit temperature coefficient of 0.3926 %/°C).

Unfortunately the platinum sensor is not fully linear. Its transfer function is described as:

$$R(T) = R_o [1 + AT + BT^2 + C(T - 100)T^3] \tag{3.68}$$

for $T \leq 0^\circ\text{C}$

$$R(T) = R_o [1 + AT + BT^2] \tag{3.69}$$

for $T > 0^\circ\text{C}$;

where: R_o is the resistance in 0°C , $A = 3.9083 \times 10^{-3} \text{ }^\circ\text{C}^{-1}$, $B = -5.775 \times 10^{-7} \text{ }^\circ\text{C}^{-2}$; $C = -4.183 \times 10^{-12} \text{ }^\circ\text{C}^{-4}$.

It can be easy to calculate that for temperature 600 °C the error of nonlinearity is about 6%. Knowing exact dependence of $R(T)$ it is possible to introduce the correction. But usually it is necessary to perform certain mathematical operation. One of such solution is described in Application Note AN-709 of Analog Device [King *et al* 2004]. The correction is performed in circuit presented in Figure 3.43.

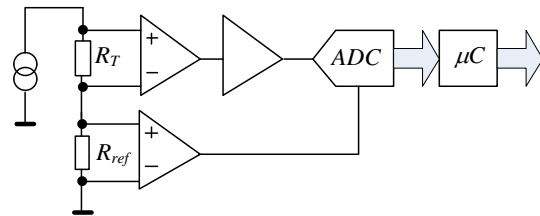


FIGURE 3.43
The measuring circuit with microcontroller for linearization [King *et al* 2004]

In the circuit presented in Figure 3.43 the resistance is calculated as U_{RT}/U_{ref} – note that in this way change of supplying current is negligible. In the presented Note authors consider three methods of linearization:

- direct mathematical method,
- single linear approximation,
- piecewise linear approximation.

In the first method following relation was calculated using the microcontroller:

$$T(R_T) = \frac{Z_1 + \sqrt{Z_2 + Z_3 \cdot R_T}}{Z_4} \tag{3.70}$$

where: $Z_1 = -A$, $Z_2 = A^2 - 4B$, $Z_3 = 4B/R_o$, $Z_4 = 2B$.

The relation (3.70) is relatively simple but it is valid only for $T > 0^\circ\text{C}$, for $T < 0^\circ\text{C}$ it is much more complex. This method of linearization is accurate but requires math library. Simple linear approximation was very fast, did not require math library and very small code space was required. But the accuracy was poor especially for wide temperature range.

The best result was reported for piecewise linear approximation. This method was sufficiently accurate and fast and the math library did not require. In

comparison with single linear approximation greater code size was necessary to use. Figure 3.44 presents other measuring circuit applying 4 wire connection and microconverter ADuC834. Note that this microconverter includes excitation, gain stage, ADC circuit and microcontroller).

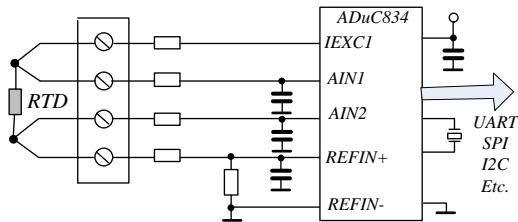


FIGURE 3.44
The measuring circuit with microconverter [King *et al* 2004]

Besides the problem of linearization in design of the measuring device with RTD two other important problem should be solved:

- self heating
- response time.

As the sensor is wound with very fine wire the current is strongly limited (usually it does not exceed 1 mA). Moreover self-heating effect can destroy distribution of measured temperature. Usually we determine acceptable current as:

$$I = \sqrt{\frac{\Delta T}{T(T)k_w}} \quad (3.71)$$

where ΔT is the increase of temperature and k_w is dissipation factor. The dissipation factor depends on the design of the sensor and environment conditions and roughly can be estimated as $k_w = 3 - 5$ mW/K for still air and $k_w = 10 - 20$ mW/K for air 1 m/s. The best solution is to determine experimental the dissipation factor by applying stepwise increase of current.

The time constant of typical temperature sensor is several seconds and depends on the external medium and its flow velocity. But usually conditions of the measurement are influenced by housing of the sensor. In the sensor with housing the time constant can increase to dozen seconds and dynamics is closer to second order (thus two time constants are present). The problem of temperature exchange between medium and sensor is quite complex and strongly influences the measurement result.

3.4.b. Thermocouple sensors

The thermoelectric effect was discovered in 1822 by Estonian physician Thomas Seebeck. He stated that the

junction of two different metal wires (thermocouple) generates voltage dependent on the temperature of the junction¹. Figure 3.45 presents the principle of operation of the thermocouple sensor.

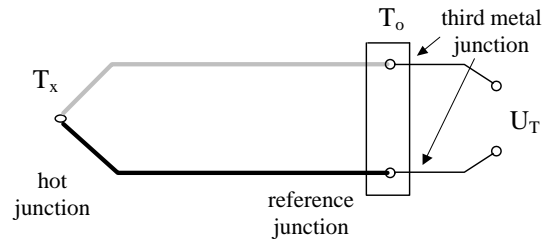


FIGURE 3.45
The principle of operation of thermocouple sensor

At the end of two different metal wires connecting as “hot junction” appears the voltage:

$$U_T = S_{12}(T_x - T_o) \text{ or } U_T = S_1 T_x - S_2 T_o \quad (3.72)$$

where S_{12} is the Seebeck constant (or S_1, S_2 – Sebeck constants related to common reference temperature, usually 0°C).

Thus we see that the thermocouple sensor *does not measure the absolute temperature* but it measures the difference of temperatures.

It would be not reasonable to extend thermocouple wires to voltmeter connection because some wires, for example platinum one, are expensive. We profit the “low of third metal”²: The algebraic sum of thermoelectric voltages in a circuit composed of any number of dissimilar materials is zero if all are at uniform temperature. Thus we can use connection of for example copper wires and no additional voltage is generated if the ends if this third materials have the same temperature.

The thermocouple sensors are commonly used to measure the temperature although they have many serious drawbacks:

- The sensitivity is poor (see Figure 3.46). For comparison: assuming current 1 mA we can expect the output voltage of the RTD sensor of about 40 mV for temperature change of 100 °C. Meanwhile the best thermocouple sensor generates the voltage of about 6 mV for similar change of temperature. That is why in thermocouple measurements the high quality, low noises, low zero drift amplifiers are necessary. We can increase the sensitivity by connecting several thermocouples in series.

¹ In original experiment of the Seebeck the current of the junction copper and bismuth was observed by applying of the compass.

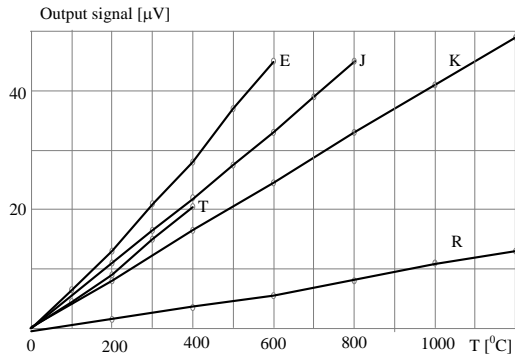


FIGURE 3.46
The transfer characteristics of typical sensors

- The transfer characteristics are nonlinear – the Seebeck coefficient changes with the temperature (see Figure 3.47). Fortunately most of the transfer characteristics are tabularized and are available in Internet (for example NIST tables available at: <http://srdata.nist.gov/its90/main>). The transfer characteristic can be described in polynomial form:

$$\Delta T = a_1 U_T + a_2 U_T^2 + a_3 U_T^3 + a_4 U_T^4 + \dots \quad (3.73)$$

The polynomial coefficients are also available at NIST Internet page and next can be used in numerical linearization [Malik 2010]. Note that for thermocouple type K the Seebeck coefficient is constant in wide range of temperature.

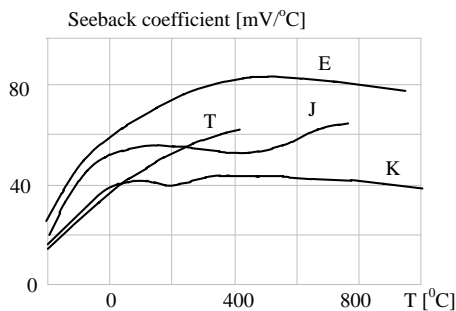


FIGURE 3.47
The dependence of the Seebeck coefficient on temperature

- It is necessary to guarantee that the reference temperature is constant. Thus the reference junction should be inserted into thermostat. More often the electronic circuit for reference temperature compensation is used.

But the thermocouples have also important advantages:

- Simple construction. It is sufficient to solder, to weld or even to twist two wires to obtain thermocouple sensor.
- Wide range of temperature, from – 200 °C to more than 2000 °C.
- Small dimensions enabling point testing of temperature distribution.
- Excitation in not necessary, thus also problem of self-heating is omitted.

Table 3.1 present typical thermocouple sensors.

TABLE 3.1
Typical thermocouples and their performances.

Type	Junction	Range °C	S (25 °C) µV/°C
B	PtRh30/PtRh6	100 - 1800	0.3
E	NiCr/CuNi	-270 - 700	61
J	Fe/CuNi	-210 - 750	52
K	NiCr/NiAl	-270 - 1000	41
N	NiCrSi/NiSi	-270 - 1000	27
R	PtyRh13/Pt	-50 - 1600	6
S	PtRh10/Pt	-50 - 1600	6
T	Cu/CuNi	-270 - 350	41

The largest sensitivity exhibits the thermocouple chromel-constantan (type E), moreover it is nonmagnetic. The most versatile is the thermocouple chromel-alumel (type K). Thermocouples based on platinum measure the largest temperature, are most stable and accurate although with low sensitivity. The thermocouples copper-constantan and iron-constantan (type T or J) are easy to prepare (these materials are commonly available), have high sensitivity and limited temperature ranges. The thermocouple nitrosil-nisil (type N) is stable and resist to oxidation. The thermocouple type B has very low Seebeck coefficient for temperatures below 100 °C and therefore can be used without compensation of the reference junction.

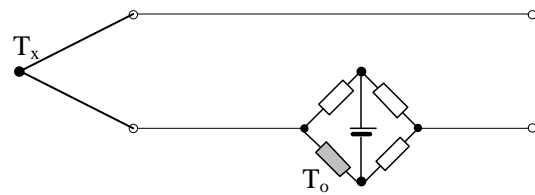


FIGURE 3.48
The compensation of the reference temperature by unbalance bridge and second temperature sensor

The thermostat for stabilization of the reference temperature is non-convenient. More often is used the temperature dependent source of the voltage. An example is presented in Figure 3.48. As such source is used the unbalanced bridge circuit with additional temperature sensor.

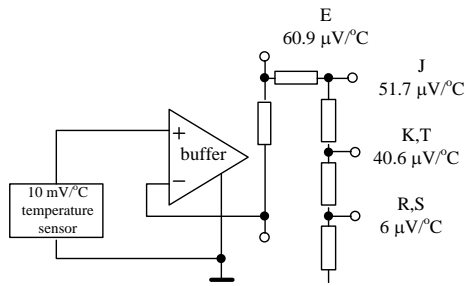


FIGURE 3.49
The thermocouple reference junction compensator – model LT1025 of Linear Technology [Williams 1988]

Figure 3.49 presents reference temperature compensator developed by Linear Technology. The various sources of compensating voltage arte delivered depending on type of the thermocouple. Figure 3.50 present the full circuit designed for temperature measurement with thermocouples.

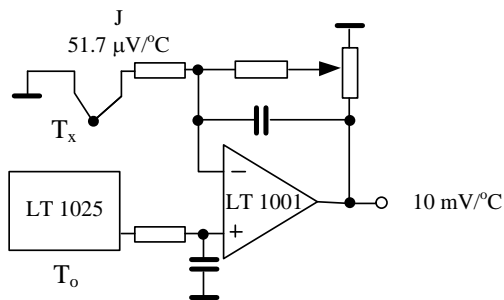


FIGURE 3.50
The circuit for temperature measurement with thermocouple reference junction compensator LT1025 proposed by Linear Technology [Williams 1988]

Also other producers proposed ready to use amplifiers specially designed for thermocouples. For example Analog Devices developed amplifier AD8497 with included cold (reference) junction compensator [Duff *et al* 2010].

3.4.c. Strain gauge sensors

The stain gauge (or strain gage) is one of the main sensors of mechanical values. The principle of operation is simple – resistance of the metal wire depends on its geometry length l and cross section A (or radius r):

$$R = \rho \frac{l}{A} = \rho \frac{l}{\pi r^2} \tag{3.74}$$

and the change of this resistance is:

$$\frac{dR}{R} = \frac{dl}{l} - \frac{2dr}{r} + \frac{d\rho}{\rho} + = (1 + 2\nu + \xi) \varepsilon = K\varepsilon \tag{3.75}$$

where: $\varepsilon = dl/l$ - strain (deformation), ν - Poisson’s ratio (dependence between longitudinal and transversal deformation), ξ - piezoresistivity constant (for metals equal to $C(1-2\nu)$, C – Bridgman constant, K – strain gauge factor.

For metals piezoresistivity constant is negligible small and strain gauge factor is:

$$K \cong 1 + 2\nu \tag{3.76}$$

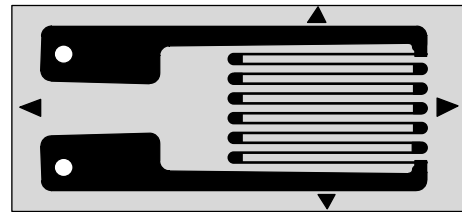


FIGURE 3.51
Typical design of the strain gauge sensor.

Figure 3.51 presents typical design of strain gauge sensor. The resistor in form of meander is etched from the foil and bonded to plastic backing. The transversal parts are wider to avoid sensitivity to transversal component of strain. The whole strain gauge is usually attached by the glue to tested material – thus the deformation of materials is transmitted to the sensor.

The strain gauge is the sensor of strain (directly) or mechanical stress σ – indirectly according to the Hooke’s law:

$$\sigma = E \frac{\Delta l}{l} = E\varepsilon \tag{3.77}$$

where E is the Young’s modulus.

As the material for strain gauge commonly is used *constantan* – alloy of copper and nickel %Cu45Ni. It has high resistivity, good plasticity and low temperature influence. It has limitation for high temperature (above 65 °C) and then special alloy known as *karma* (NiCrFeAl) is used. Karma is especially recommended for long time static measurements. Both constantan and karma have Poissons’s ratio close to 0.5 and therefore the strain gauge factor is usually equal to 1.8 – 2.4.

Both materials enable to prepare so called STC (Self Temperature Compensated) strain gauges. The

influence of temperature can be described by following relation:

$$\frac{\Delta R}{R}(T) = [\alpha + K(\gamma - \beta)] \Delta T \quad (3.78)$$

where α is temperature coefficient of resistance of strain gauge material, β is thermal expansion coefficient of substrate (tested material) while γ is thermal expansion coefficient of strain gauge material. The α coefficient is relative small (40ppm/°C). It is possible to select material in such a way to obtain condition $\gamma - \beta = 0$ for chosen tested materials. These materials are known as A-alloys.

The measured deformation are usually very small and expressed in microstrain ($\epsilon = 10^{-6}$ for 1 μ strain). If we measure small deformation of several μ strains it means that the output signal of the bridge circuit with strain gauge is very small – in μ V range). It is the main measurement problem in application of strain gauges. It means that even if we have STC gauges the changes of temperature can influence the result (we cannot distinguish which part of the change of resistance comes from temperature and which from strain). That is why usually it is recommended to use second “temperature compensation” sensor as it is presented in Figure 3.52.

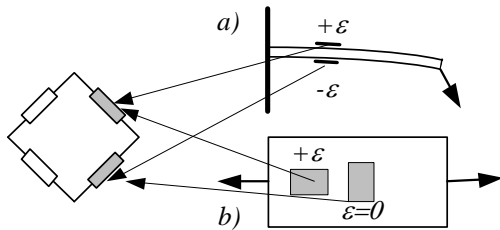


FIGURE 3.52
Connecting of the sensors to a bridge circuit to eliminate temperature error: a) two active sensors, b) active and passive sensors

Of course the best is the case when we can organize two differential sensors – as it is presented in Figure 3.52. If we do not have differential sensors accepted is to connect the second dummy (passive) sensor to adjacent arm of the bridge circuit. In the case presented in Figure 3.52b the dummy sensor is in transverse direction to be insensitive to the longitudinal measured stress.

As it was mentioned above the main problem of instrumentation is very small signal of the sensor. Therefore formerly as strain bridge instruments have been used special carrier amplifiers to decrease zero

drift and interferences. This bridge circuit was supplied by AC voltage next modulated by sensor signal. The principle of operation of such bridge is presented in Figure 3.53.

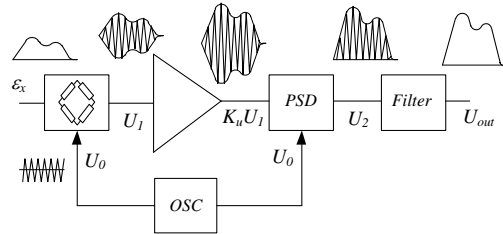


FIGURE 3.53
Strain gauge bridge instrument with carrier amplifier

If the measured strain ϵ varies periodically with the frequency ω then the variation of the resistance of the sensor with the constant K is

$$\frac{\Delta R_x}{R_x} = \delta R_x = K \epsilon_x = K \epsilon_m \sin \omega t \quad (3.79)$$

The output voltage of the bridge circuit of the sensitivity factor S supplied by the voltage signal $U_0 = U_{om} \sin \Omega t$ is

$$U_1 = S \delta R_x U_0 = SK \epsilon_m U_{om} \sin \omega t \sin \Omega t \quad (3.80)$$

After simple calculations we obtain

$$U_1 = U_{1m} [\cos(\Omega - \omega) t + \cos(\Omega + \omega) t] \quad (3.81)$$

where $U_{1m} = SK \epsilon_m U_{om}$.

From the equation (3.81) we can see that the bridge circuit supplied by the AC voltage works as a modulator device – the magnitude of the output signal of the frequency the same as the supply voltage is modulated according to the variation of resistance (and stress). The spectral characteristics of these signals are presented in Fig. 3.54.

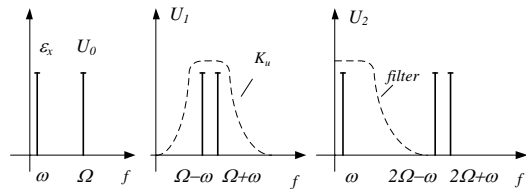


FIGURE 3.54
The spectral characteristics of the signals of the circuit presented in figure 3.53

The transfer characteristic of phase sensitive detector PSD is

$$U_2 = K_u U_1 |\cos \Omega t| \quad (3.82)$$

or as a series

$$U_2 = \frac{2}{\pi} K_u U_1 \left(1 - \frac{2}{3} \cos \Omega t - \frac{2}{15} \cos 4\Omega t + \dots \right) \quad (3.83)$$

thus

$$U_2 = \frac{2}{\pi} K_u U_{1m} \left[\begin{array}{l} \sin \omega t + \frac{1}{3} \sin(2\Omega - \omega) t + \\ \frac{1}{3} \sin(2\Omega + \omega) t + \dots \end{array} \right] \quad (3.84)$$

The phase sensitive detector acts as a selective filter. Now it is only necessary to connect the low-pass filter to correctly recover the measured signal

$$U_{out} = \frac{2}{\pi} K_u U_{1m} \sin \omega t \quad (3.85)$$

The carrier amplifier is rather complex, the AC supplying require sometimes additional phase balance of the bridge circuit and the useful frequency bandwidth is limited to the 20% of carrier frequency. Meantime on the market appeared low noise, low zero drift monolithic amplifiers. Therefore recently as strain amplifier the DC supplied bridge instruments are commonly used. Nevertheless for very small deformations and strong interferences the AC supplied bridge instruments can be recommended. Table 3.2 presents comparison of two instruments of the same company Showa Measuring Instruments Inc. - one with AC 5 kHz bridge (carrier amplifier) model 5683 and DC bridge model 5693.

TABLE 3.2
Comparison of AC and DC strain gauge bridges instruments.

Parameter	AC bridge	DC bridge
Sensitivity [V/ μ strain]	10/200	10/1000
Smallest range [μ strain]	200	1000
Noise level [μ strain]	0.6	20
Zero drift [μ strain/ $^{\circ}$ C]	0.1	1
Zero drift [μ strain/24h]	0.5	5
Frequency bandwidth	DC - 2 kHz	DC - 500kHz
Nonlinearity	0.1% FS	0.01% FS
Stability	0.2%/24h	0.05%/24h
T	Cu/CuNi	-270 - 350

From this comparison we see that AC bridge exhibits much better resolution while DC bridge exhibits much better frequency bandwidth and linearity.

3.4.d. Linear Variable Differential Transformer

The *linear variable differential transformer LVDT* sensor is the most frequently used sensor of displacement.

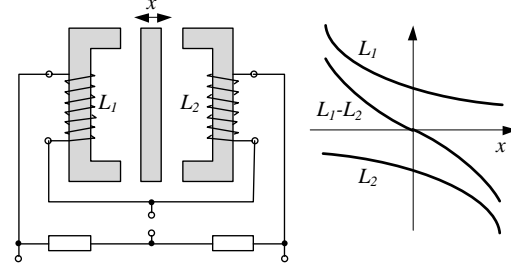


FIGURE 3.55
Inductive sensors and their transfer characteristics

Let us start with simple inductive sensor with reluctance variation presented in Figure 3.55. The inductivity of single sensor is:

$$L = \frac{n^2}{R_\mu} = \frac{n^2}{\frac{l_o}{\mu_o A_o} + \frac{l_{Fe}}{\mu_{Fe} A_{Fe}}} \quad (3.86)$$

where l , μ , A are length, permeability and cross section of air and iron part, while n is number of turns and R_μ is the reluctance. For $\mu_{Fe} \gg \mu_o$ we can write:

$$L = n^2 \mu_o A_o \frac{1}{l_o} \quad (3.87)$$

If we assume movement of internal iron part then $l = 2x + 2l_o$ and reluctance is:

$$R_\mu = \frac{2l_o}{\mu_o A_o} + \frac{2x}{\mu_o A_o} \quad (3.88)$$

and the inductance is

$$L_o = \frac{1}{2} n^2 \frac{\mu_o A_o}{l_o} \quad \text{where} \quad L_o = \frac{1}{2} n^2 \frac{\mu_o A_o}{l_o} \quad (3.89)$$

Thus the change of inductivity (and output signal of a sensor) $(L-L_o)/L_o$ is:

$$\frac{\Delta L_l}{L_l} = \frac{\frac{x}{l_o}}{1 + \frac{x}{l_o}} = \frac{x}{l_o} - \left(\frac{x}{l_o} \right)^2 + \left(\frac{x}{l_o} \right)^3 - \dots \quad (3.90)$$

The output signal of single inductive sensor is nonlinear (see Figure 3.55). We can significantly improve the linearity by connecting into bridge circuit two differential sensors because:

$$\frac{\Delta L_1}{L_1} - \frac{\Delta L_2}{L_2} = \frac{x}{l_o} + \left(\frac{x}{l_o}\right)^3 + \left(\frac{x}{l_o}\right)^5 \dots \quad (3.91)$$

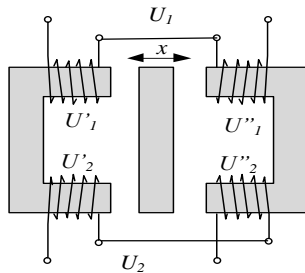


FIGURE 3.56
Differential transformer sensor

We can significantly improve properties of the same sensor connecting it in transformer circuit (Figure 3.56) instead of bridge circuit. The input voltages are:

$$U'_1 = \frac{L_1}{L_1 + L_2} U_1 \quad \text{and} \quad U''_1 = \frac{L_2}{L_1 + L_2} U_1 \quad (3.92)$$

while the output voltages are:

$$U'_2 = \frac{n_2}{n_1} U'_1 \quad \text{and} \quad U''_2 = \frac{n_2}{n_1} U''_1 \quad (3.93)$$

The output signal is the difference of the secondary voltages thus:

$$U_2 = \frac{n_2}{n_1} U_1 \frac{L_2 - L_1}{L_2 + L_1} \quad (3.94)$$

Assuming that air gaps are: $2l_o - 2x$ and $2l_o + 2x$ and taking into account Eq. (3.87) we obtain:

$$U_2 = \frac{n_2}{n_1} U_1 \frac{x}{l_o} \quad (3.95)$$

The transformer sensor is linear. Usually instead of choke sensor presented in Figure 3.56 the other solenoid sensor (presented in Figure 3.57) is recently used. It is more convenient in use (non-limited distance of moving part) and to design (simply three coils on the plastic frame).

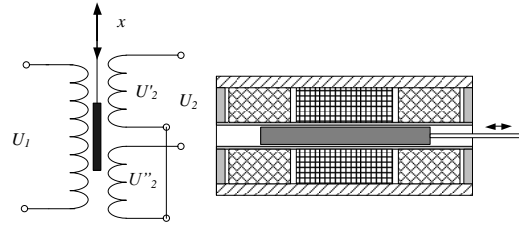


FIGURE 3.57
The solenoid type linear variable differential transformer LVDT

In transformer sensor presented in Figure 3.57 if the moving high permeability ferromagnetic part is in the central position both secondary voltages are the same. Because output voltage is the difference of the secondary voltages the output signal for central position of the moving part is zero. Movement of the ferromagnetic part causes that one of the secondary voltages (and its phase shift) is dominating and output signal increases as it is presented in Figure 3.58.

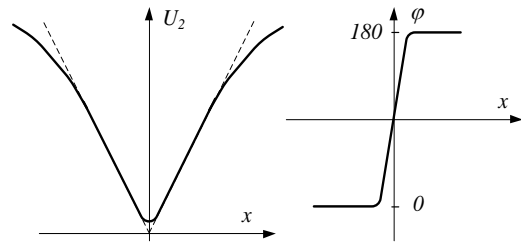


FIGURE 3.58
The transfer characteristics of typical LVDT sensor – output voltage and phase shift (related to input voltage)

In the real LVDT sensor transfer characteristic is usually slightly nonlinear – mainly in $x = 0$ point. The reason is not completely compensation of two AC voltages – due to possible asymmetry. The solution is to use the conditioning circuit with synchronous detector (Figure 3.59).

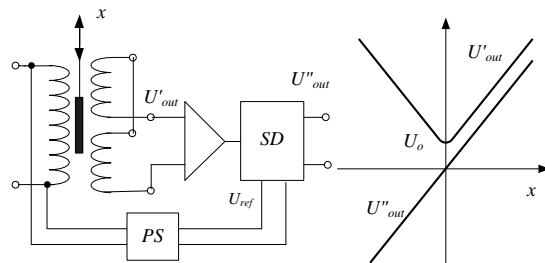


FIGURE 3.59
The conditioning circuit of LVDT sensor – with synchronous detector

Synchronous detector removes the orthogonal component and the transfer characteristic becomes linear. And moreover what is important DC output signal enables to detect direction of the movement. But if we apply the synchronous detector it is necessary to add the phase shifter because the phase shift between excitation reference voltage and output signal is other than 0/180°. Moreover this phase shift changes with temperature. That is why sometimes simple rectifiers are used as it is presented in Figure 3.60.

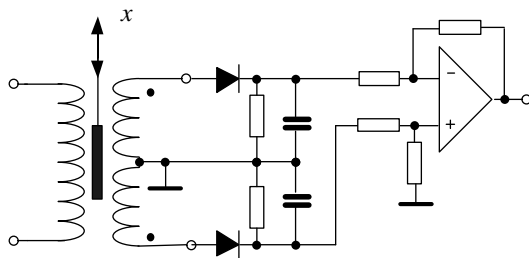


FIGURE 3.60
The conditioning circuit of LVDT sensor – with diode rectifiers and differential amplifier [after Nyce 2004]

In the circuit presented in Figure 3.60 diodes load the sensor, voltage drops on the diodes decrease output signal, parameter of diodes should be the same. More sophisticated rectifying circuit includes in their conditioning circuit AD 598 Analog Devices. Additional advantage of this solution is independence of the output signal on the value of exciting voltage.

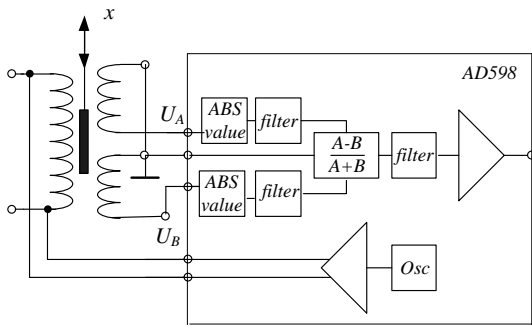


FIGURE 3.61
The conditioning circuit of LVDT sensor developed by Analog Devices.

The LVDT sensor enables measurement of the displacement with resolution of μm . Beside the linear sensors often are used also Rotating Variable Differential Transducer RVDT used to the angle measurement. Figure 3.62 present an example of such sensor known as resolver.

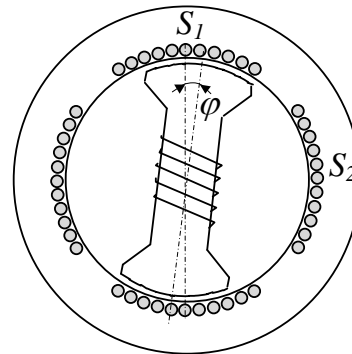


FIGURE 3.62
The RVDT sensor (resolver) for measurement of the angle [after Padmanabhan 2000].

Voltages induced in two stators depends on the rotation angle of the rotor:

$$U_{S1} = A_1 = E_m \sin \varphi \text{ and } U_{S2} = A_2 = E_m \cos \varphi \quad (3.96)$$

The angle can be calculated as:

$$\varphi = \sin^{-1} \frac{A_1}{\sqrt{A_1^2 + A_2^2}} \quad (3.97)$$

3.4.e. Glass sensor for pH measurement

Measurements of the pH are important not only in chemical industry but also in many other areas, as medicine, food industry, agriculture etc. For pH measurement most commonly the glass sensor is used. The pH is the measure of acidity (less than 7) or basicity (alkalinity) (more than 7) (Figure 3.63).

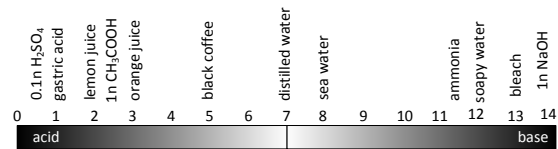


FIGURE 3.63
Typical values of pH of various substances.

In distilled water the concentration of hydrogen ions is the same as concentration of hydroxide ion:

$$[H^+] = [OH^-] = \sqrt{10^{-14}} = 10^{-7} \quad (3.98)$$

And as pH unit it was assumed concentration of hydrogen:

$$pH = -\log [H^+] \quad (3.99)$$

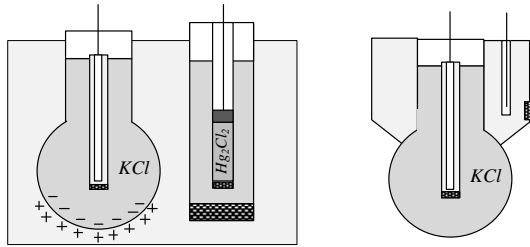


FIGURE 3.64
Two electrodes for pH measurement (glass and reference calomel one) or combined electrode.

For measurement of concentration of hydrogen ion (pH value) commonly is used glass electrode. On the thin glass bulb (thickness of 50 – 200 μm) are concentrated charges depending on the pH value. As a glass specially doped by lithium ions is used. As result on the glass electrode appears the potential described by the Nernst equation:

$$E = E_o - \frac{2.303RT}{F} \text{pH} \quad (3.100)$$

where E_o is standard electrode potential, R is universal gas constant $R = 8.314472(15) \text{ J K}^{-1} \text{ mol}^{-1}$, T is absolute temperature, while F is Faraday constant $F = 9.64853399(24) \times 10^4 \text{ C mol}^{-1}$.

After substitution of constants we obtain that the electrode generates potential

$$E = -0.19847 \cdot T \cdot \text{pH} \text{ [mV]} \quad (3.101)$$

or

$$E = -58.13 \cdot \text{pH} \text{ [mV]} \quad (3.102)$$

The glass bulb is filled by KCl solution and to obtain the potential the reference electrode is included. As the reference electrode silver-chloride electrode or calomel electrode is used. Because on the glass electrode we have only the potential to obtain voltage it is necessary to use the second reference electrode with potential independent on pH. Usually it is the same electrode as used in the glass electrode.

The calomel reference electrode is presented in Figure 3.64. The glass tube ended with porous seal and filled with KCl solution. The inner electrode is filled by calomel Hg_2Cl_2 and mercury. Recently often instead of two electrodes one combined electrode is used. The example of such electrode is presented in Figure 3.64.

Figure 3.65 present typical dependence of $E = f(\text{pH})$ of glass electrode.

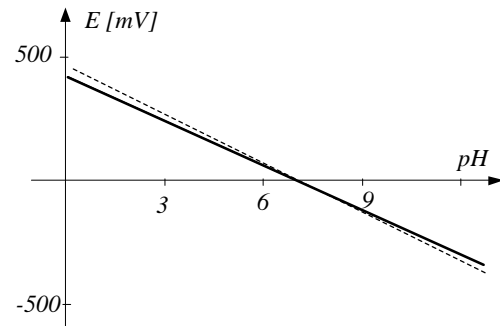


FIGURE 3.65
Typical $E=f(\text{pH})$ dependence of the glass electrode.

The slope of $E = f(\text{pH})$ dependence is about 58 mV/pH and increase of about 2 mV/10°C. The common point for all temperatures (point of rotation) is called *isopotential point*. For the designers of the glass electrodes it is recommended if this point is close to pH = 7.

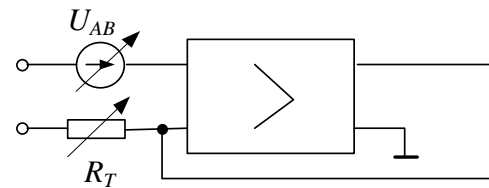


FIGURE 3.66
Typical circuit of the pH meter instrument.

There are two main problems in pH measurements. The first one is that the resistance of electrodes (source of the voltage) is usually very large – 500 M Ω or more. Thus the input resistance should be much larger (see Figure 2.39). Typical voltmeter cannot be used for pH measurement because its input resistance is not so large – the special electronic circuits with feedback should be designed.

The second problem is that the transfer characteristics of the electrodes (presented in Figure 3.65) can be different for various electrodes. Therefore for accurate pH measurements it is recommended to scale the instrument by using special standard buffer solutions. The point of zero voltage of electrodes should correspond with pH = 7 and to correct this point the adjustable voltage source U_{AB} can be used. The change of slope can be corrected by resistor R_T – this resistor is sometimes the temperature sensor to auto temperature correction. As the transfer characteristic $E = f(\text{pH})$ is close to straight line it is sufficient to use two buffer solutions to calibrate the pH meter.

3.5 AC to DC conversion

3.5a. The diode rectifying devices

It is relatively easy to convert the value of AC signal to the DC signal using diode rectifiers. A typical rectifying diode conducts the current for only one direction of applied voltage. An example of the transfer characteristic of a silicon rectifying diode is presented in Figure 3.67.

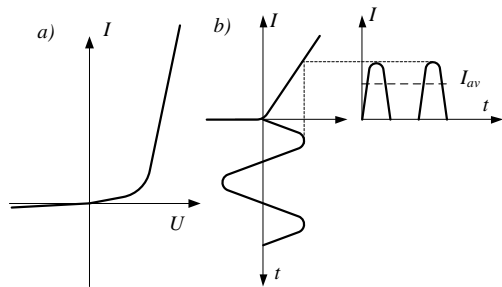


FIGURE 3.67
The principle of diode rectifying.

A typical transfer characteristic of the rectifying diode is presented in Figure 3.67a. In the conducting direction the characteristic is nonlinear and the conductance starts from a certain non-zero threshold voltage ($U_p \approx 0.5\text{ V}$). Moreover, a small inverse current will be conducted in the “non-conducting” direction. For that reason, the simple rectifying diode circuits can be used only in non-accurate devices – for measurement purposes it is necessary to support the diode with a more sophisticated electronic circuit, for example containing an operational amplifier.

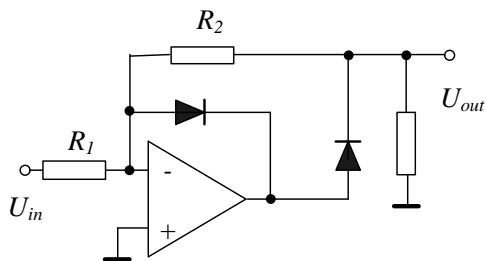


FIGURE 3.68
AC/DC converter with rectifying diodes and the operational amplifier.

Figure 3.68 presents the typical AC/DC converter with rectifying diodes and operational amplifier. The amplifier operates as a current transducer – rectified current flows in the feedback circuit. For a strong

feedback the threshold voltage U_p' decreases to negligible small value $U_p' \approx U_p/K_u$. (K_u – gain of the amplifier). In such case the converter behaves as a practically linear transducer of input voltage u_{in}

$$U_{out} = -\frac{R_2}{R_1}|U_{in}| \quad (3.103)$$

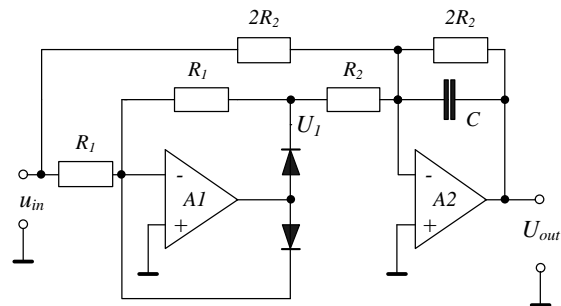


FIGURE 3.69
The full-wave converter of average value of AC voltage to the DC voltage (Tran Tien Lang 1978)

Figure 3.69 presents another converter of average value of AC voltage to DC voltage. The amplifier A1 works a half-wave rectifier according to the following conditions

$$U_1 = \begin{cases} -u & \text{for } u \geq 0 \\ 0 & \text{for } u \leq 0 \end{cases} \quad (3.104)$$

The second amplifier (A2) adds two voltages

$$U_{out} = -(u_{in} + 2U_1) \quad (3.105)$$

thus, the full-wave rectification is achieved:

$$U_{out} = \begin{cases} u & \text{for } u \geq 0 \\ -u & \text{for } u \leq 0 \end{cases} \quad (3.106)$$

3.5b. The peak value converters

Figure 3.70 presents the principle of the conversion of the peak value of the AC signal. The rectified voltage is connected to the capacitor C. If the time constants of the RC circuits (circuits of charge and discharge respectively) are designed in such a way that process of charging is fast and discharging is slow then the voltage across the capacitor is equal to the peak value of the supplying voltage. By connecting two converters it is possible to detect peak-to-peak U_{pp} value as it is presented in Figure 3.71.

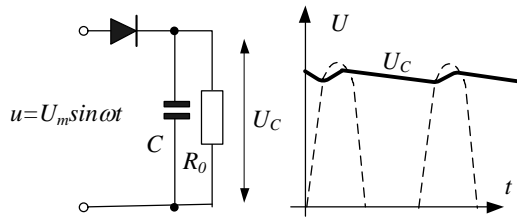


FIGURE 3.70
The principle of operation of the peak detector.

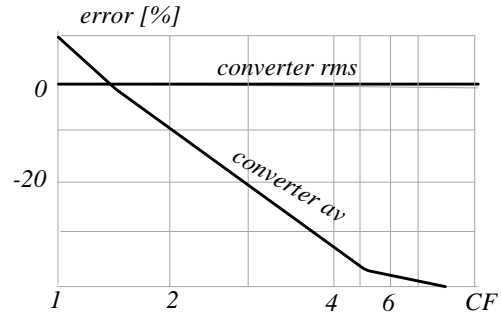


FIGURE 3.73
The error of conversion depending on the crest factor (converter rms and rectifying (averaging)/converter).

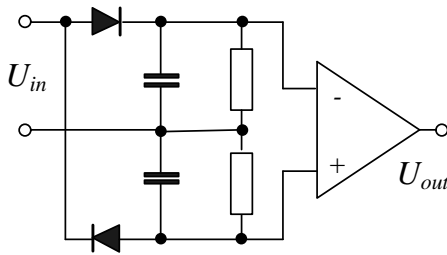


FIGURE 3.71
The principle of operation of the peak-to-peak detector.

In the circuit presented in Figure 3.72 the capacitor C_1 is charged to the maximal (peak) value. The feedback circuit (elements R_1 and D_1) protects the amplifier from the saturation when $U_{in} < U_c$. Periodical connection of the resistor R_p enables the capacitor to discharge and repeat the conversion.

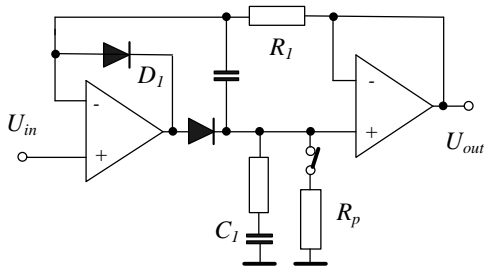


FIGURE 3.72
The precise peak detector circuit.

3.5c. The true rms value converters

The converters presented in Section 3.5.a allow determining averaged rectified value of AC signal. On many digital instruments is added notice “true rms”. Indeed old instruments used simple rectifying device and they were scaled for sinusoidal shape. But if the signal is distorted the error of rectifying converters can be large. Figure 3.73 presents error of conversion versus crest factor $CF = U_{max}/U_{rms}$.

TABLE 3.3
Crest factor of different signals.

Waveform	rms value	CF	Error [%]
Sine	0.707	1.41	0
Square	1	1	11
Triangle	0.577	1.73	-3.8
Noise	0.333	3	
Pulse	0.1	10	-44

If the rectifying measuring device is calibrated for sinusoidal waveform the measuring error for square waveform is larger than 10%, and for crest factor equal to 10 error is very large.

The conversion of the *rms* value of the AC signal to the DC voltage is more difficult. According to the equation:

$$U_{rms} = \sqrt{\frac{1}{T} \int u^2(t) dt} \tag{3.107}$$

we should perform the following operations: square, mean value calculation and root operation (*root-mean-square*). These mathematical operations are possible to perform using two multipliers, as is schematically shown in Figure 3.74.

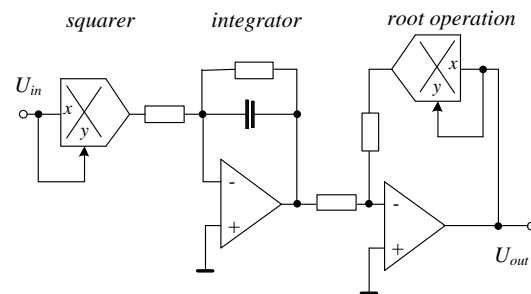


FIGURE 3.74
The true rms converter using two multipliers.

In the circuit presented in Figure 3.74 the first multiplier is squaring the input voltage, then this voltage is averaged in the integrator circuit and next rooting is performed. The root operation is achieved by second multiplier in the feedback circuit of operational amplifier.

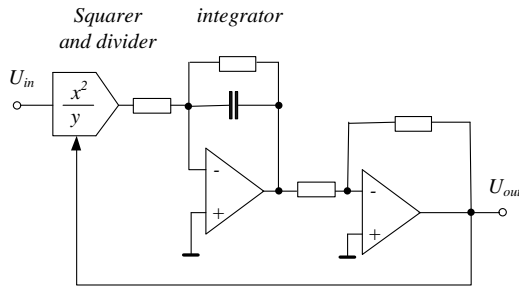


FIGURE 3.75
The true rms converter with indirect calculation of rms value.

The converter presented in Figure 3.74 is realized seldom due to its poor dynamics. More often is used circuit presented in Figure 3.75 with indirect calculation of rms value. Indeed in this circuit we have fulfilled following relation:

$$U_{out} = \frac{U_{in}^2}{U_{out}} \quad (3.108)$$

Thus we have

$$U_{out} = \sqrt{U_{in}^2} \quad (3.109)$$

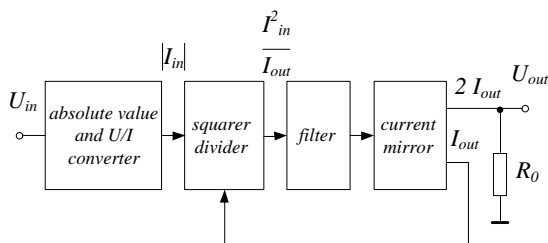


FIGURE 3.76
The principle of operation of the AD636 rms converter of Analog Devices (Kitchin 1986)

There are two strategies of true rms calculation. In the first one presented in Figure 3.76 the multiplier is used. Instead of multiplier the logarithmic amplifier can be used as it is presented in Figure 3.77.

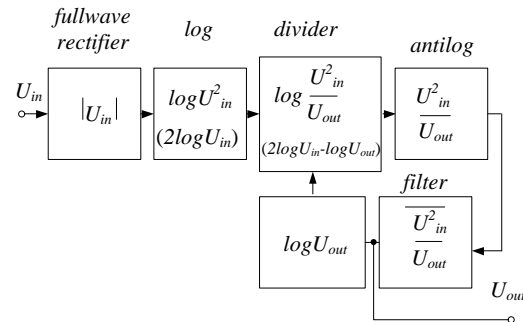


FIGURE 3.77
The principle of operation of the AD637 rms converter of Analog Devices (Kitchin 1986)

Figure 3.77 presents the principle of operation of another true rms converter - utilizing the log-antilog circuit (logarithmic and exponential amplifier – described in next Section). This converter performs the following operations:

- 1) $2\log U_{in}$ the same as: $\log U_{in}^2$
- 2) $2\log U_{in} - \log U_{out}$ the same as: $\log(U_{in}^2 / U_{out})$
- 3) $\text{anti log}(\log U_{in}^2 / U_{out}) = U_{in}^2 / U_{out}$
- 4) $\overline{U_{in}^2 / U_{out}}$
- 5) $U_{out} = \overline{U_{in}^2} / U_{out}$

Thus, as the result of these operations we obtain:

$U_{out} = \sqrt{U_{in}^2}$ which is exactly the definition of the rms value.

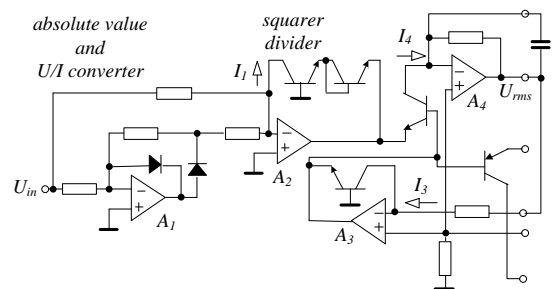


FIGURE 3.78
The simplified circuit of the AD637 rms converter of Analog Devices

In the circuit presented in Figure 3.78 realized is operation

$$I_4 = I_1^2 / I_3 = I_1^2 / I_4 \quad (3.110)$$

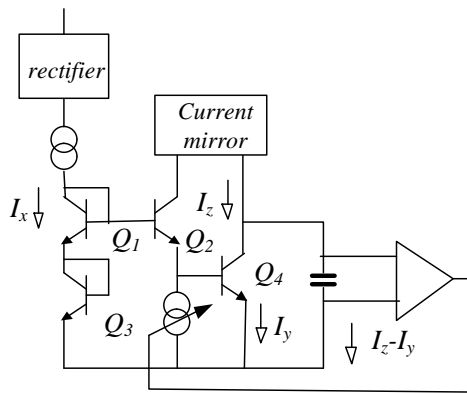


FIGURE 3.79
Structure of translinear rms-dc converter [Wassenar *et al* 1988]

Very often as the rms core the translinear circuit introduced by Gilbert is used [Gilbert 1975, Wassenar *et al* 1988]. For the loop Q3 – Q1 – Q2 – Q4 according to Kirchhoff’s law we can write:

$$U_{BE3} + U_{BE1} = U_{BE2} + U_{BE4} \quad (3.111)$$

Assuming exponential relationship between the base-emitter voltage and collector current:

$$\frac{kT_3}{q} \ln \frac{I_{c3}}{I_s} + \frac{kT_1}{q} \ln \frac{I_{c1}}{I_s} = \frac{kT_2}{q} \ln \frac{I_{c2}}{I_s} + \frac{kT_4}{q} \ln \frac{I_{c4}}{I_s} \quad (3.112)$$

Assuming the same temperature T and the same saturation current I_s we obtain translinear principle:

$$I_{c3} I_{c1} = I_{c2} I_{c4} \quad (3.113)$$

In the circuit presented in Figure 3.79 $I_{c3} = I_{c1} = I_x$ and $I_{c4} = I_y$ and $I_{c2} = I_z$. Thus we obtain:

$$I_x^2 = I_z I_y \quad \text{and} \quad I_z = \sqrt{I_x^2 I_y} \quad (3.114)$$

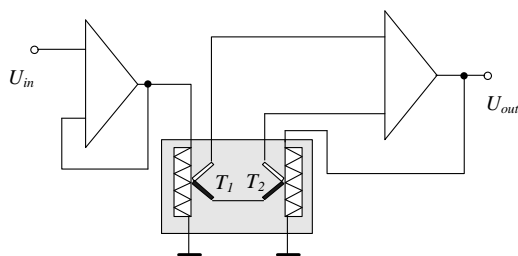


FIGURE 3.80
The thermal true rms converter

Instead of utilizing the relationship (3.107), it is also possible to perform AC/DC conversion by applying the physical definition of the effective value: “the effective (rms) value of the AC current is equal to the DC current value, which in the same resistance R in the time of one period causes emission of the same value of the heat”. Such idea was realized by the rms converter of Linear Technology (model LT1088)² presented in Figure 3.80.

The voltage generated by the thermocouple is a measure of the heat emission on the resistor and is compared with the voltage generated by the second thermocouple sensor heated by the AC current. Thus, we compare the heat effects of both currents. Such a transducer enabled AC/DC conversion in very large bandwidth (up to 300 MHz) with a large crest factor. Recently is available only in laboratory scale

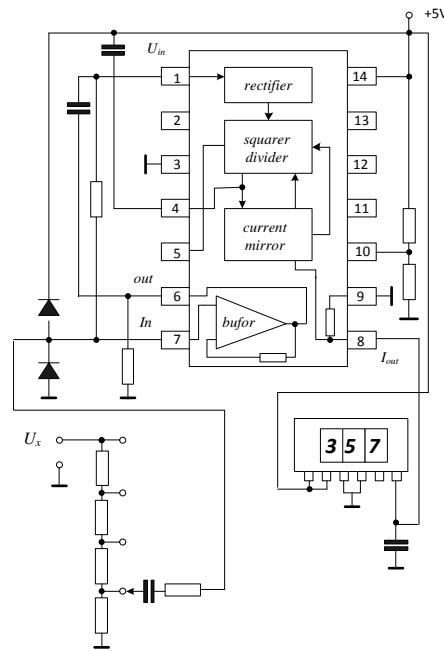


FIGURE 3.81
The design of the true rms voltmeter design – the proposal of Analog Devices

Fig. 3.81 presents an example of the application of the rms converter – as the true rms voltmeter (proposed by the Analog Devices).

Table 3.4 presents performances of different rms converters. Beside the log/antilog converters Linear Technology designed converters basing on sigma-delta conversion.

² LT1088 is not currently manufactured by LT.

TABLE 3.4
Performances of market available rms converters.

IC	Bandwidth 1% error	Accuracy	CF
AD637	200 kHz/1%	1 mV	10
AD737	33 kHz/1%	0.2 mV	5
AD8436	65 kHz/1%	0.01 mV	10
ADL5502	450 MHz-6GHz	0.25 dB	10
LMH2120	50 MHz-6GHz	0.5 dB	
LTC1966	6 kHz/1%	0.1%	4
LTC1968	500 kHz/1%	0.1%	3
LT1088	300MHz	0.01 Fs	40

Note1: AD – Analog Devices, LT – Linear Technology, LMH – Texas Instruments

Note2 – LT1088 (finished production - only for comparison)

The translinear circuits enable also conversion in high frequency range – up to 6 GHz [Nash *et al* 1999]. As an example we can consider ADL5502 converter designed for microwave power measurements. This circuit converts both – rms value and envelope value and this way the measurement of CF is possible.

Of course the rms value computation is possible by digital signal processing.

3.5d. Phase sensitive detectors

Synchronous detectors (known also as *synchronous detector or phase-sensitive demodulators*) play a very important role in the measurements and instrumentation. It helps in the separation of two signal components – in phase and 90 degrees out of phase, as it was presented in the example earlier. But the main their feature is excellent sensitivity enabling noise rejection and small signal amplification as lock-ion amplifier (next Section)..

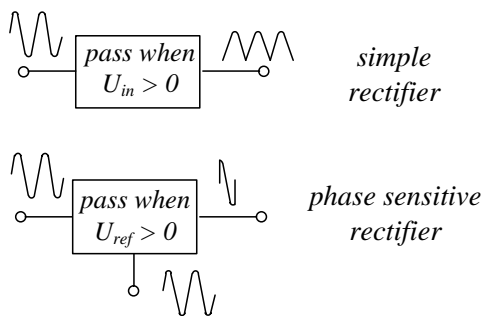


FIGURE 3.82
The difference between simple and phase-sensitive rectifier.

The phase-sensitive rectifier converts the measured voltage U_x with respect to additional reference voltage U_{ref} . Thus, it is equipped at least with two inputs and one output. The reference voltage switches the rectifying elements in such a way that the mean value of the output signal depends on the phase shift between

both input signals. This principle of operation is presented in Figures 3.82 and 3.83.

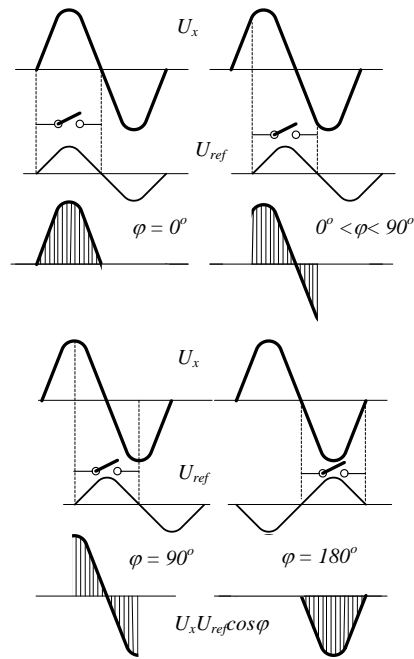


FIGURE 3.83
The principle of the operation of phase-sensitive rectifier.

The phase-sensitive rectifier works according to the following equation

$$U_{out} = U_{ref} U_x \cos \phi \tag{3.115}$$

where $\cos \phi$ is the cosine of the phase shift between U_x and U_{ref} .

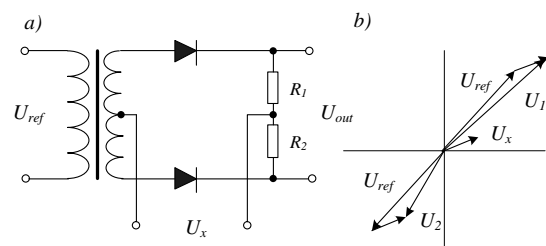


FIGURE 3.84
The simplest diode phase-sensitive rectifier.

A typical diode polarized as conducting and non-conducting element can be used as the switch in phase sensitive rectifier. An example of such a rectifier is presented in Figure 3.84.

In the phase-sensitive rectifier circuit presented in Figure 3.84 the voltage signal U_x is added to the reference voltage U_{ref} in the first half-period of this signal and is subtracted from this voltage in the second half of the period. According to the phasor diagram presented in Figure 3.84b the output signal U_{out} is

$$U_1 = \sqrt{U_{ref}^2 + 2U_{ref}U_x \cos \phi + U_x^2}$$

$$U_2 = \sqrt{U_{ref}^2 - 2U_{ref}U_x \cos \phi + U_x^2} \quad (3.116)$$

and

$$U_{out} = U_1 - U_2 =$$

$$2U_x \cos \phi \left(1 - \frac{U_x^2}{U_{ref}^2} \sin^2 \phi \right) \cong 2U_x \cos \phi \quad (3.117)$$

For correct operation of this rectifier it is required that $U_{ref} > U_x$. The full-wave version of diode phase-sensitive rectifiers is presented in Figure 3.85.

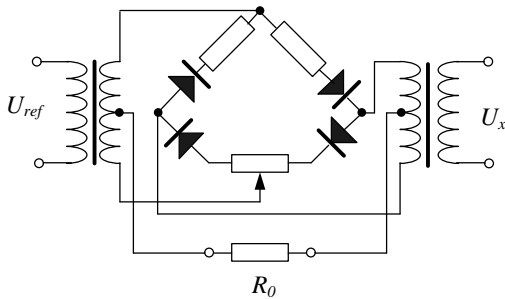


FIGURE 3.85
The full-wave version of diode phase-sensitive rectifiers.

Figure 3.86 present the phase sensitive detector basing on the operational amplifier.

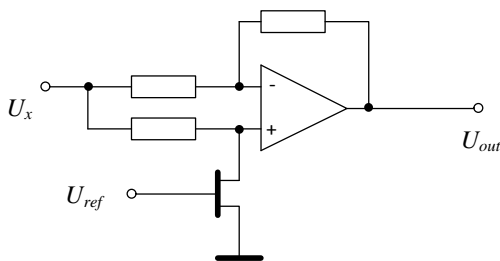


FIGURE 3.86
The phase-sensitive rectifier with the operational amplifier.

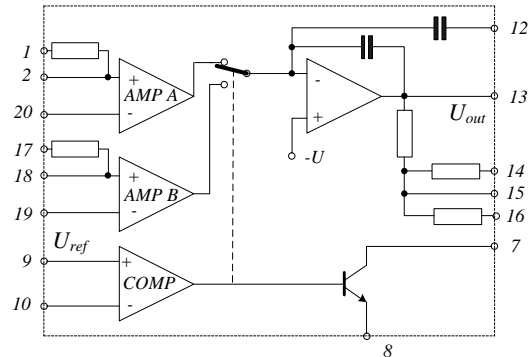


FIGURE 3.87
The functional block diagram of phase-sensitive detector model AD630 of Analog Devices

There are also available ready-to-use monolithic phase-sensitive rectifiers. As an example a functional block of the AD630 circuit developed by the Analog Devices is presented in Figure 3.87. This IC includes two precise input amplifiers and a third amplifier switched by the reference voltage connected to the input 9.

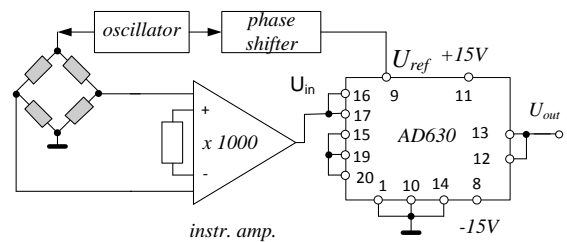


FIGURE 3.88
The application of the phase-sensitive rectifier as the output circuit of the unbalanced type AC bridge

Phase sensitive detectors are commonly used as:

- to reject noises in lock-in amplifiers;
- to separate real and imaginary components, for example in impedance analysis;
- as output device of alternating bridge circuit do improve balancing and detect the direction of the change of impedance.

The lock-in amplifiers are described in the next Section. Figure 3.88 present the application of AD630 circuit to alternating bridge. By using the synchronous detector we are able to detect increasing or decreasing of the tested impedance – for example direction of movement of LVDT sensor (Figure 3.59) or strain gauge sensor (Figure 3.53). Figure 3.89 presents the application of synchronous detector to impedance analysis.

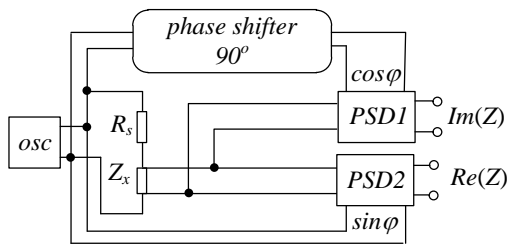


FIGURE 3.89
The application of the phase-sensitive rectifier to the impedance analysis.

By using of the synchronous detector in lock-in amplifiers we are able to measure small alternating voltages even in the nV range. In measurement small resistance (Figure 3.90b) or small change of resistance (Figure 3.90a) the output signal is very small. By supplyin the measuring circuit by alternating voltage and using this voltage as reference we are able to measure this very small signal. Figure 3.90b presents the application of phase sensitive detector to measure of $\mu\Omega$ resistors.

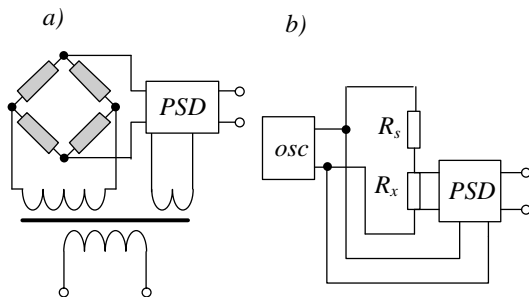


FIGURE 3.90
The application of the phase-sensitive rectifier to measure of small changes of resistance or small resistances.

3.6 The measuring amplifiers

3.6.1. Operational amplifiers

The amplifiers are generally used for the amplification of the voltage signal. However, the amplification process enables also improvement of the signal quality – mostly the signal-to-noise ratio. A good amplifier should exhibit sufficiently large and steady amplification factor (gain) $K_u = U_{out}/U_{in}$, large input resistance and small output resistance.

It is also required to perform the amplification without the distortion. The amplifier can process the signal with *frequency distortion* caused by the unequal gain of all frequencies comprising the signal. To obtain small linear distortion the bandwidth of frequency

should be sufficient. Also the gain K_u should be the same for all frequencies in the bandwidth. There is also *amplitude distortion* caused by non-linear transfer characteristics and introduction to the signal additional harmonics. The non-linear distortion appears when the input signal is large. Therefore it is recommended to limit input signal of the amplifier by applying the negative feedback. If the change of the phase with frequency in not linear also the *phase distortion* can decrease of output signal quality.

Usually, it is assumed that the *frequency bandwidth* is the frequency range for which the K_u factor does not roll off more than $3dB$. And another important factor – the *dynamics of the amplifier* (ratio between the smallest detectable signal and the largest – limited by the supply voltage signal). Dynamics (the smallest signal) depends mostly on the level of noises and zero drifts.

The real revolution in the amplification technique was the development of the integrated operational amplifiers, and later the instrumentation amplifiers. No wonder that operational amplifier is one of the most frequently described electronic circuits (Coughlin 2000, Franco 2001, Jung 2004, Mancini 2002, Stanley 2001, Zumbahlen 2008).

The operational amplifier (*OpAmp*) is a special kind of the integrated amplifier with the following performances: very large amplification factor – larger than 10^5 , very large input resistance and small output resistance. Additionally, small temperature errors coefficient, small level of noises, small zero drifts and large *CMR* (*common mode rejection*) factor are required.

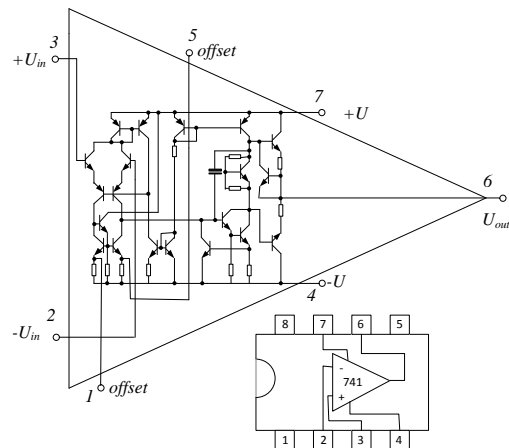


FIGURE 3.91
An example of the design of the operational amplifier – historical amplifier 741.

Figure 3.91 presents the typical design of the operational amplifier. The operational amplifier practically does not work intrinsically – with such large amplification it would be immediately saturated. Therefore the operational amplifier works always with suitable feedback. We can say that the operational amplifier is some kind of semi-finished product designed for the construction of various electronic circuits. By connecting an appropriate feedback circuit we can obtain the required device: multiplier, adder, integrator, generator, filter and of course amplifier.

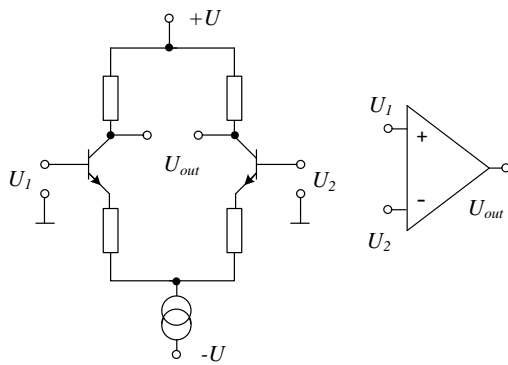


FIGURE 3.92 The differential amplifier and its symbolic representation.

Modern operational amplifiers can be quite complex but in all the main input part constitutes the differential amplifier (Figure 3.92). The important advantage of such an amplifier is the possibility of suppression of the parasitic signals. The input signal is processed as the difference of two inputs signals

$$U_{out} = K_u(U_1 - U_2) \quad (3.118)$$

The parasitic interference signals ΔU are the same on both inputs. Therefore the output signal is

$$U_{out} = K_u[(U_1 + \Delta U) - (U_2 + \Delta U)] = K_u(U_1 - U_2) \quad (3.119)$$

Thus it is possible to amplify the voltage difference with the large common signal ΔU in the background.

The possibility of the rejection of the common parasitic component is described by the coefficient $CMRR$ – *Common Mode Rejection Ratio* defined as

$$CMRR = \frac{K^-}{K^+} \quad (3.120)$$

where K^- is the amplification of the voltage difference and K^+ is the amplification of the common signal. In

use is also the parameter CMR – *Common Mode Rejection* defined as

$$CMR = 20 \log CMRR \quad (3.121)$$

Taking into account this parameter the output voltage is

$$U_{out} = (U_1 - U_2)K^- \left[1 + \frac{1}{CMRR} \frac{\Delta U}{(U_1 - U_2)} \right] \quad (3.122)$$

The second component in the square brackets of the equation (3.122) describes the error caused by the presence of the common component.

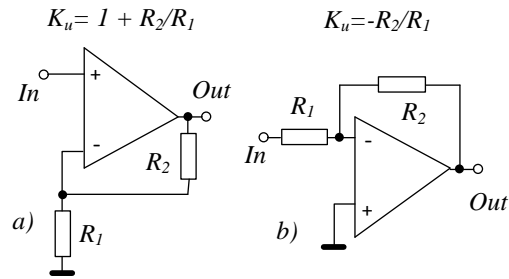


FIGURE 3.93 Non-inverting (a) and inverting (b) configuration of the amplifier.

The main idea of operational amplifiers consists in application of feedback. If gain of the amplifier is high the performances of the amplifier with feedback depends only on the feedback loop. Thus by design different feedback we can obtain amplifier with desired performances. Figure 3.93 presents the two main configurations of the amplifier. By joining both these configuration we obtain the differential amplifier - as it is presented in Figure 3.94.

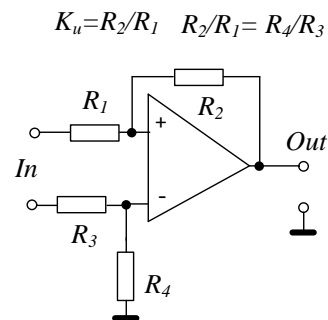


FIGURE 3.94 Configuration of differential amplifier.

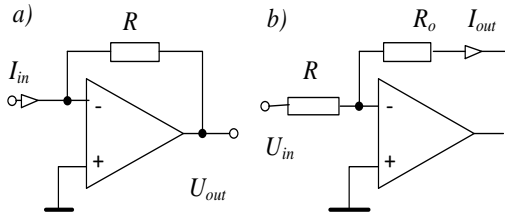


FIGURE 3.95
Converters: current-voltage (a) and voltage-current (b).

The application of appropriate feedback enables to design various performances of the amplifier. Figure 3.95 presents examples of two main transducers: *current to voltage* converter (high resistance input/low resistance output) and *voltage to current* converter (low resistance input/high resistance output).

In the current to voltage converter (Figure 3.95a) the output signal U_{out} is proportional to the input current according to the following equation

$$U_{out} = -RI_{in} \tag{3.123}$$

while in the voltage-to-current converter (Figure 3.95b) the output current is:

$$I_{out} = \frac{U_{in}}{R} \tag{3.124}$$

The conversion factor depends on the value of resistance R , which we can set very precisely.

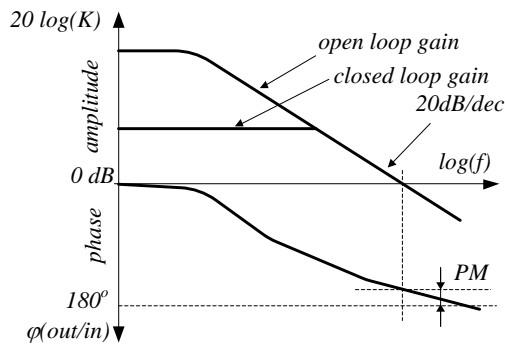


FIGURE 3.96
Bode plot of typical opamp.

The frequency bandwidth of the operational amplifier depends on the gain – it decreases as the gain is increasing. The relationship between gain and bandwidth often is presented as the Bode plot – dependence of logarithm of gain versus logarithm of

frequency. Figure 3.96 present typical Bode plot of operational amplifier. The gain usually is presented in decibels³ – most often the fall-off (the slope) of the gain versus frequency is 20 dB/dec starting from certain cutoff frequency (Figure 3.96). Because product of gain and bandwidth is constant often this product is presented as GBW factor.

From Bode plot presented in Figure 3.96 results that we can increase the gain at the cost of the frequency bandwidth - the largest is for $K = 1$). From the Bode plot we can also consider the problem of stability. Indeed if the gain K of the closed loop is:

$$K = \frac{K_u}{1 + \beta K_u} \tag{3.126}$$

(where K_u is the gain of open loop and the β is feedback coefficient) it is possible that the denominator can be equal to zero and the whole circuit is then unstable.

It is unacceptable if the phase shift is larger than 180° for the gain larger than 1 because it means that the negative feedback is changed to positive. Therefore usually it is determined the phase margin PM (Figure 3.96) as the margin to unstable state.

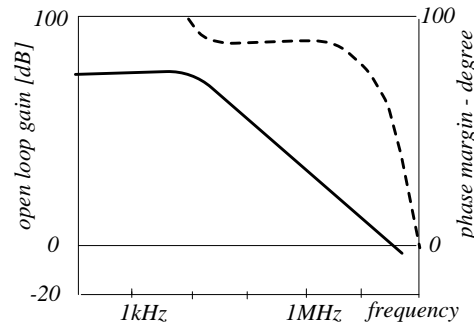


FIGURE 3.97
Bode plot of AD847 opamp.

³ Decibel dB is logarithmic unit of ratio of power P or voltage U:

$$dB = 10 \log \frac{P_2}{P_1} = 20 \log \frac{U_2}{U_1} \tag{3.125}$$

dB	P_2/P_1	U_2/U_1
-40	0.0001	0.01
-20	0.01	0.1
-3	0.5	0.707
0	1	1
1	0	0
20	100	10
40	10 000	100
100	10 000 000 000	100 000

Fortunately as it is presented in Figure 3.97 the opamps producers design such devices with sufficient phase margin. But in certain work conditions, for example capacity load this margin can be at risk of the loss of stability. In such case appropriate compensating element should be connected to the circuit.

There are many factors influencing the quality of signal conversion by the opamp circuit, as noises, offset, zero drift, bandwidth etc. It is not possible to design the circuit with the best of all these factors - therefore available are specialized amplifiers, as for example: low noise, low zero drift, high speed or energy saving amplifiers.

The datasheets usually described many various properties of the amplifier, as: open loop gain, offset voltage, offset voltage drift, noise level, 1/f noise, input bias current, input offset current, total harmonic distortion, input resistance, output resistance, 0.1 dB bandwidth or GBW, slew rate, settling time, overshoot of pulse response, phase margin, CMR ratio, supply voltage, quiescent current, power consumption. Almost all these parameters depend on temperature and frequency - therefore often they are presented in form of a graph. Table 3.5 presents the main parameters of three popular operational amplifiers and Table 3.6 presents the best performances of AD opamps.

TABLE 3.5
Main parameters of typical opamps.

	LM358	TL071	LM833
GBW	0.7 MHz	3 MHz	16 MHz
Slew rate	0.3 V/ μ s	13 V/ μ s	7 V/ μ s
Bias current	250 nA	200 pA	700 nA
Offset	7 mV	10 mV	2 mV
Offset drift	7 μ V/ $^{\circ}$ C	18 μ V/ $^{\circ}$ C	2 μ V/ $^{\circ}$ C
Noise 1 kHz	40 nV/rtHz	18 nV/rtHz	5 nV/rtHz
CMRmin	65dB	70 dB	80 dB

TABLE 3.6
The best performances of opamps.

	AD549 Low bias I	AD8630 Low drift	AD797 Low noise
Bandwidth	1 MHz	2.5 MHz	8 MHz
Slew rate	3 V/ μ s	1 V/ μ s	20 V/ μ s
Bias current	0.04 pA	30 pA	250 nA
Offset	0.3 mV	1 μV	25 μ V
Offset drift	5 μ V/ $^{\circ}$ C	2 nV/$^{\circ}$C	0.2 μ V/ $^{\circ}$ C
Noise 1 kHz	35 nV/rtHz	22 nV/rtHz	0.9 nV/rtHz
Noise < 10Hz	4 μ Vpp	0.5 μ Vpp	0.05 μVpp

The small bias current is especially important when the source of signal exhibits large impedance (electrometer mode) - for example the piezoelectric sensor, photodiode or pH electrode. Usually in low bias current opamps in the input circuit the FET transistors are used. It is possible to obtain the bias current as small as 40 fT what correspond with input impedance as large as $10^{15} \Omega$.

The offset voltage is not a great problem because we are able to compensate it - internally or by external resistors. But danger is offset temperature drift because we are not able to separate it from the input signal with DC component - as in the case of infrared sensors, strain gauge or thermocouple sensors. Recently the best method to decrease this drift to the level of 20 nV/ 10° C is auto-zero principle joined with chopper technique. But due to improvement of technology it is possible to obtain similar small temperature drift without auto-zero what is important because auto-zero operation limits the frequency bandwidth.

The noises level is especially important if we are interested in large dynamics and low distortion. For example presented in table 3.6 low noise amplifier AD797 enables to obtain the total harmonic distortion THD⁴ as high as 130 dB. We separately consider the noise density in nV/rtHz and low frequency 1/f noise in the frequency range 01 - 10 Hz as peak-to-peak voltage.

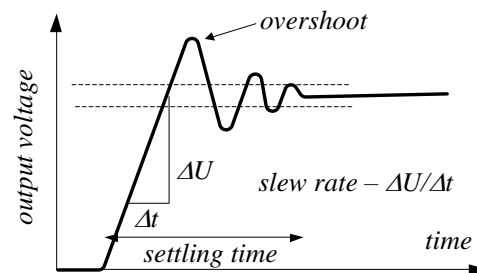


FIGURE 3.98
Answer to step change of the input signal.

The speed of the amplifier can be evaluated by testing the answer to the step change of the input signal - as it is presented in Figure 3.98. Modern high speed amplifiers have by 2 GHz bandwidth the slew rate as high as 10 kV/ μ s and settling time less than 2 ns.

3.6.2. Instrumentation amplifiers

The operational amplifier should exhibit large gain but it is not absolutely indispensable to have steady and precise value of this factor - it depends on the feedback elements. For accurate signal processing it is reasonable to use special kind of IC amplifier, known as *the instrumentation amplifier*. Such amplifier is designed for measurement purposes, with precise laser trimmed resistors.

⁴ The THD is usually calculated as ratio of rms value of the first nine harmonics to rms value of total voltage.

The instrumentation amplifier is not a special kind of operational amplifier. Operational amplifier is used as a basis of various devices: amplifiers, filters, oscillators etc. The instrumentation amplifier is almost exclusively designed for amplification. It should exhibit following feature: differential input with large input resistance $> 10^9 \Omega$ and large CMR enabling to process of small signal in presence of large common voltage; small error or nonlinearity, small error of gain, small noises and temperature zero drift. Table 3.7 presents performances of two typical instrumentation amplifiers.

TABLE 3.7
Main parameters of instrumentation amplifiers.

	AD620 G = 1	AD620 G = 100	AD8228 G = 100
Bandwidth	1 MHz	120 kHz	110 kHz
Offset drift	0.1 $\mu\text{V}/^\circ\text{C}$	0.1 $\mu\text{V}/^\circ\text{C}$	0.5 $\mu\text{V}/^\circ\text{C}$
Bias current	0.5 nA	0.5 nA	0.4 nA
Gain error	0.01%	0.15%	0.05%
Gain(T)	10 ppm/ $^\circ\text{C}$	10 ppm/ $^\circ\text{C}$	1 ppm/ $^\circ\text{C}$
Noise 1 kHz	9 nV/rtHz	9 nV/rtHz	8 nV/rtHz
Noise 1/f	3 μVpp	0.3 μVpp	0.3 μVpp
Nonlinearity	10 ppm	10 ppm	5 ppm
CMRR	90 dB	130 dB	120 dB
R_{in}	10 G Ω	10 G Ω	100 G Ω
Slew rate	1.2 V/ μs	1.2 V/ μs	2.5 V/ μs

All parameters influence the accuracy in different way. Table 3.8 presents the error budget analysis of general purpose IA given by a manufacturer Analog Devices.

TABLE 3.8
Error budget of AD 620 IA for input values $R_s = 350 \Omega$, $U_{in} = 100$ mV, ,gain 100, temp.; 25 $^\circ\text{C}$ [after MT-066]

		Error [ppm]
Offset U_{os}	55 μV	550
Offset I_{os}	350 $\Omega \times 0.5$ nA	1.8
Gain error	0.15%	1500
Nonlinearity	40 ppm	40
CMRR error	120 dB, 1 ppm $\times 5$ V	50
1/f noise	280 nV	2.8
Total unadjusted error		2145
Resolution		42.8

Because gain, CMR error can be decreased by calibration the remaining errors are considered as resolution. The dominating error is caused by gain error – unfortunately this error increases with gain and for the same IA and gain $G = 1000$ it is 0.35%. Presented in the table error 0.05% for $G = 100$ is the smallest available.

Similarly as in the opamps case there are available variety different amplifiers of specialized performances. Table 3.9 presents the data for very small zero drift (auto-zero function) and very small bias current (FET input).

TABLE 3.9
The best parameters of instrumentation amplifiers.

	AD8429 G = 100	AD8230 G = 100	AD8220 G = 100
Bandwidth	1.2 MHz	2 kHz	120 kHz
Offset drift	0.1 $\mu\text{V}/^\circ\text{C}$	50 nV/$^\circ\text{C}$	5 $\mu\text{V}/^\circ\text{C}$
Bias current	150 nA	0.15 nA	10 pA
Gain error	0.3%	0.01%	0.2%
Gain(T)	5 ppm/ $^\circ\text{C}$	14 ppm/ $^\circ\text{C}$	3 ppm/ $^\circ\text{C}$
Noise 1 kHz	1 nV/rtHz	240 nV/rtHz	14 nV/rtHz
Noise 1/f	0.1 μVpp	3 μVpp	0.8 μVpp
Nonlinearity	2 ppm	20 ppm	30 ppm
CMRR	90 dB	120 dB	100 dB
R_{in}	1.5 G Ω		10 ⁴ G Ω
Slew rate	22 V/ μs	2 V/ μs	2 V/ μs

The differential amplifier presented in Figure 3.94 requires very precise selection of the resistors. Even small changes or differences significantly deteriorate the CMR ratio. Also if the resistance of the source is not fully symmetrical (what can be for example in case of bridge circuit) the CMR ratio is also decreased. Therefore for professional applications the differential amplifier is constructed from two or three amplifiers [Zumbahlen 2008, Kitchn and Counts 2006], as it is presented in Figures 3.99 and 3.100.

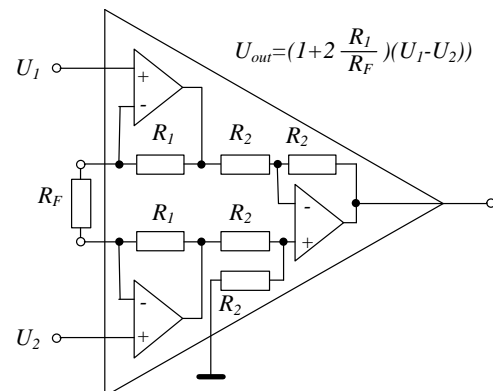


FIGURE 3.99
Configuration of typical instrumentation amplifier.

In the amplifier presented in Figure 3.99 only one external resistor is used to adjust the gain. Such solution is recently often substituted by internal, precise laser trimmed resistor adjusted by pin-strap. The external resistor can have other properties than the rest of internal resistors what can cause additional gain error. Available are also amplifiers with fixed one/two gains. The best solution is to use programmable gain amplifiers PGA [Zumbahlen 2008, Kitchn and Counts 2006].

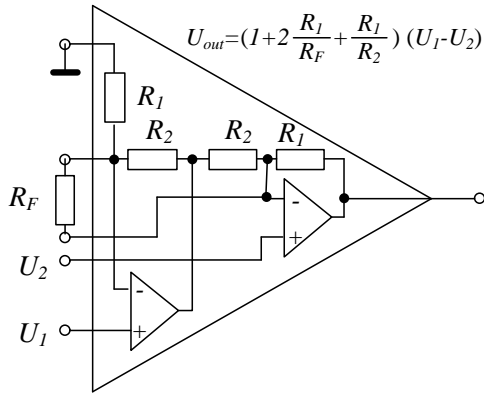


FIGURE 3.100
Two opamps version of differential amplifier.

Sometimes it is necessary to have differential output – for example to connect it to AS device. Figure 3.101 presents an example of the full input/output differential amplifier.

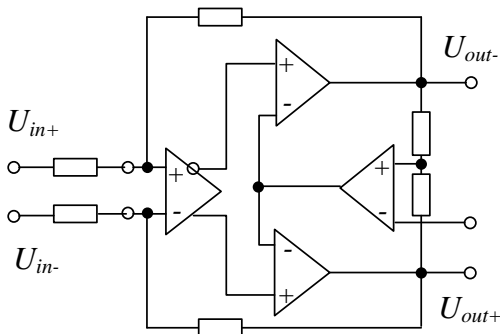


FIGURE 3.101
Full input/output differential amplifier [Zumbahlen 2008].

On the market there are many various specialized instrumentation amplifiers ready to use as measuring devices, as for example strain gauge bridge, thermocouple temperature meter, shunt current measurement etc. They are often equipped with useful tools as for example EMI filters. Figure 3.102 present the CMOS instrumentation amplifier AD8290 designed to cooperation with sensors and bridge circuit. It is equipped with precise excitation current source to supply the bridge circuit or RTD temperature sensor. It has fixed gain $G = 50$ with gain error 0.5%, gain nonlinearity 0.0075%, low noise level and low temperature drift and high CMRR coefficient.

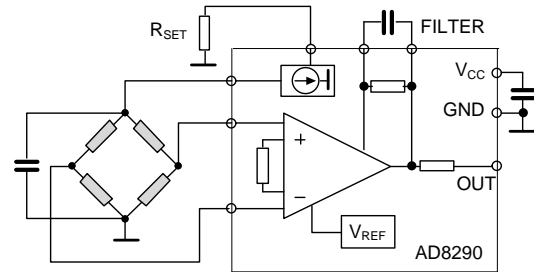


FIGURE 3.102
Instrumentation amplifier designed to bridge circuit.

Figure 3.103 present other instrumentation amplifier designed to cooperation with shunt resistor – for current measurement. Due to high CMRR coefficient it is enable to measure small shunt voltage drop in presence of high up to 80 V voltage. The amplifier works in temperature range $-40 - +125^{\circ}\text{C}$ with fixed gain $G = 20$, small offset drift $0.1 \mu\text{V}/^{\circ}\text{C}$ and $5 \text{ ppm}/^{\circ}\text{C}$ gain drift. The circuit is protected before overvoltage by the internal low dropout regulator LDO.

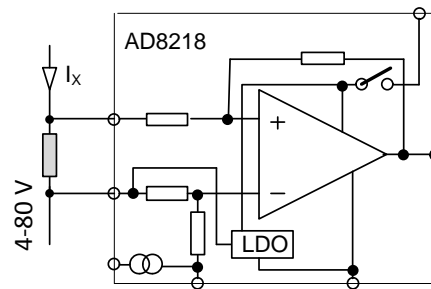


FIGURE 3.103
Instrumentation amplifier designed to shunt current measurement.

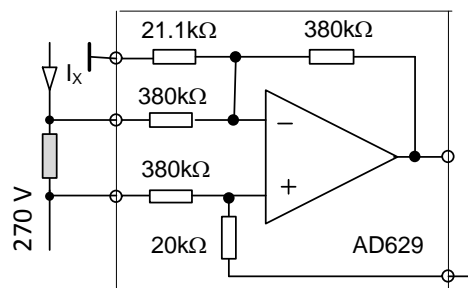


FIGURE 3.104
Instrumentation amplifier designed to shunt current measurement in presence of high voltage.

Often the shunt voltage is measured in presence of much higher common voltage. In such case solution is to use separating transformer but it introduces additional errors. Other solution is to use more expensive insulating amplifiers – described in next Section. Relative simple solution is to use voltage dividers. Figure 3.104 presents the instrumental amplifier known as difference or subtraction amplifiers with high CMR ration. The internal voltage dividers enable to measure the shunt voltage drops in presence the common voltage as high as ± 270 V – with protection to 500 V.

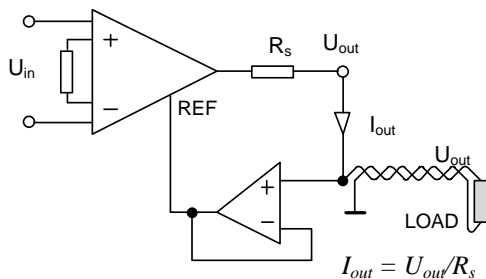


FIGURE 3.105
Instrumentation amplifier with current output.

In industrial practice the output signal can be transmitted and in this case the current output is preferred (as eliminating the increase of resistance change of transmission wires). In the market there are special instrumentation amplifiers known as 4-20 mA drivers (or current out drivers). Figure 3.105 presents simple method to obtain current output in typical instrumental amplifier PGA [Zumbahlen 2008, Kitchn and Counts 2006].

3.6.3. Isolation amplifiers

There are circumstances, when it is necessary to ensure the galvanic separation of the input and output circuit. For example, when we measure very small differential signal superimposed on large common signal. Such a case is presented in Figure 3.106 where the relatively low voltage (with the level of tens *mV*) across the shunt resistor R_b is measured in the presence of relatively high voltage (several hundred *V*), which is used for supplying the load R_o . Between the ground of the indicating instrument connected to the amplifier and the ground of the supply source there could be a voltage difference dangerous for the servicing personnel (and also the amplifier could be damaged due to this large potential difference).

Also dangerous is the situation when the input circuit is distant from the rest of the circuit and even more

when these both parts are supplied from different sources. The difference between the ground potential of both circuits can be as large as hundreds of volts. Without galvanic separation such difference can cause destruction of the amplifier (and of course could be dangerous to the servicing personnel). Therefore in medical equipment it is indispensable to use the isolation amplifiers. Galvanic isolation helps also in rejection of various electromagnetic interferences.

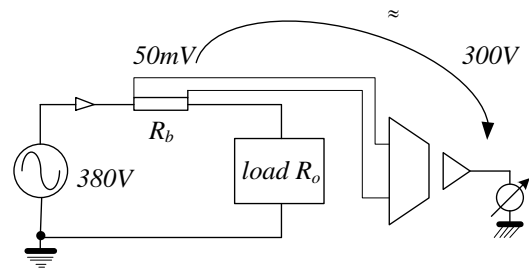


FIGURE 3.106
The application of the isolation amplifier for separation supply source and receiver when the potential difference of grounding can be large.

In the isolation amplifier the connection between input terminals and output terminals does not exist (and the same applies for input ground and output ground). Sometimes, also the supply sources are physically separated. The rejection of the isolation voltage U_{IM} (voltage between common parts of input and output circuits) is described by *IMRR* – *Isolation Mode Rejection Ratio*

$$U_{out} = K_u \left(U_{in} + \frac{\Delta U}{CMRR} \right) + \frac{U_{IM}}{IMRR} \quad (3.127)$$

There are different tools of galvanic separation – the use of transformer, capacitor, light or magnetic field. In all these methods relatively easy is to separate AC signals – but from isolation amplifiers is required to separate both AC and DC components.

It is convenient to use a small transformer as the isolation device. Because transformer does not transform *DC* signals it is needed to use the modulator (signal is transformed as the magnitude varying carrier *AC* signal) and next the demodulator to recover again the *DC* signal. Such idea is realized in the isolation amplifiers of Analog Devices (Figure 3.107). In the AD215 model presented in Figure 3.107 (two-port isolator) the power section is not isolated from the output. In other model AD215 (three port isolator) both input and output are isolated form power section by additional transformer.

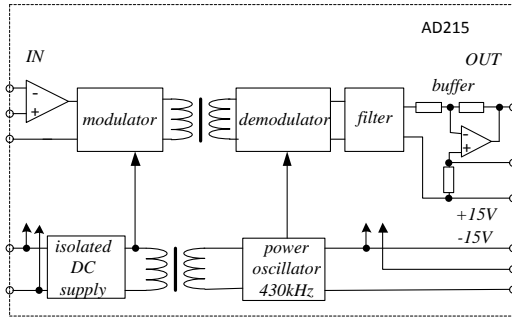


FIGURE 3.107
Isolation amplifier with transformer separation – model AD215 of Analog Devices.

Presented in Figure 3.107 isolation amplifier provides 1500 V common mode voltage protection. With fixed gain $G = 1$ it converts voltages in bandwidth 120 kHz with low nonlinearity error 0.005% and low harmonic distortion 80 dB by 1 kHz.

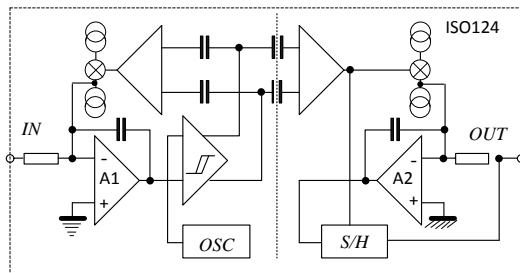


FIGURE 3.108
Isolation amplifier with capacitor separation – model ISO124 of Texas Instruments.

Another principle of galvanic separation is applied in the isolation amplifier of *Texas Instruments* – for example in model *ISO124* presented in Figure 3.108. In this case a capacitor with capacitance 2 pF is used as the isolation device. The input signal is converted to AC signal using integrating analogue to digital circuit A1. Next, this signal transmitted by the capacitance is again converted to the DC signal using integrating amplifier A2. Additional sample-and-hold circuit is used to obtain the output signal without the ripple voltage inherent the demodulation process.

Presented isolation amplifier enables conversion of the voltage with gain fixed to $G = 1$ in the presence of the common mode voltage 1500 V (IMR coefficient is equal to 140 dB). The nonlinearity error is better than 0.01%, zero drift better than $200\text{ }\mu\text{V}/^\circ\text{C}$ and frequency bandwidth is 50 kHz.

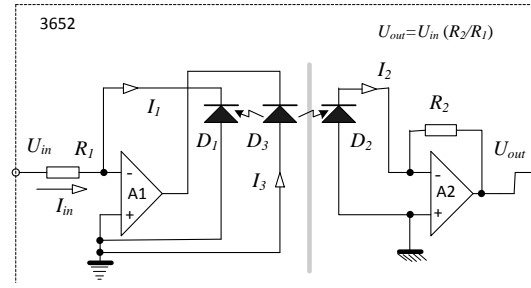


FIGURE 3.109
Isolation amplifier with light separation – model 3652 of Burr-Brown.

The light separation could be an excellent tool for isolation amplifiers. Unfortunately the conversion is with large nonlinearity error. Therefore two strategies are used: one with feedback to eliminate this nonlinearity, the second with conversion to digital form where influence of nonlinearity is negligible.

The first principle is utilized in the isolation amplifier developed by Burr-Brown – model 3652 (Figure 3.109). The LED diode D3 illuminates two identical photodiodes D2 in the output circuit (converter current/voltage) and D1 in the input circuit (converter voltage/current). The diode D1 is in feedback circuit, which enables to minimize the nonlinearity errors. Since both diodes are illuminated identically therefore $I_1 = I_2 = I_{in}$.

Similar principle isolation amplifiers with two infrared phototransistors developed Clare Inc. Company. The LOC110 linear optocoupler enables to convert voltage with nonlinearity error less than 0.01%, THD 87dB and bandwidth 200 kHz.

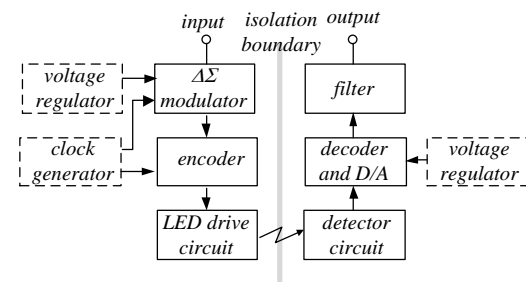


FIGURE 3.110
Isolation amplifier with light separation – model HCPL-7850 of Avago Technologies.

Figure 3.110 presents the isolation amplifier based on the second principle. The input signal is converted to digital form by sigma-delta converter. Next digital signal is transmitted by the optocoupler and the analog signal is used by applying digital-to-analog converter.

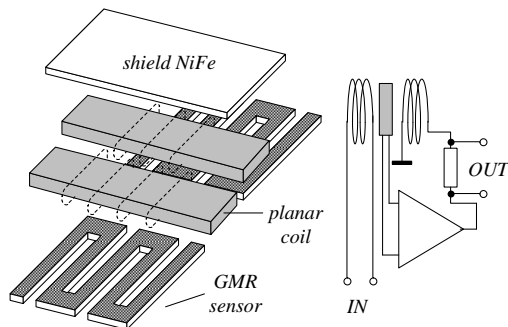


FIGURE 3.111 Isolation amplifier with magnetic separation – model developed by Nonvolatile Electronics Inc.

Figure 3.111 presents the magnetic galvanic separation IC device developed by Nonvolatile Electronics Inc. The main advantage of magnetic separation is that it correctly converts both DC and AC signals (transformer and capacitor convert only AC signals). The current in the planar coil generates the magnetic field detected by the *GMR* (giant magnetoresistance) sensor. Signal of the sensor is the source of the current generating the balancing feedback magnetic field. The *GMR* sensor only detects the presence of magnetic field and thus its nonlinearity does not influence the linearity of the device. This device can operate in analog or in digital mode with transmission speed even above 1 GB/s .

3.6.4. Amplifiers of very small signals

From the data presented in Table 3.7 we see that the resolution of general purpose AD620 instrumentation amplifier is limited by following factors:

- voltage input noise: $U_{Ni} = 10\text{ nV/rtHz}$,
- voltage output noise: $U_{no} = 70\text{ nV/rtHz}$
- $G = 100$ $1/f$ voltage noise: $0.3\text{ }\mu\text{V}$,
- current input noise: $I_{Ni} = 1\text{ nA/rtHz}$,
- $1/f$ current input noise: 10 pA ,
- offset drift of about $\Delta U = 1\text{ }\mu\text{V}/10^\circ\text{C}$.

Thus in the case of AC+DC small signals the temperature zero drift and $1/f$ noise are predominating and in this case the resolution is on the level of μV . In the case of only AC signals it is possible to eliminate the influence of zero drift and only noises influence the resolution. In this case the resolution is on the level of tens of nV .

The total noise when the input source has Resistance R_s is:

$$U_N = \sqrt{(U_{Ni})^2 + (U_{No}/G)^2 + (R_s I_{Ni})^2} \quad (3.128)$$

To this noise budget also noise generated by the circuit resistors should be added. For resistor R this noise in temperature T for the bandwidth B is:

$$U_R = \sqrt{4kTBR} \quad (3.129)$$

where k is the Boltzmann constant $K = 1.38 \cdot 10^{-23}\text{ J/K}$.

At room temperature this noise approximately is $4\text{ nV}/\sqrt{\text{Hz}} \times \sqrt{R}$ where R is in $\text{k}\Omega$. Figure 3.112 presents the noise of one of the best low noise amplifiers on the market.

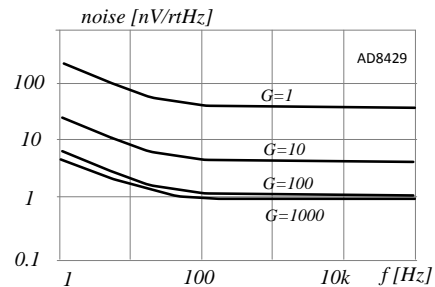


FIGURE 3.112 Voltage noise of low-noise instrumentation amplifier AD8429.

The noise consists of unlimited number of signals with various frequencies distributed randomly (white noise) and sometimes the noise itself is larger than the useful input signal. If we know the frequency of this input signal we can separate this signal from noises using a selective amplifier or filter. The use of the selective amplifiers (tuned to certain known frequency) is limited because it is difficult to ensure stable amplification. Small deviation from the resonance frequency causes large variation of the amplification. For that reason recently the best tool for the amplification of small AC signals is the *lock-in amplifiers* (Scofield 1994, Blair and Sydenham 1975).

In the lock-in amplifiers a phase sensitive detector is used as the selective element. This detector selects from the input signal only these components that have the same frequency as the reference voltage. When the ordinary selective amplifier exhibits the Q factor of about 50 - 100, the lock-in amplifier can exhibit this factor as large as 100 000 (it is possible to select the signals of 10 kHz in the frequency bandwidth 0.01 Hz). In this way it is possible to select from the noises signals of the level below nV .

The synchronous detector can be realized as special device (as presented in Section 3.5.d) but the same effect we can obtain using simply a multiplier.

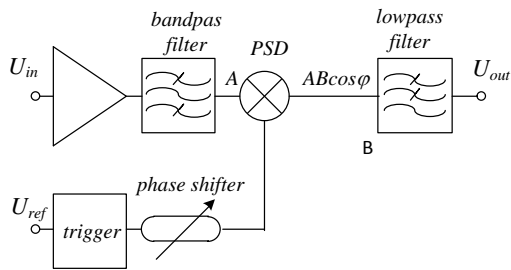


FIGURE 3.113
The operation principle of the lock-in amplifier.

Figure 3.113 presents the operation principle of the lock-in amplifier. After preliminary amplification the input signal is connected to the synchronous detector, where it is rectified with respect to the frequency and phase of the reference signal. Next, this signal is filtered by low-pass filter.

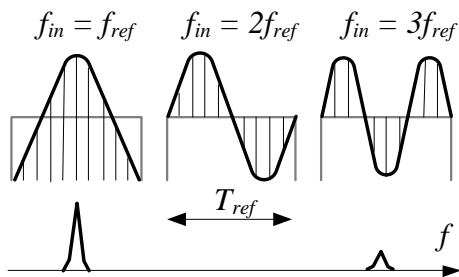


FIGURE 3.114
The signal in the “window” of period of rectangular reference signal.

In Figure 3.14 is presented the frequency effect of synchronous rectifying. If input signal has the same frequency as the reference signal its value is the largest. For second harmonics (1 octave) this signal is zero. For comparison the first order RC filter decreases the signal by 6dB/octave). This selectivity effect is amplified by the phase relations because as it is presented in Figure 3.83 the “in phase” signal is the largest but for the phase shift by 90° the signal is zero. It is assumed that by using the lock-in amplifier it is possible to recover signal buried in 60 dB larger noises.

The making impression results of experiment are presented in Figure 3.115. As synchronous rectifier was used monolithic circuit AD630 of Analog Devices. To the signal was added the noise larger of 100 dB. It was possible to recover the measured signal in presence of noises 100 000 times greater.

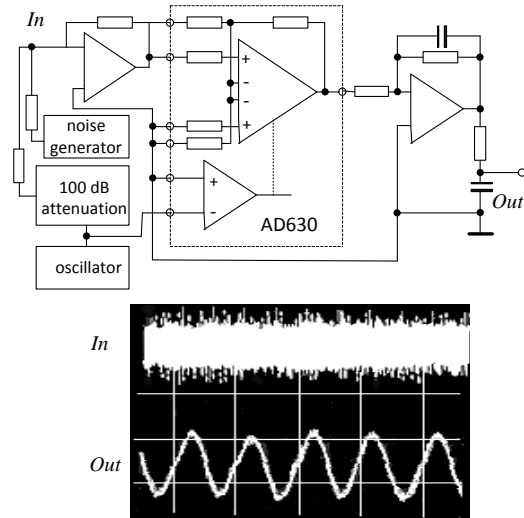


FIGURE 3.115
An example of the lock-in amplifier based on the AD630 device of Analog Devices. Output signal when to the sinusoidal input signal are added noises 100 dB larger. (From Data Sheet of AD630).

In applying of lock-in amplifier it is necessary to have the reference signal. Often this signal is in natural case available in all carrier amplifiers where the high frequency signal is modulated by low frequency small signal. The carrier signal can be used as the reference signal.

The amplitude modulation is realized by multiplying high and low frequency signals:

$$U_{mod} = U_{in} \sin \omega t \cdot U_{ref} \sin \Omega t = U_{in} U_{ref} [\cos(\Omega - \omega) t + \cos(\Omega + \omega) t] \quad (3.130)$$

Such multiplication is realized by every bridge circuit as it is presented in the example of strain gauge bridge (Section 3.4.c) or in the Figure 3.90 because:

$$U_{out} = U_o \sin \Omega t \cdot \frac{\Delta R}{R} \sin \omega t \quad (3.131)$$

Sometimes for obtain the modulation effect the multiplier device can be used. Figure 3.116 presents the example when the reference modulated signal is added artificially. Because output signal of DC SQUID device is small and noisy usually the supporting magnetizing winding is added supplied by the oscillator. This additional signal is next modulated by the measured SQUID signal.

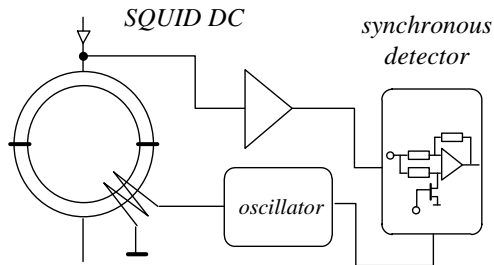


FIGURE 3.116
Application of the lock-in amplifier in DC SQUID magnetometer.

The professional lock-in amplifiers are equipped with internal precise PLL oscillator and it is possible to tune this oscillator to find the main frequency component of amplified signal.

To demodulation of the carrier modulated signal usually the multiplier is used. Indeed according to the relationship (3.115) the phase sensitive rectifier also performs multiplication of two signals.

$$U_{dem} = AU_{in} \sin \omega t \cdot U_{ref} \sin \Omega t \cdot U_{ref} \sin \Omega t = \frac{A}{2} U_{in} U_{ref}^2 [\sin \omega t + \sin(2\Omega - \omega) t + \sin(2\Omega + \omega) t] \quad (3.132)$$

It is relatively easy to remove high 2Ω frequency components by using the low-pass filter and to recover input low frequency signal. To correct carrier modulation it is recommended if $\Omega > 5\omega$. Looking at the Figure 3.112 by using the amplifier near carrier frequency we escape from the large $1/f$ noises band.

Figure 3.117 presents typical functional block diagram of lock-in amplifier. Usually two multipliers are used as synchronous detectors for two components of measured signal: in-phase and orthogonal one. For measurement of orthogonal component the 90° phase shifter is used. Lock-in amplifiers often are equipped with internal oscillator to use in the case when reference signal is not available.

Typical lock-in amplifier, for example model 850 of Stanford Research System has following parameters: sensitivity: 2 nV – 1 V; input noise: 6 nV/rtHz for 1 kHz, gain accuracy 1 %, frequency bandwidth 1 mHz – 100 kHz, phase resolution 0.001°, dynamics 100 dB, demodulator time constant 10 μ s – 30 ks.

The analogue lock-in amplifier exhibits several drawbacks: it is necessary to use an analog low-pass filters, the dynamics is rather poor, and the bandwidth is limited. Therefore, recently on the market are available digital lock-in amplifiers. In such device both

signals (measured and reference) are converted to the digital signals and as synchronous detection the digital multiplication is used.

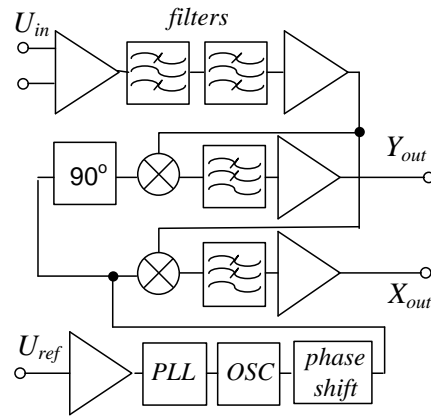


FIGURE 3.117
Functional block diagram of typical lock-in amplifier.

The main problem in the amplification of small DC signals is the temperature zero drift of the amplifier, because it is very difficult to separate this zero drift signal and the useful DC signal. The temperature zero drift is caused by non-ideal technology – even small differences in various parts of the circuit can be the source of DC offset signal. This effect is minimized by laser trimming to the level of $1 - 50 \mu\text{V}/^\circ\text{C}$, but even such small offset is still limiting the amplification of small DC signals.

To decrease the zero drift influence there are two main techniques. The first one is based on the conversion of the DC signal to the AC signal. Then it is possible to separate DC zero drift and AC useful signal. The AC signal can be amplified and converted back to the DC one. This technique is called a *chopper amplifier* - the conversion to the AC signal is achieved by very fast connecting and disconnecting the signal to the input.

The second technique employs the *auto-zero* principle. The amplifier is periodically disconnected from the input, then the input is short-circuited to ground and the zero component is detected. The auto-zero technique enables to eliminate the zero drift down to the level of $5\text{nV}/^\circ\text{C}$.

The principle of operation of the chopper amplifier is illustrated in Figure 3.118. The signal is switched with frequency of up to tens of kHz. To the amplifier are delivered pulses with amplitude modulated by the input signal. After amplification this signal is demodulated by the synchronous switching (or using the phase-sensitive detector).

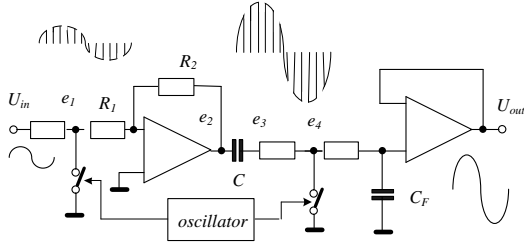


FIGURE 3.118
The principle of operation of the chopper amplifier.

If the input signal is $u_{in}(t)$ and the commutation frequency is ω_o , then the signal at the input of amplifier is

$$e_1 = u_{in}(t) \left(\frac{1}{2} + \frac{2}{\pi} \cos \omega_o t - \frac{2}{3\pi} \cos 3\omega_o t + \frac{2}{5\pi} \cos 5\omega_o t \dots \right) \quad (3.133)$$

If we describe the zero component as U_o and the zero drift as ΔU_o and the analysis is limited to the first harmonics (we can eliminate higher harmonics using the filter at the output) the output voltage of the amplifier is

$$e_2(t) = -\frac{R_2}{R_1} u_{in}(t) \left(\frac{1}{2} + \frac{2}{\pi} \cos \omega_o t \right) + \left(1 + \frac{R_2}{R_1} \right) U_o + \left(1 + \frac{R_2}{R_1} \right) \Delta U_o \quad (3.134)$$

The DC components are blocked by the capacitor C , thus the e_3 signal is

$$e_3(t) = -u_{in}(t) \frac{R_2}{R_1} \left(\frac{2}{\pi} \cos \omega_o t \right) \quad (3.135)$$

After the second commutation the signal is

$$e_4(t) = e_3(t) \left(\frac{1}{2} + \frac{2}{\pi} \cos \omega_o t - \frac{2}{3\pi} \cos 3\omega_o t \dots \right) \quad (3.136)$$

Thus after the filtration we obtain the output signal

$$u_{out}(t) = -u_{in}(t) \frac{R_2}{R_1} \frac{4}{\pi^2} + U_{o2} \quad (3.137)$$

The U_{o2} component is the zero drift of the last amplifier and it is negligible because it is added to the large output signal.

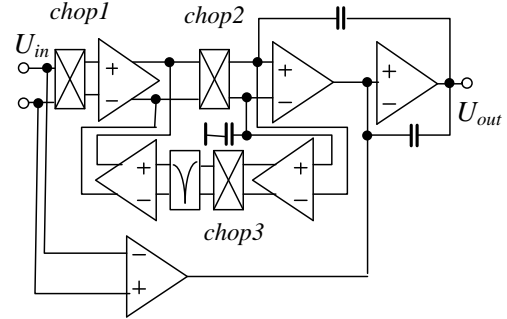


FIGURE 3.119
The chopper amplifier with autocorrection feedback.

The chopper amplifier exhibits several drawbacks: the limitation of frequency bandwidth (it is limited by the frequency of the carrier signal), necessity of the signal filtration. For that reason the chopper technique is often substituted by auto-zero technique. But last time it can be observed renaissance of this technique [Wong 2011, Moghimi 2011]. Analog Devices developed chopper amplifier of next generation - presented in Figure 3.119. This amplifier has high chopping frequency of 200 kHz and special correction feedback loop helping in remove of ripples. As result the amplifier ASA4528 has offset drift 2 nV/°C and noise 5.6 nV/rtHz – the best parameters currently available.

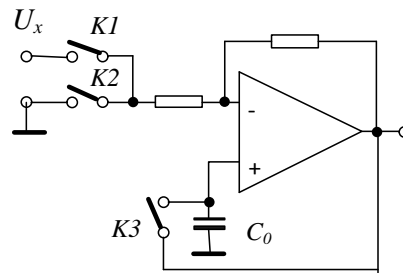


FIGURE 3.120
The principle of operation of the auto-zero amplifier.

The operation principle of auto-zero method is presented in Figure 3.120. The amplifier works in two phases. In the first phase the input is shortened, the amplifier is amplifying its own zero drift voltage and the result is stored in capacitor C_o . In the second phase the input voltage is connected to amplifier and the voltage stored on capacitor is subtracted from input voltage.

The real auto-zero amplifier is more complex to avoid break in the amplifying process and to improve quality of amplifier (Figure 3.121). The amplifier is

now composed of two amplifiers – wideband A and nulling B. These amplifiers have three inputs and work as:

$$U_{out} = A(U_1 - U_2) + \beta U_N \quad (3.138)$$

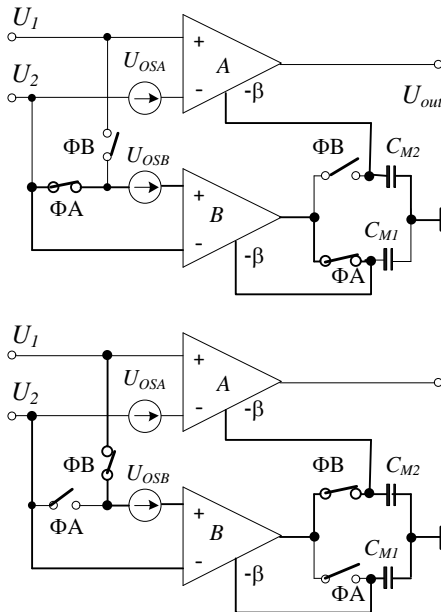


FIGURE 3.121
The principle of operation of the auto-zero amplifier – model AD8551 of Analog Devices.

The real auto-zero amplifier is more complex to avoid break in the amplifying process and to improve quality of amplifier (Figure 3.121). The amplifier is now composed of two amplifiers – wideband A and nulling B. These amplifiers have three inputs and work as:

$$U_{out} = A(U_1 - U_2) + \beta U_N \quad (3.138)$$

Two amplifiers are commuted by switches ΦA and ΦB . When switches ΦA are closed realized is phase A – auto-zero phase. When switches ΦB are closed the second phase is realized – the output phase.

In phase A the amplifier A is connected to input voltage while the amplifier B has shortened input. Thus amplifier B simplifies its own zero voltage U_{OSB} and amplified voltage is stored on capacitor C_{M1} . To the third input of amplifier A is connected voltage previously stored on the capacitor C_{M2} .

In phase B the input voltage is connected to both amplifiers. The output voltage of amplifier B is

connected to third input of amplifier A. To third inputs of both amplifiers are connected voltages stored on capacitors C_{M1} and C_{M2} .

As result of switching between two phases the output voltage is (AD 8551):

$$U_{out} \cong A\beta U_{in} + A(U_{OSA} + U_{OSB}) \quad (3.139)$$

Thus the input voltage is amplified by a factor of $A\beta$, while the zero drifts are amplified by the factor β -times smaller. The resultant zero drift component U_{OS} is

$$U_{OS} = \frac{U_{OSA} + U_{OSB}}{\beta} \quad (3.140)$$

Because β is large the resultant zero component is reduced to the nV level. Thus these two steps of the auto-zero operation significantly reduce the zero drift components without limitation of the frequency bandwidth and with the possibility of the differential mode of amplification.

Both methods of decrease of the zero drift – chopping and auto-zero have pros and cons [Moghimi 2011]. Auto-zero exhibits low zero drift at the expense of higher low frequency noise due to aliasing the wideband noise into the low frequency band. The chopper amplifier has limited bandwidth and ripple of the chopping frequency. Therefore it was developed the new low zero drift amplifier AD 8628 combining these both technique.

TABLE 3.10
The performances of low zero drift amplifiers.

	AD4051	AD8551	AD8628
Bandwidth	125 kHz	1.5 MHz	2.5 MHz
Offset drift	20 nV/°C	50 nV/°C	2 nV/°C
Offset	2 μV	1 μV	1 μV
Noise 1 kHz	95 nV/rtHz	42 nV/rtHz	22 nV/rtHz
Noise 1/f	2 μV_{pp}	1 μV_{pp}	0.16 μV_{pp}
Current noise	100 fA/rtHz	2 fA/rtHz	5 fA/rtHz

AD4051 – chopper, AD 8551 – auto-zero, AD8628 – chopper + auto-zero

It should be noted that modern amplifiers due to improvement of technology have now very low zero voltage drift even without more complex auto-zero or chopper techniques. For example ultra-precision opamp OP 177 of Analog Devices exhibits noise 11 nV/rtHz and zero drift 100 nV/°C.

3.6.5. Charge amplifiers (electrometers)

The operational and instrumentation amplifiers exhibit usually very large input resistance. For example general purpose IA AD620 has input bias current 1 nA

and input resistance $10\text{ G}\Omega$. One of the commonly used methods to increase resistance is to use in the input FET transistors. For example general purpose opamp TL071 of Texas Instruments has bias current 65 pA and input resistance $10^{12}\ \Omega$.

The special designed amplifiers with FET transistors can have input resistance as large as $10^{13}\ \Omega$. For example opamp AD549 of Analog Devices has bias current only 60 fA and input resistance $10^{13}\ \Omega$. Figure 3.122 presents the circuit of FET transistors instrumentation amplifier AD8220 with bias current 600 fA and input resistance $10^{13}\ \Omega$.

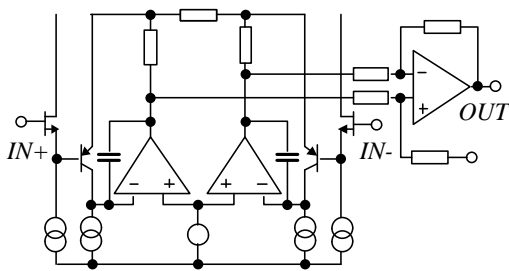


FIGURE 3.122
Simplified circuit of the FET transistors input instrumentation amplifier AD8220.

Even such large input resistance in certain applications can be insufficiently large. For example some piezoelectric sensors, photoelements, pH sensors exhibit very large input resistance close to the insulator state and conventional amplifiers are in this case short-circuit of the sensors output.

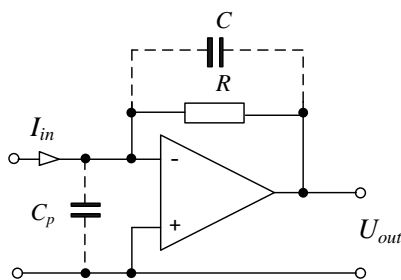


FIGURE 3.123
An example of transimpedance amplifier (C_p – capacity of the cable).

Special kinds of amplifiers or instruments with extremely large input resistance, for potential measurement are designed. They are called *electrometers*. For example, Keithley Company developed the electrometers with the input resistance of $10\text{ P}\Omega$ ($1\text{ P}\Omega$ (*penta*) = $10^{15}\ \Omega$) and input current 400

aA (1a (*atto*) = 10^{-18}). To put that into perspective consider that the voltage of about 10 V causes in a typical insulator a current of several pA.

We can obtain very large input resistance by special technology (special kind of insulation and connections) and also by using special electrical circuits. As the amplifier with large input resistance we can use current-voltage transducers presented in Figure 4.123. This circuit is also known as *transimpedance amplifier*. For this circuit we can write that

$$U_{out} = -I_{in}R \quad (3.141)$$

In the circuit presented in Figure 3.123 the small capacitor C is sometimes added to prevent gain peaking [Pallas-Areny, Webster 1999]. The time constant depends on RC and for large R it can be as large as several seconds. Therefore this circuit exhibits low-pass filtering characteristics with relatively small cut-off frequency. The application of very large $T\Omega$ resistance R can be inconvenient and therefore the modified amplifier circuit presented in Figure 3.124 can be recommended [Pallas-Areny, Webster 1999].

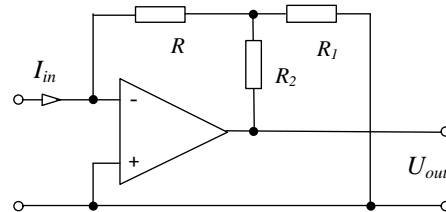


FIGURE 3.124
An example of transimpedance amplifier with extended input resistance.

For this circuit presented in Figure 3.124 we can write the following dependence

$$U_{out} = -I_{in} \left[R_2 + R \left(1 + \frac{R_2}{R_1} \right) \right] \approx -I_{in} R \left(1 + \frac{R_2}{R_1} \right) \quad (3.142)$$

Thus we obtain multiplication of the input resistance by the ratio R_2/R_1 . The transimpedance amplifier with the input signal source in form of capacitor is sometimes called the *charge amplifier* (Figure 3.125). In this case in the feedback circuit resistance R is substituted by capacity C (parallel resistance R_F can be added to correct frequency characteristic). For this circuit we can write that

$$U_{out} = \frac{Q}{C_F + (C + C_F)/K_u} \approx \frac{Q}{C_F} \quad (3.143)$$

We obtain the transducer of the charge with negligible influence of the cable capacitance C (when the gain of amplifier K_u is sufficiently large).

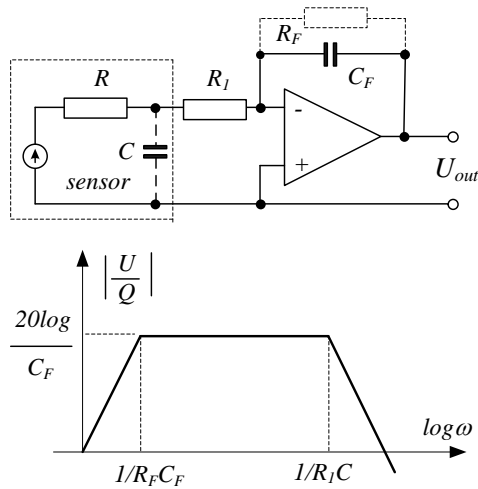


FIGURE 3.125
An example of the charge amplifier and its frequency characteristic.

Figure 3.125 present the typical frequency characteristic of the charge amplifier. The time constant of this transducer depends on the $R_F C_F$. For example for $R_F = 10 \text{ G}\Omega$ and $C_F = 100 \text{ pF}$ the low cut-off frequency is 0.16 Hz . The high cut-off frequency depends on $R_1 C$ and for example for $R_1 = 50 \text{ }\Omega$ and $C = 200 \text{ pF}$ it is 1.6 MHz .

3.6.6. The mathematical amplifiers

By appropriate application of the feedback we can create various transfer characteristics of amplifier and in this way we can realize various mathematical functions as: integration, differentiation, logarithm, exponential dependence, etc.

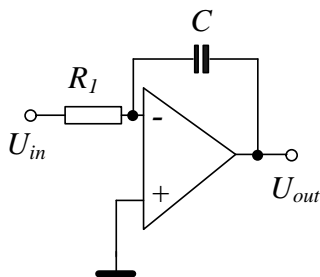


FIGURE 3.126
The circuit of the ideal integrator.

Figure 3.126 presents the circuit of the amplifier realizing the integration of the input signal – the *integrator*. For ideal *integrator circuit* we can write the following dependence

$$u_{out}(t) = -\frac{1}{R_1 C} \int_{t_0}^{t_0+T} u_{in}(t) dt + U_0 \quad (3.144)$$

Thus the circuit realizes integration with time constant $R_1 C$ and U_0 is the voltage across the capacitor C before start of the integration.

The presence of the zero voltage and associated zero drift is quite significant problem of the operation of integrator circuit. It depends on quality of the amplifier (low bias current, low zero drift) but also on the quality of capacitor [Stata 1967, Scholes 1970]. Especially this problem is troublesome in when input signal contains DC components. In such case usually it is necessary to perform discharge of the capacitor (by shortening it) and correct zero. To obtain low frequency operation the capacitor leakage resistance R_4 should be very large. In the case of AC signal the frequency bandwidth and problems with zero drift can be limited by inserting additional resistor R_4 (Figure 3.127).

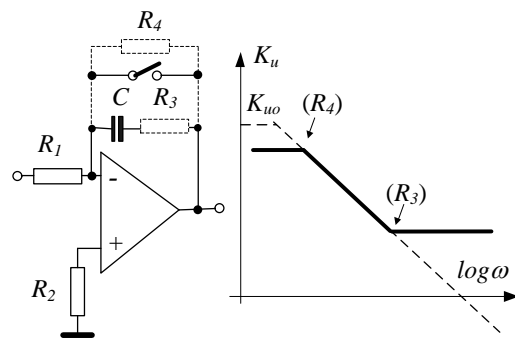


FIGURE 3.127
The practical circuit of the integrator.

We can set low and high cut-off frequencies by appropriate choice of resistance R_3 and R_4 . Figure 3.127 presents the transfer characteristic without (dashed line) and with correction resistors.

The integrator is a very important circuit in the measurements. Figure 3.128 presents the main application of this circuit. In magnetic measurements it can substitute old-fashioned moving coil fluxmeter device for measurement of the change of magnetic flux $\Delta \Phi$ (it practically measures charge – see Figure 3.125). If it is connected to the coil with n turns the output voltage is:

$$e = \frac{n}{RC} \Delta\Phi \quad (3.145)$$

In the case of AC magnetic circuit the voltage induced in the secondary winding is proportional to dB/dt . Thus to recover the flux density value it is necessary to integrate this voltage (Figure 3.128a).

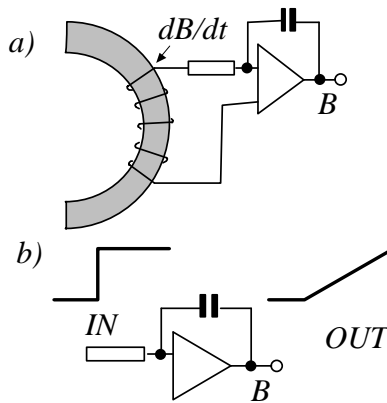


FIGURE 3.128
The main applications of the integrator.

Integrating circuit is the main part of two analog to digital converters – dual slope and sigma delta. In these converters is utilized feature of integrating circuit that for stepwise change of input signal the output signal is increased linearly versus time.

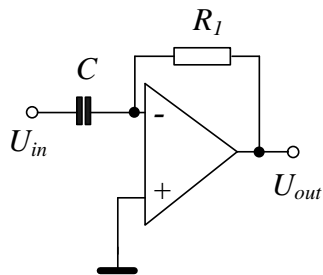


FIGURE 3.129
The circuit of the ideal differentiator.

By simply interchanging positions of resistor and capacitor we obtain the *differentiator circuit*. For an ideal differentiator circuit (Figure 3.129) there is:

$$u_{out}(t) = -R_1 C \frac{du_{in}(t)}{dt} \quad (3.146)$$

The ideal circuit presented in Figure 3.129 exhibits inherently instability because gain is increasing with frequency (Figure 3.130). Therefore usually additional elements are added to limit the frequency.

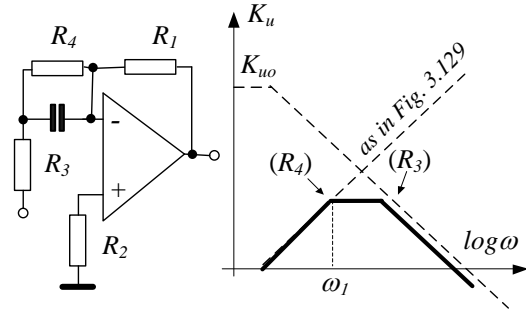


FIGURE 3.130
The practical circuit of the differentiator.

The risk of instability and increase of high frequency noise can be prevented by inserting additional resistors R_3 and R_4 (Figure 3.130). Thus this circuit operates as differentiator only to the frequency ω_1 .

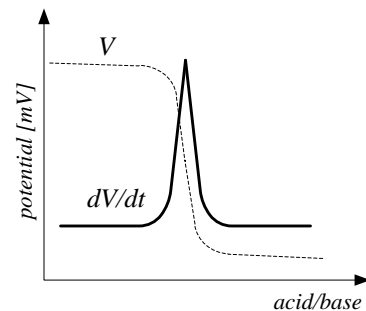


FIGURE 3.131
The derivative as the method of detection of the deflection point.

The differentiator is not as commonly used as integrator. It can be used as the high-pass filter. Figure 3.131 present the possible application of the differentiator to detect the deflection point in the potentiometric titration. Similarly it can be used to detection the peak value of the signal.

Between the collector current I_c and base-emitter voltage U_{BE} of silicon bipolar transistor is exponential dependence:

$$I_c = I_s e^{U_{BE}/U_T} \quad (3.147)$$

where k is the Boltzman constant, q is the electron charge, T is temperature, I_s is the collector reverse saturation current and $U_T = kT/q$.

Thus by appropriate connection of such transistor into the feedback circuit of operational amplifier we can obtain logarithmic *log amp* or exponential amplifier *antilog amp* (Figure 3.132).

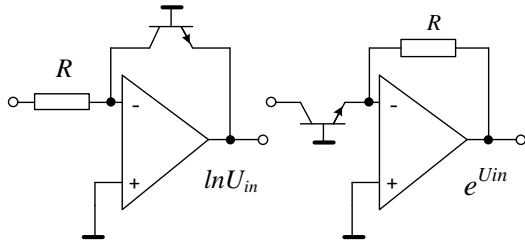


FIGURE 3.132
The principle of operation of logarithmic and exponential amplifiers.

For the logarithmic amplifier we can write the following dependence:

$$U_{out} = -U_T \ln \frac{I_{in}}{I_s} = -U_T \ln \frac{U_{in}}{R I_s} \quad (3.148)$$

$$U_{out} = I_s R \cdot e^{-U_{in}/U_T} \quad (3.149)$$

where $U_T = kT/q$ is thermal voltage - in ambient temperature $U_T \approx 25$ mV.

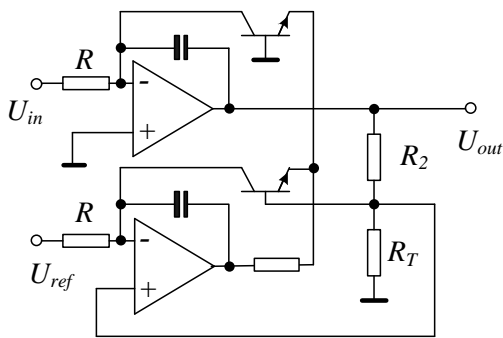


FIGURE 3.133
An example of the logarithmic amplifiers.

The transfer characteristic $U_{out} = f(U_{in})$ depends on the temperature (also current I_s depends on the temperature). Therefore, the practical circuit of the logarithmic amplifier is more extended, as it is presented in Figure 3.133 (Tran Tien Lang 1978). With correction the transfer characteristic is described as

$$U_{out} = -\frac{R_T + R_2}{R_T} U_T \ln \frac{U_{in}}{U_{ref}} \quad (3.150)$$

It is possible to correct the temperature characteristic of the whole amplifier by appropriate choice of the temperature characteristic of the R_T element.

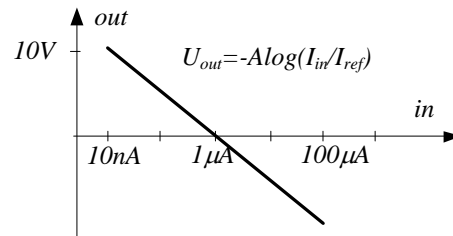
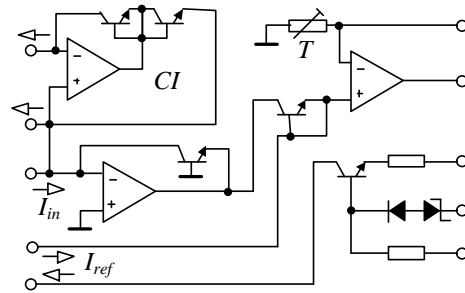


FIGURE 3.134
Simplified functional diagram of 4127 logarithmic amplifier of Texas Instruments.

Figure 3.134 presents the circuit of logarithmic amplifier model 4127. This amplifier converts $\log(I_{in}/I_{ref})$ to output voltage. Depending in the direction of the input current it can be connected directly to the input or by current inverter CI. The voltage input signal is connected with serial resistor. The amplifier is equipped with internal source of reference current. By appropriate connection it can be transformed to antilog amplifier. The accuracy of the amplifier is 0.5% and frequency bandwidth to 250 kHz.

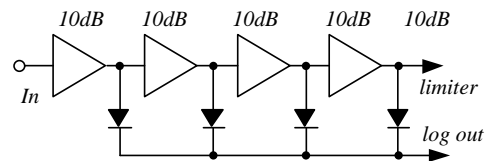


FIGURE 3.135
Successive detection log amplifier.

Logarithmic amplifiers are commonly used as light diodes amplifier in fiber-optic data transmission for compress and demodulate RF signal. In such case the amplifier presented in Figure 3.134 has to small bandwidth. Much higher bandwidth is possible to obtain in the successive detection logarithmic amplifier

presented in Figure 3.135. Basing on this principle AD641 demodulating logarithmic amplifier of Analog Devices operates in bandwidth from DC to 250 MHz.

The logarithmic amplifiers can be used for compression of the signals or linearization of the transfer characteristic (when the characteristic of the sensor is exponential). Using the logarithmic amplifier it is easy to perform many mathematical operations because:

$$\log X + \log Y = \log XY; \log X - \log Y = \log \frac{X}{Y} \quad (3.151)$$

$$2 \log X = \log X^2; 0.5 \log X = \log \sqrt{X}$$

After operation it is sufficient to perform antilog operation to realize multiplication or squaring. Basic on this principle operates true rms converters (see Figure 3.77) or multipliers (later in this Section).

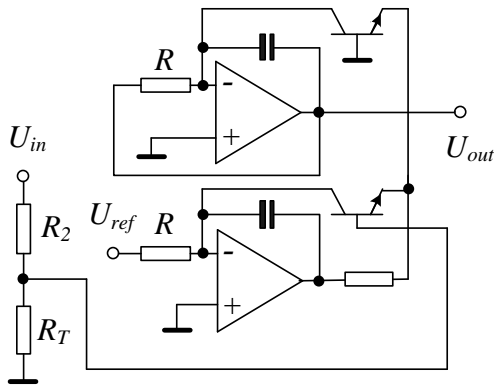


FIGURE 3.136 An example of the antilog amplifiers.

Figure 3.136 present the example of exponential amplifier. For this *antilog circuit* the transfer characteristic is described as:

$$U_{out} = R_1 \frac{U_{ref}}{R} \exp\left(-\frac{q}{kT} \frac{R_T}{R_T + R_2} U_{in}\right) \quad (3.152)$$

One of the most important devices in analogue signal processing is the *multiplier*, enabling to perform various operations: multiplication, division, square, root, trigonometric functions, *rms* calculation, electrical power calculation, phase sensitive modulation or demodulation.

Recently, there are available various monolithic multipliers with a multiplying error not larger than 0.1% and frequency bandwidth up to tens of MHz. In

such circuits two techniques of multiplying are applied: *Gilbert transconductance multiplier* or *log/antilog operation*.

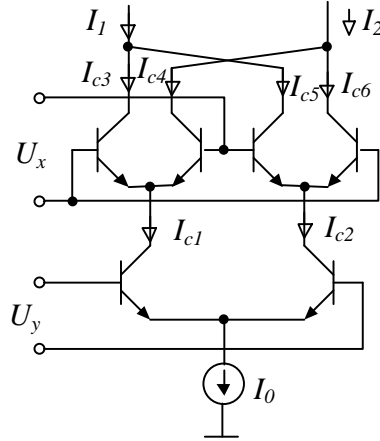


FIGURE 3.137 The transconductance Gilbert cell.

Designed by Gilbert in 1968 (Gilbert 1968, Gilbert 1972) the multiplier circuit is still (with modifications) used in analogue semiconductor devices. Its main advantage is that it is easy to implement such a device into the integrated circuit (the same semiconductors as the rest of the circuit), large frequency bandwidth and what is important it can be implemented as four quadrant multiplier. For the Gilbert multiplier presented in Figure 3.137 we can describe currents as:

$$\begin{aligned} I_{c1} &= \frac{I_0}{1 + \exp(-U_y / U_T)}; I_{c2} = \frac{I_0}{1 + \exp(U_y / U_T)} \\ I_{c3} &= \frac{I_0}{[1 + \exp(-U_x / U_T)][1 + \exp(-U_y / U_T)]} \\ I_{c4} &= \frac{I_0}{[1 + \exp(U_x / U_T)][1 + \exp(-U_y / U_T)]} \\ I_{c5} &= \frac{I_0}{[1 + \exp(U_x / U_T)][1 + \exp(U_y / U_T)]} \\ I_{c6} &= \frac{I_0}{[1 + \exp(-U_x / U_T)][1 + \exp(U_y / U_T)]} \end{aligned} \quad (3.153)$$

and

$$\begin{aligned} I_1 - I_2 &= I_{c3} + I_{c5} - (I_{c4} + I_{c6}) = (I_{c3} - I_{c6}) - (I_{c4} - I_{c5}) \\ &= I_0 \tanh \frac{U_x}{2U_T} \tanh \frac{U_y}{2U_T} \end{aligned} \quad (3.154)$$

For small value of $U_x, U_y < U_T$ we can assume $\tanh(x) = x + x^3/3 + \dots \approx x$ and

$$\Delta I = I_1 - I_2 = \frac{I_0}{4U_T^2} \cdot U_x U_y = K \cdot U_x U_y \quad (3.155)$$

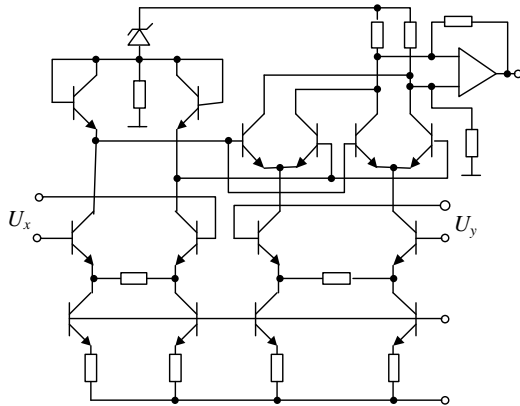


FIGURE 3.138
The four quadrant multiplier AD534.

Figure 3.138 present the circuit 1 MHz, 0.25% accuracy multiplier AD534. Figure 3.139 presents its functional diagram.

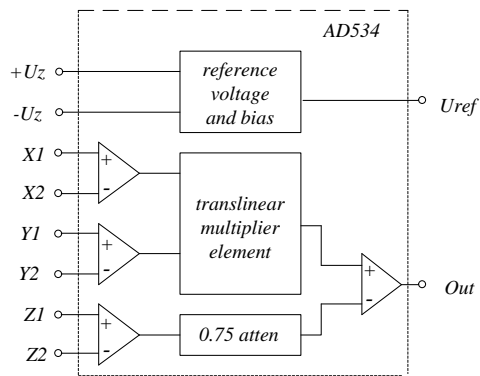


FIGURE 3.139
The functional diagram of multiplier AD534.

The multiplier device enables calculation of the following equation

$$U_{out} = \frac{(X_1 - X_2)(Y_1 - Y_2)}{10V} + (Z_1 - Z_2) \quad (3.156)$$

By appropriate connection of the multiplier it is possible to realize various operations. Several examples

proposed by Analog Device (Data Sheet of AD534) are presented in Figure 3.140.

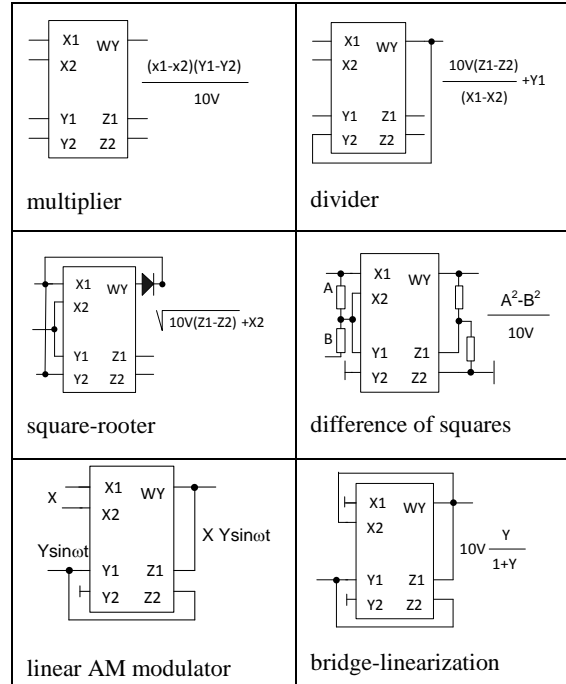


FIGURE 3.140
Various examples of the applications of a typical multiplier device (proposed by Analog Devices).

It is possible to design a multiplier as the log/antilog principle presented in Eq. 3-151. An example of such multiplier is presented in Figure 3.141.

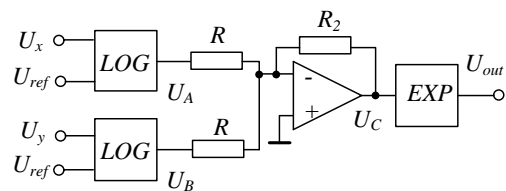


FIGURE 3.141
The log/antilog multiplier.

$$U_A = K_1 \log \frac{U_x}{U_{ref}}, \quad U_B = K_2 \log \frac{U_y}{U_{ref}} \quad (3.157)$$

and assuming that $K_1=K_2=K$

$$U_C = -(U_A + U_B) = -K \log \frac{U_x U_y}{U_{ref}^2} \quad (3.157)$$

and at the output

$$U_{out} = U_{ref} 10^{-U_c / K_3} = \frac{U_x U_y}{U_{ref}} \quad (3.158)$$

The multiplier based on the logarithmic function usually realizes the following equation

$$U_{out} = U_y \left(\frac{U_z}{U_x} \right)^M \quad (3.159)$$

Figure 3.142 presents the operational diagram of a typical log/antilog multiplier. The parameter M is set by connection of suitable resistors.

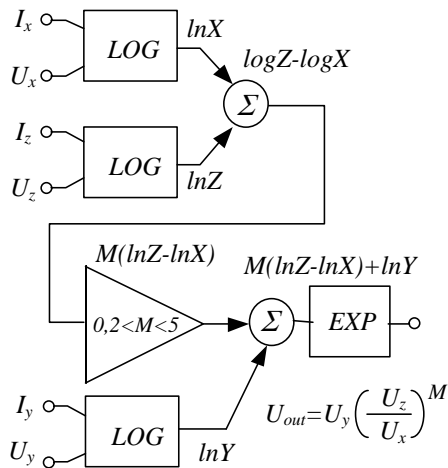


FIGURE 3.142
The operational diagram of typical log/antilog multiplier – model AD538 of Analog Devices.

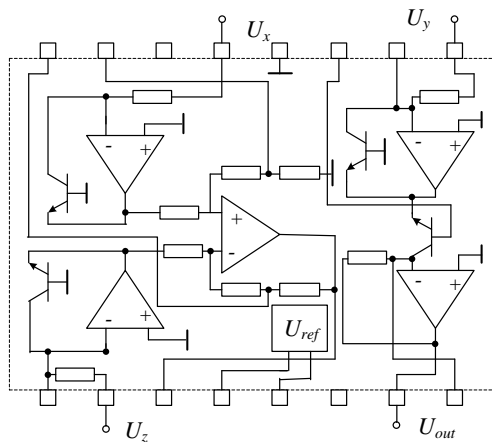


FIGURE 3.143
The log/antilog multiplier – model AD538 of Analog Devices.

Figure 3.143 presents the circuit of log-antilog multiplier AD538. Beside typical multiplier functions it is possible to use it as logarithmic amplifier. In comparison with transconductance Gilbert cell multiplier AD534 the multiplier AD538 has narrower bandwidth to 400 kHz, larger error equal to 1%. As AD534 enables to multiply in 4-quadrant the AD538 operates only in single quadrant.

The operational amplifier allows performing the operations of addition or subtraction. An example of such device is presented in Figure 3.144.

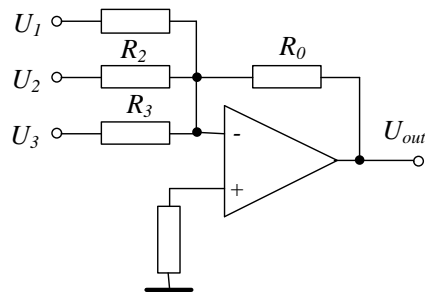


FIGURE 3.144
The operational amplifier used for addition of the signals.

The output voltage of adder presented in Figure 3.144 is:

$$U_{out} = - \left(\frac{U_1}{R_1} + \frac{U_2}{R_2} + \frac{U_3}{R_3} \right) R_0 \quad (3.160)$$

If all input resistors are the same we have averager device.

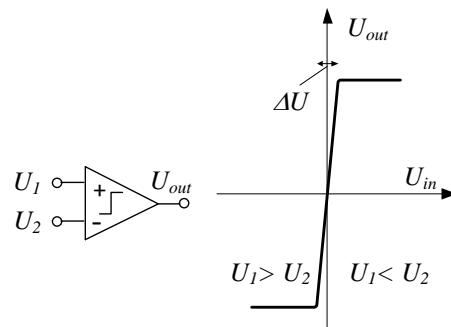


FIGURE 3.145
The operating principle of the comparator.

In the measurements often occurs the necessity of comparison of two signals. The devices called *comparators* realizes the following function

$$\begin{cases} U_{out} = 1 & \text{for } \varepsilon = U_+ - U_- > 0 \\ U_{out} = 0 & \text{for } \varepsilon = U_+ - U_- < 0 \end{cases} \quad (3.161)$$

where output signal are logical 0 or 1 corresponding with $\pm U_{out}$.

Figure 3.145 illustrates the operating principle of the comparator device. Theoretically, every operational amplifier without feedback acts as a comparator. But in the typical operational amplifier time of switching is relatively large – several μs . Therefore, there are available specially designed devices – comparators with switching time of several ns . If it is necessary to perform the comparison very fast, for example for detection of zero crossing by measurement of phase shift, the comparator is very useful. For slow processes, for example monitoring of the level of the signal, ordinary operational amplifier is sufficient. Comparators play a very important role in digital signal processing, as main part of analog to digital converters.

3.7 The analog filters

The analog filters are used mainly to pass only selected part of the frequency bandwidth. By using the *lowpass filters LP* we can reject the high frequency interferences (for example radio frequency interferences). And *vice versa* by using the *highpass filter HP* we can eliminate the industrial frequency interferences (if our signal is in the bandwidth above these frequencies). Also, we can separate the useful signal from the interference signals by using the *bandpass BP filter*. And inversely we can use the *bandreject filters*. Exist also *all-pass filters* – used as a phase shifters.

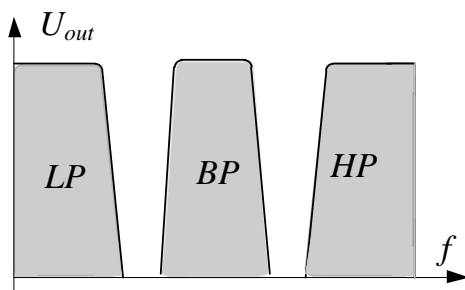


FIGURE 3.146 Typical filters and their frequency characteristics: LP – low-pass filter, BP – band-pass filter, HP – high-pass filter.

The ideal filter should pass the signals in assumed frequency bandwidth and stop the signals of other frequencies. The real analogue filter can exhibit ripples

in the passband frequency characteristics⁵ and the transition between the passband and stopband is not vertical (there is a finite transition frequency bandwidth). The width of transition band depends on the dynamic of the signal and order of the filter).

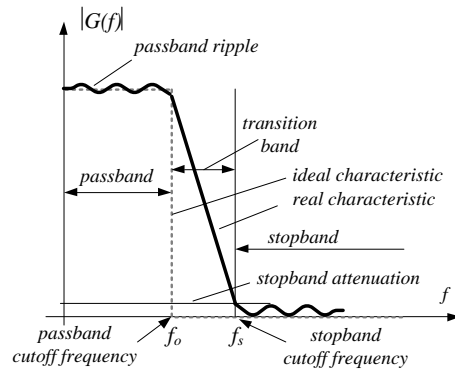


FIGURE 3.147 The transfer characteristic of the real lowpass filter.

The performance of the filter is described by the amplitude and phase frequency characteristics (Bode characteristics) – Figure 3.148. The ideal amplitude characteristic should be flat in the passband till cut-off frequency (attenuation 0 dB). For real characteristic we assume that the passband is for the attenuation 0 – 3dB. As the stopband we assume the frequency band where the attenuation is larger than the assumed value (for example 100 dB).

The slope of the characteristic in the transition band depends on the order of the filter – for the first order filter it is 20 dB/decade (6 dB/octave⁶), for the second order filter it is 40 dB/decade (12 dB/octave) etc.

The phase frequency characteristic is also important because incorrect phase performances mean that the filter introduces signal distortions (various phase shift of harmonics). To obtain correct phase performances it is required that the phase varies linearly with the frequency. Usually the phase characteristic is not linear in the whole bandwidth (see Figure 3.148). Moreover it is very difficult to ensure both performances simultaneously: the filters with excellent amplitude characteristic exhibit poor phase linearity and *vice versa*.

⁵ Exist also filters for example Cauer filter with ripples in the stopband.

⁶ Octave it is the ratio of frequency equal to 1:2, while the decade corresponds with the ratio of frequency 1:10.

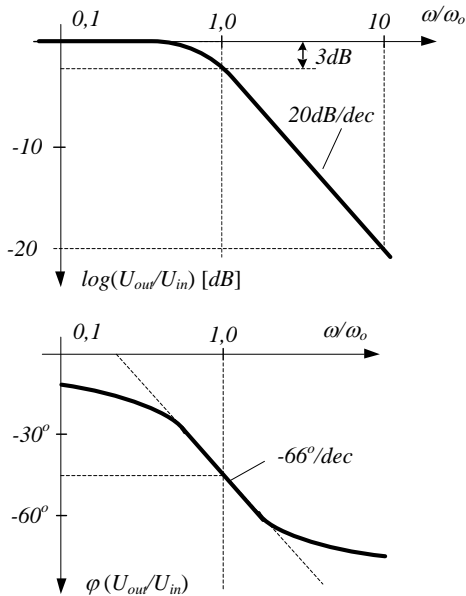


FIGURE 3.148
An example of the amplitude and phase frequency characteristics of the lowpass filter.

In the time domain usually is analyzed answer of the filter to stepwise or pulse input signal. The examples of such characteristics are presented in Figure 3.149.

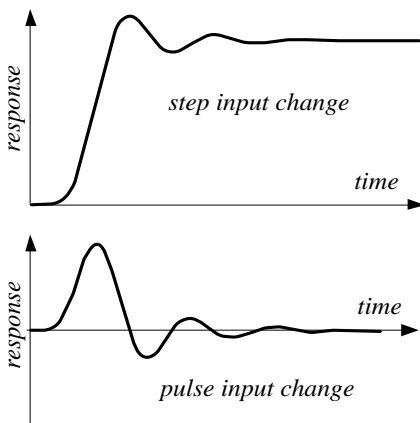


FIGURE 3.149
The examples of the time domain characteristics of typical filter.

It has been designed several types of the filters optimized by taking into account requirements. Figure 3.150 presents typical amplitude characteristics of the

most commonly used filters: Butterworth, Chebyshev, Bessel and Cauer.

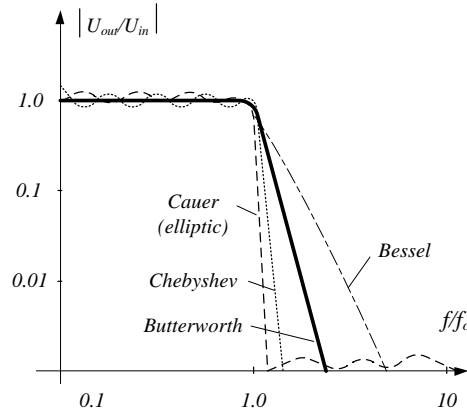


FIGURE 3.150
The comparison of the frequency amplitude characteristics of the main filters.

The *Butterworth filter* is designed to obtain the optimal parameters – almost flat characteristic in the passband and modest slope in the transition band. Therefore it is most commonly used. The *Chebyshev filter* has much better steepness of the transfer characteristic but at the cost of ripples in the pass band. It is possible to design various values of the ripples but as smallest ripples as weaken slope at the transition band (in the Figure 3.150 is presented the characteristics for 0.5dB ripples). Exists also inverse *Chebyshev filter* with flat passband and ripples in stopband. The best steepness exhibits the *elliptic Cauer filter* but this filter has ripples in both passband and stopband. The *Bessel filter* exhibits poor amplitude characteristic but the best phase characteristic what results in the small signal distortion (Figure 3.151).

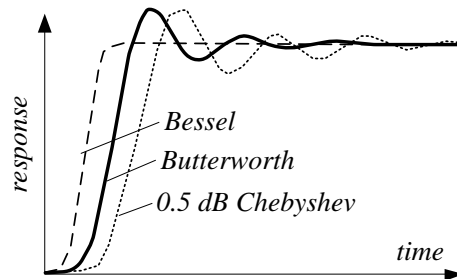


FIGURE 3.151
The time response of the main filters after stepwise change of the input signal (after Zumbahlen 2008).

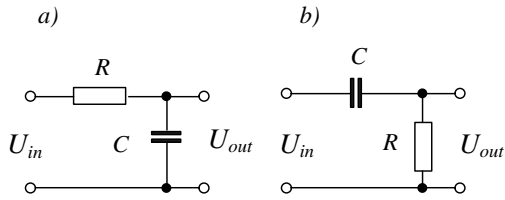


FIGURE 3.152
The passive RC filters: a) low-pass filter, b) high-pass filter.

Figure 3.152 presents the examples of realization of simple passive RC filters. The low-pass RC filter presented in Figure 3.152a is described by the equation

$$G(j\omega) = \frac{1}{1 + j\omega RC} \quad (3.162)$$

The cut-off frequency of such filter is $\omega_0 = 1/RC$. Because it is the first order filter the attenuation is only 20 dB/dec. We can improve performances of the filter by connecting several filters in the cascade (Figure 3.153).

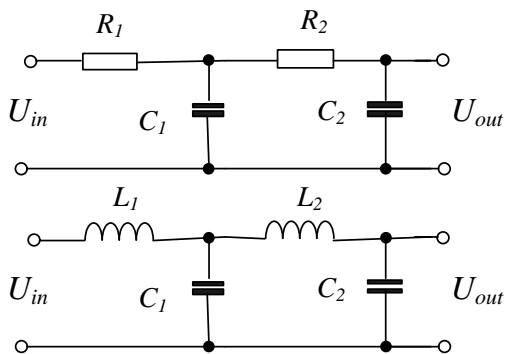


FIGURE 3.153
The passive RC filter of second order and LC filter of fourth order.

For cascade connected RC filters (Figure 3.153) the frequency characteristic is described in the form

$$G(j\omega) = \frac{1}{1 + j\omega(R_1C_1 + R_2C_2 + R_1C_2) - \omega^2 R_1C_1R_2C_2} \quad (3.163)$$

By connecting several filters in series we obtain an increase of the order of the filter and the same the steepness of the characteristic in the transition band. But it is not reasonable to connect many filters in the

cascade (more than three) because each of the filters significantly attenuates also the useful signal. Moreover, the cascade type filter is not a simple sum of single filters because each following filters loads the previous one, thus influencing the frequency characteristic (the dependence (3.163) was derived under assumption that the source resistance is negligibly small and the load resistance is large).

It is possible to obtain better performances by using LC filters instead of RC one because simple LC filter is the second order filter with slope of 40 dB/dec.

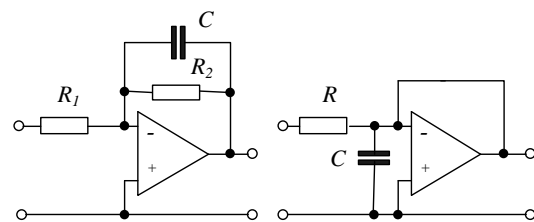


FIGURE 3.154
The active first order lowpass RC filters.

The effect of attenuation of the signal by the passive RC filters can be decreased by supporting such filters with the amplifier circuit – as presented in Figure 3.154. But such filters do not ensure sufficient steepness of the frequency characteristic in the transition state. It is possible to obtain improvement of the analogue filter performances by application of the special active filters presented in Figure 3.155.

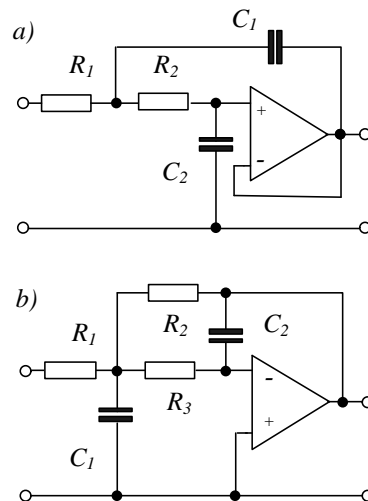


FIGURE 3.155
The active second order lowpass RC filters: a) Sallen-Key, b) multifeedback MFB.

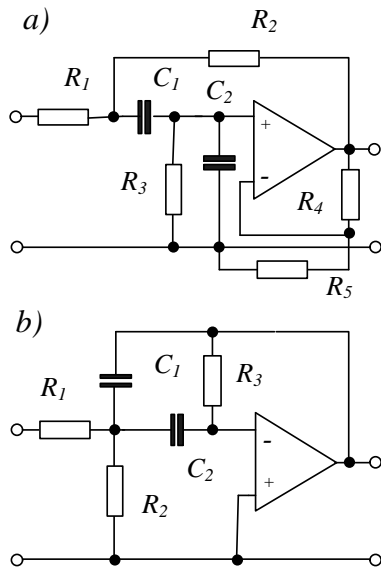


FIGURE 3.156
The active second order bandpass RC filters: a) Sallen-Key, b) multifeedback MFB.

The active filters use the operational amplifiers and the RC elements in the feedback circuit. Figure 3.155a presents one of the most commonly used filter – *Sallen-Key filter* (called also *filters with voltage controlled source - VCS*). Figure 3.,155b present other active filter - MFB filters (*multi-feedback filters*). Note that the low-pass filters and high-pass filters are obtained simply by swapping around the *R* and *C* elements. The band-pass filters are obtained by the combination of low-pass and high-pass filters – Figure 3.156.

For the Sallen-Key lowpass filter the transfer characteristic can be described by the following *s*-operator function:

$$H(s) = \frac{1}{s^2 + \frac{1}{R_1 C_2} s + \frac{1}{R_1 R_2 C_1 C_2}} = \frac{\omega_o^2}{s^2 + \frac{\omega_o}{Q} + \omega_o^2} \quad (3.164)$$

where

$$\omega_o = \sqrt{\frac{1}{R_1 R_2 C_1 C_2}}; \quad Q = \sqrt{\frac{R_1 C_2}{R_2 C_1}}$$

For the special case when $R_1 = R_2 = R$ the capacitances can be calculated from the following conditions (Jamal 2003)

$$C = \frac{1}{2\pi R f_o}; \quad C_1 = 2QC; \quad C_2 = C/2Q \quad (3.165)$$

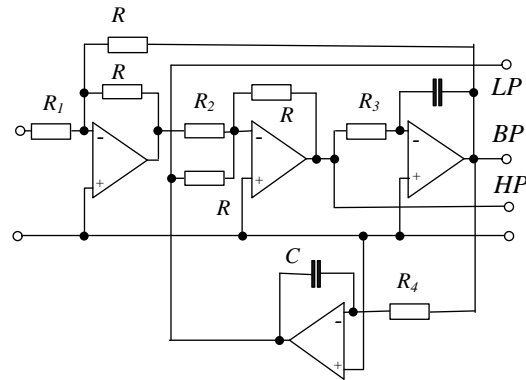


FIGURE 3.157
The active second order State variable RC filters.

Figure 3.157 presents other commonly used active RC filter – *state variable filter*. This filter enables to obtain simultaneous three types of filters: low-pass LP, high-pass HP and band-pass filters BP. The modification of this filter known as *biquadratic filter* is used for design of Cauer and inverse Chebyshev filter.

The design of the analogue filters requires quite complicated calculations (Huelsman 1993, Thede 2004, Schaumann 2001, Winder 2002, Volkenburg 1995). Fortunately, there are available various design procedures enabling fast design of the filter with desired performances. For example, the *Matlab* software offers various tools for the design of the filters (Lutovac 2000). Also, in the *LabVIEW* platform there are ready to use design procedures of the filters.

Usually, the filter is described using *s*-operators. A simple RC filter (equation 3.162) can be described in the form:

$$H(s) = \frac{1}{1 + sRC} \quad (3.165)$$

For design of filters commonly it is used normalized form with assumption that $R = 1 \Omega$, $C = 1 F$, $\omega_o = 1 rad/s$ and the dependence (3.165) can be rewritten as:

$$H(s) = \frac{1}{1 + s} \quad (3.166)$$

Similarly the fourth order filter is described by the equation:

$$H(s) = \frac{1}{a + bs + cs^2 + ds^3 + s^4} \quad (3.167)$$

The general transfer equation of the filter has the form:

$$H(s) = \frac{a_m s^m + a_{m-1} s^{m-1} + \dots + a_1 s + a_0}{b_n s^n + b_{n-1} s^{n-1} + \dots + b_1 s + b_0} \quad (3.168)$$

In analysis of the properties of the filter usually are determined roots of the denominator (poles) and numerator (zeros). In the s-plane (Figure 3.158) all poles should be in the left side to guarantee the stability.

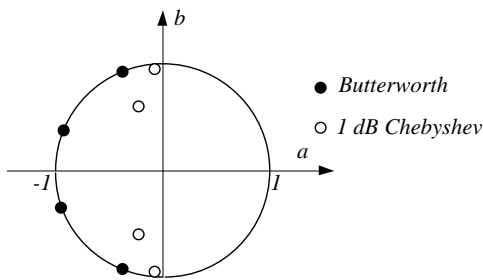


FIGURE 3.158
The poles of the 4-th order Butterworth and 1 dB Chebyshev filters.

All most popular filters are described as the polynomials representing the denominator in equation (3.168). Usually the poles of all filters are completed as tables in various publications. Knowing poles it is possible to calculate coefficients of polynomial. For example the poles of Butterworth filter of 4th order are (Figure 3.158):

$$a \pm jb = \begin{cases} -0.9239 \pm j0.3827 \\ -0.3827 \pm j0.9239 \end{cases} \quad (3.169)$$

The polynomial of denominator can be calculated as [Maxim 2003]

$$s^2 + 2as + a^2 + b^2 \quad (3.170)$$

Combining equation (3.169) and (3.170) we obtain the polynomial:

$$(s^2 + 1.848s + 1)(s^2 + 0.765s + 1)$$

Table 3.11 presents the Butterworth denominator polynomials.

TABLE 3.11
Butterworth filter denominator polynomials.

Order	Polynomials
1	$s + 1$
2	$s^2 + \sqrt{2}s + 1$
3	$s^3 + 2s^2 + 2s + 1$
4	$s^4 + 2.61s^3 + 3.414s^2 + 2.61s + 1$

The active filters presented in Figure 3.156 represent the second order filters. The simplest way to obtain higher order of the filter is to connect the filters in a cascade form – for example, to obtain the fourth order filter usually there are connected two filters of the second order, and to obtain the fifth order filter additional first order filter is connected. Table 3.12 presents the denominator polynomials derived under the assumption that we dispose to connect the first and second order filters.

TABLE 3.12
Butterworth filter denominator polynomials for the filter composed from the first and second order components.

Order	Polynomials
1	$s + 1$
2	$1 + 1.414s + s^2$
3	$(1 + s)(1 + s + s^2)$
4	$(1 + 1.848s + s^2)(1 + 0.765s + s^2)$
5	$(1 + s)(1 + 1.618s + s^2)(1 + 0.618s + s^2)$

Let us design the low-pass Butterworth filter of the fourth order with the cut-off frequency 1000 Hz (Maxim 2003). The characteristic of the Sallen-Key filter can be described using the following equation:

$$G(s) = \frac{G_1 G_2}{G_1 G_2 + (G_1 + G_2) C_2 s + C_1 C_2 s^2} \quad (3.171)$$

where resistances R are presented as conductances G (for simplifying further calculations). With normalized resistors 1Ω the equation (3.171) can be rewritten in a form:

$$G(s) = \frac{1}{1 + (2C_2)s + (C_1 C_2)s^2} \quad (3.172)$$

According to the polynomial $(s^2 + 1.8478s + 1)(s^2 + 0.7654s + 1)$ and the equation (3.172) in the first

filter $C_1C_2 = 1$ and $2C_2 = 1.8478$ thus the capacitances in the first filter are $C_2 = 0.9239 F$ and $C_1 = 1.08 F$. Similarly in the second filter $C_1C_2 = 1$ and $2C_2 = 0.7654$ thus the capacitances in the first filter are $C_2 = 0.3827 F$ and $C_1 = 2.61 F$.

If we assume that the resistors are $1 k\Omega$ (multiplied by factor 1000) the capacitances should be divided by 1000. To obtain the cut-off frequency as $1 kHz$ (instead of $1 rad/s$) we should divide the capacitances by $2\pi \cdot 1000$. As result we obtain the circuit of the filter presented in Figure 3.159.

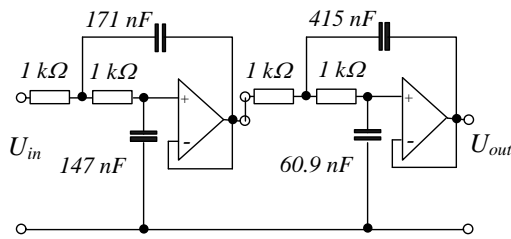


FIGURE 3.159
The 4th-order Butterworth low-pass filter with the cut-off frequency $1 kHz$ - after (Maxim 2003).

In the integrated circuit technology it is rather difficult to obtain precise values of the RC elements. Therefore, instead of resistors there are developed filter circuits with *switched capacitors* because in the integrated circuit technology it is relatively easy to design the switch element.

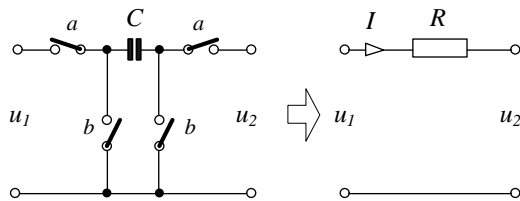


FIGURE 3.160
The switched capacitor as the simulator of the resistance.

Consider the circuit presented in Figure 3.160. If the capacitor is switched with the period T (first time to the input u_1 the second time to the output u_2) the charge transfer is

$$\Delta Q = C(u_1 - u_2) \tag{3.173}$$

and the equivalent current is

$$I = \frac{\Delta Q}{T} = \frac{C(u_1 - u_2)}{T} \tag{3.174}$$

The circuit with a switched capacitor is equivalent to the circuit with the resistor R

$$R = \frac{u_1 - u_2}{I} = \frac{T}{C} = \frac{1}{fC} \tag{3.175}$$

Thus it is possible to design the filters with the R element substituted by the switched capacitor. The important advantage of this solution is the possibility of the tuning of filter by the change of the frequency of switching. Figure 3.161 presents the design of the switched capacitor filter.

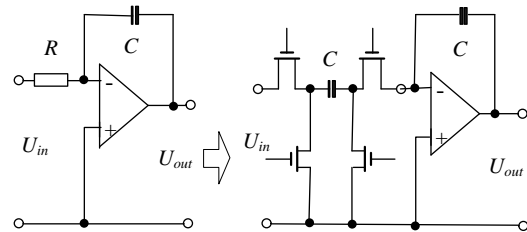


FIGURE 3.161
The RC filter and equivalent filter with switched capacitor.

Figure 3.162 presents the *state variable* universal filter circuit designed for the programmable active filters with the switched capacitors. This filter can operate as the low-pass filter LP, high-pass filter HP, band-pass filter BP and additionally band-reject filter BR. The cut-off frequency can be changed of the switching frequency of capacitor C_1 simulating resistor:

$$\omega_o = \frac{1}{R_f C} = \frac{1}{fC_1 C} \tag{3.176}$$

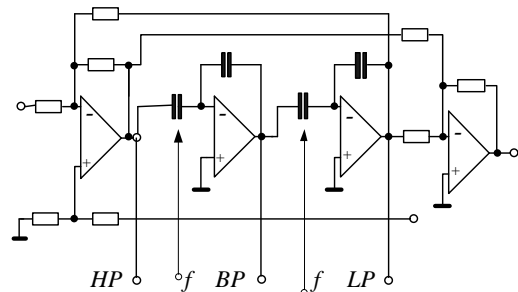


FIGURE 3.162
The state variable filter with the possibility of application of the frequency tuning.

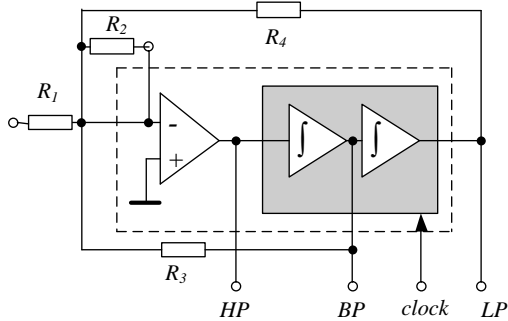


FIGURE 3.163
The functional circuit of the high performance dual switched capacitor filter model LMF100 of National Semiconductor.

Figure 3.163 presents the integrated filter circuit developed by the *National Semiconductor* - model *LMF100*. This circuit utilizes the operation principle of the state variable filter presented in Figure 3.162. The integrated circuit of the filter with switched capacitors enable to design the second order filter (high-pass, low-pass or band-pass). The external resistors can be used to the setting of the band-pass gain or low-pass gain. The center frequency is tuned by the external clock frequency.

3.8 The noises and interferences

The measured signals are usually accompanied by some noises and interferences, sometimes of the level comparable to the level of the measured signal. As the noises and interferences we assume all signals other than the measured signal – the noises are the stochastic signals with indefinite frequency and magnitude (*the white noise* is the signal with theoretically all frequency components). The interferences are the signals coming from various external sources; very often these signals are of the main frequency 50 Hz (or 60 Hz) and harmonics of this frequency.

The typical interference signals are generated by the electric power lines, electrical machines, lighting equipment, commutating devices, radio communication transmitters, atmospheric discharges or cosmic noises. The sources of noises are usually internal – all resistors and semiconductors intrinsically generate noises.

In the previous chapters various methods of rejection of noises or interferences have been described:

- application of the differential input of amplifiers (common mode signals rejection) or application of differential sensors (for example to eliminate the external temperature influence);
- application of the galvanic separations of the circuits (isolation amplifiers);

- application of the phase sensitive detectors – in lock-in amplifiers to rejection of the noises;
- elimination of the temperature zero drift by application of the auto-zero function;
- correct grounding and shielding of various parts of the circuit, for example application of the *Wagner earth* in the AC bridge circuits.

Modern signal recovering techniques enable us to eliminate the noises and interferences significantly larger than the measured signal. But we can look at the problem of noises and interferences from other point of view. By using incorrect connections of the signal or by applying the incorrect grounding we can deteriorate the quality of the measuring signal.

One of the most difficult to elimination interference is the signal deteriorated by the zero drifts. The zero drift can be caused by several sources: the connections of two metals (thermoelectric voltage), instable contacts, vibrations of various parts of the circuit, bad quality insulation, piezoelectric effects, electrochemical effects, etc. The basis of the zero drift is very often technological (quality of contacts, uniformity of materials) and it can be amplified by the temperature differences of various parts of the circuit. For that reason it is important to exclude the formation of the temperature differences (for example non-uniform heating of various parts). Sometimes, conversion of the DC into the AC signals can be helpful (carrier amplifiers, chopper amplifiers, etc.).

One of the basic sources of the noises is the resistor R . The *thermal Johnson noise* U_{nT} is generated due to the chaotic thermal movement of the charges. This noise can be described by the *Nyquist relation*

$$U_{nT} = \sqrt{4kTR\Delta f} \quad (3.177)$$

where k is the Boltzman constant ($k = 1.38 \cdot 10^{-23}\text{ Ws/K}$), T is the temperature, and Δf is the frequency bandwidth.

The thermal noises can be reduced by the decrease of the resistances, by the limitation of the bandwidth and of course by the control of the temperature.

Another important source of noises is the semiconductor junction. When the current is on the potential barrier a number of charges q are randomly crossing this barrier and these random current fluctuations are the source of the *shot noises* I_{ss} described by the *Schottky relation*

$$I_{ss} = \sqrt{2qI\Delta f} \quad (3.178)$$

where q is the electric charge ($q = 1.6 \cdot 10^{-19}\text{ C}$).

In the low frequency range there are *1/f* type noises (sometimes called *low frequency noise*, *flicker noise* or *excess noise*). There are many sources of these noises, most of them unknown. Such noises are inversely proportional to the frequency, and the power spectral density $S(f)$ of this noise is:

$$S(f) = \frac{E_f^2}{f^\alpha} \tag{3.179}$$

where E_f is the *rms* voltage of noises and α coefficient is $\alpha = 0.8 - 1.3$.

Because the noise level depends on the frequency these noises are not the white noises (noises containing every frequency of signals) and are called *pink noise* – random noise having the same amount of energy in each octave.

Due to the random character of the noises usually they are described not by the voltage level U_n but by the spectral density $S(f)$ (see Figure 2.16):

$$S(f) = \frac{U_n^2}{\Delta f} = \left(\frac{U_n}{\sqrt{\Delta f}} \right)^2 \tag{3.180}$$

The $U_n / \sqrt{\Delta f}$ value is called the *spectral density of noises* and it means the *rms* value of the voltage signal in relation to the square root from the frequency bandwidth. Often the noises are characterized by the *SNR factor – signal to noise ratio*:

$$SNR = 20 \log \frac{U_n}{U} \tag{3.181}$$

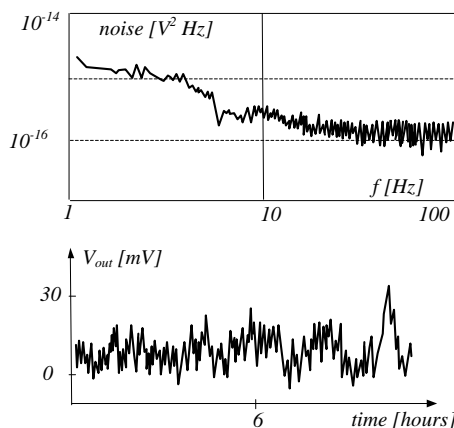


FIGURE 3.164 An example of the noises in Hall sensor (From Schott *et al.* 1997).

Figure 3.164 presents the example of the noise characteristics of Hall sensor – spectral density and low frequency signal. When there are many sources of noises necessary is to perform noise budget calculation, as it is presented for amplifier in Section 3.6.4 (Eq. 3.128). As noises are characterized by V / \sqrt{Hz} finally it is necessary to calculate U_{nrms} as:

$$U_{nrms} = U_n \cdot \sqrt{\Delta f} \tag{3.182}$$

The low frequency *1/f* noises are usually characterized by U_{nrms} determined for certain frequency bandwidth, for example 0.1 – 10 Hz.

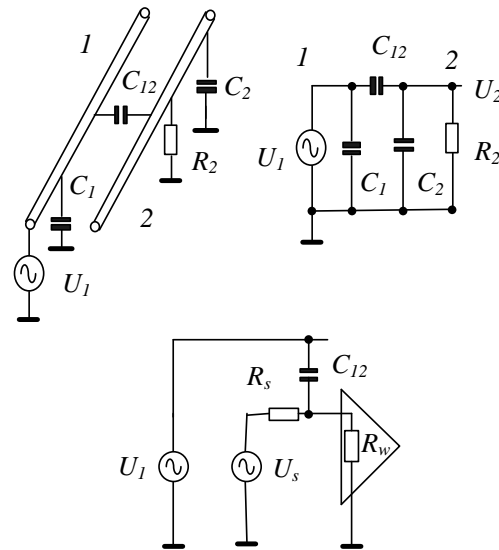


FIGURE 3.165 The interferences connected to the amplifier by the capacitive coupling: the access to the adjacent wire and access to the amplifier input.

The external interferences can penetrate the measuring circuit by the capacitive, inductive or conductive coupling. Figure 3.165 presents two examples of the interferences connected to the measuring circuit by the *capacitive coupling*. The wire 2 infiltrates the signal from the wire 1 by the inter-wire capacitance C_{12} . Or the amplifier connected to the measured signal U_s is additionally connected to the signal U_1 by the coupling capacitance C_{12} .

For the large frequency is created the capacitance voltage divider and the interference signal in the wire 2 is:

$$U_2 = \frac{C_{12}}{C_2 + C_{12}} U_1 \tag{3.183}$$

For lower frequencies the interference signal depends on the frequency f and the resistance R_2 (Pallas-Areny 1999)

$$U_2 = j\omega R_2 C_{12} U_1 \quad (3.184)$$

A typical example of capacitance coupling is the penetration of the interferences by the inter-turns capacitance of the separation transformer. The researcher performing experiments would expect that the connection of the galvanic separation (by use of the separation transformer) makes the circuit free from the 50 Hz interferences. To effectively obtain such rejection of interferences it is necessary to introduce between turns the copper grounded electrostatic shield (this way we eliminate the capacitive coupling of signals).

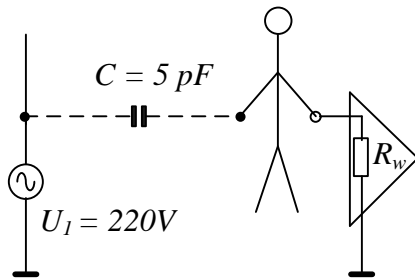


FIGURE 3.166
The interferences connected to the amplifier by the capacitive coupling and human body (after van Putten 1996).

Other example is presented in Figure 3.166 (taken from the book of van Putten – van Putten, 1996). It illustrates what happens when we touch the input of oscilloscope with typical impute impedance $> 1 \text{ M}\Omega$. Assuming impedance of the human body as about $1 \text{ M}\Omega$ and the coupling typical capacity as 5 pF we obtain that in the input of oscilloscope appears voltage signal as high as about 4 V .

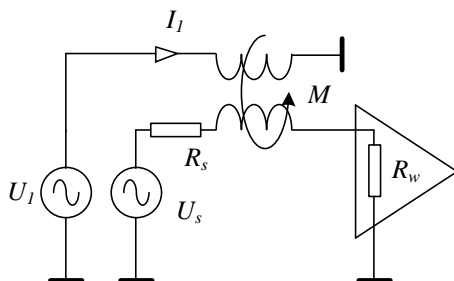


FIGURE 3.167
The interferences connected to the amplifier by an inductive coupling.

Figure 3.168 presents the inductive coupling when the current in adjacent wires can induce an additional interference voltage:

$$U_L = \omega M I_1 \quad (3.185)$$

A typical example of *inductive coupling* is the penetration of the measuring circuit by the voltages induced by the external sources of electromagnetic fields, from radio transmitters or mobile telephony communication. Therefore, such interferences are often called as *RFI – radio frequency interferences* or *electromagnetic interferences IMI*.

Problem of generation of interferences by electromagnetic fields increases due to increase of *electromagnetic pollution*. It is main subject of interest *electromagnetic compatibility EMC*. Generally EMC looks at the interferences from both point of view:

- how to design the electrical devices to reduction the emitted electromagnetic field,
- how to design the electric devices to obtain immunity to EMI.

Fortunately recently are in power many international standards strictly prohibited emission of introduced to the market electric devices.

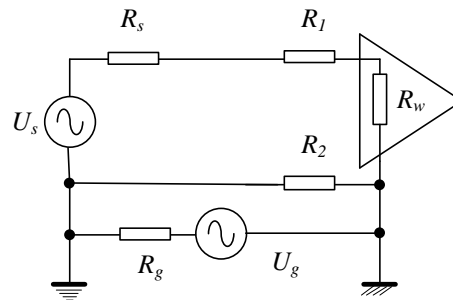


FIGURE 3.168
The interferences connected to the amplifier by the conductive coupling.

A typical example of the *conductive coupling* of interferences is voltage U_g (Figure 3.168) appeared in the case of connection of two various grounding points. The inter-ground difference of potentials can be introduced as the voltage drop U_i on the resistor R_2 :

$$U_i = U_g \frac{R_2}{R_2 + R_g} \quad (3.186)$$

There are several universal methods and tools of rejection or limitation of the interference. The capacitive coupling can be reduced by the application of the electrostatic shield. A conducting plate or foil

grounded at one point can be used as the electrostatic shield (Figure 3.169). After introduction of this shield most of the currents coming from the interference source U_1 are shorted to the ground by the shield and do not penetrate the measuring circuit (Figure 3.169b).

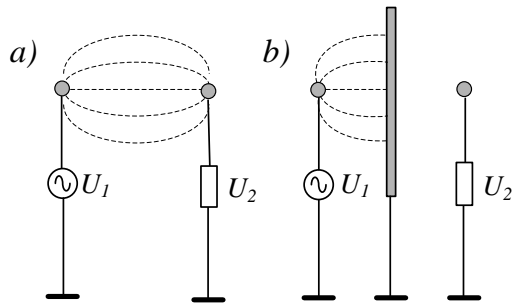


FIGURE 3.169
The reduction of the capacitive coupling by the electrostatic shield.

Figure 3.170 presents the method of reduction of magnetic coupling by the application of a magnetic shield. The magnetic shield is prepared from high-permeability magnetic material. The lines of magnetic field are closed in the shield and do not penetrate the area of the measuring circuit.

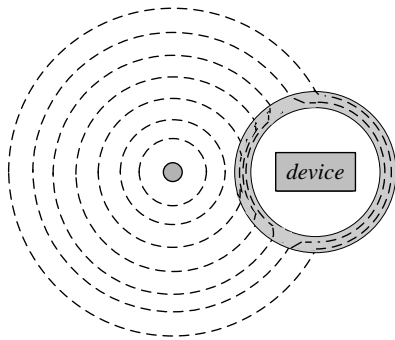


FIGURE 3.170
The reduction of the magnetic coupling by the magnetic shield.

To obtain effective shielding the material of the shield should be properly chosen – for low magnetic fields it is necessary to use different material than for high magnetic field since the magnetic permeability strongly depends on the level of magnetic field. Also for DC magnetic field different magnetic materials should be used than for the AC magnetic fields (Figure 3.171). Therefore, sometimes the magnetic shield is composed of several shields prepared from various materials.

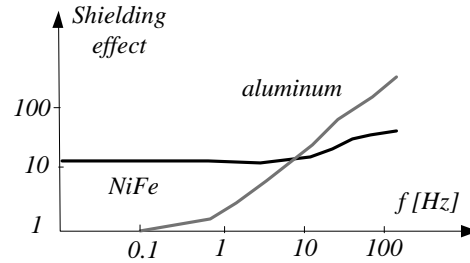


FIGURE 3.171
Comparison of effectiveness of shielding of ferromagnetic and non-magnetic materials versus frequency (Yamazaki 2006).

The effectiveness of shielding is described by the shielding factor S as the relationship between external H_e and internal H_i magnetic field

$$S = \frac{H_e}{H_i} \quad (3.187)$$

For simple shapes of the shield (sphere, cylinder or cube) there were calculated approximate formulas enabling determination of the shielding factor for DC magnetic field. For a long cylinder with diameter D the shielding factor is:

$$S = 1 + \frac{\mu t}{D} \quad (3.188)$$

The most important factor is the relative permeability μ of the material. That is why for shields are usually used materials of high permeability as NiFe (*mumetal*) with relative permeability of about 500 000 or amorphous materials reaching permeability as high as 800 000. The second factor influencing the shielding effect is the wall thickness. However it was proved that instead of increasing of the wall thickness more effective is to use multiple shells. For example a cylinder consisting of two layers with diameter D_1 and D_2 shielding factors S_1 and S_2 the resultant shielding factor is

$$S = 1 + S_1 + S_2 + S_1 S_2 \left[1 - \left(\frac{D_2}{D_1} \right)^2 \right] \quad (3.189)$$

A mumetal alloy commonly used as the shield material is very sensitive to stress and mechanical shocks, so it should be carefully annealed. Both mumetal and amorphous materials are rather expensive and in many cases the shield made from much cheaper SiFe electrical steel can be an alternative [Okazaki *et al*

2009]. At higher frequencies it can also be effective to use a shield made from aluminum in which eddy-currents aid the shielding. Also for high frequencies (for example in microwave range) the *Faraday cage* (a mesh prepared from conducting material) is commonly used as a shield. Ideally the shield should be designed in such a way as to make possible its periodic demagnetization, because magnetized shield exhibit lower performance.

We can destroy the signal by not correct connection to the measuring instrument. Figure 3.172 presents the results of experimental investigation of the various connecting cables presented in well-known book of Ott (Ott 1988). The connecting cables were influenced by artificially generated external 50 kHz magnetic field. At the end of the cable the attenuation of parasitic 50 kHz signal was measured.

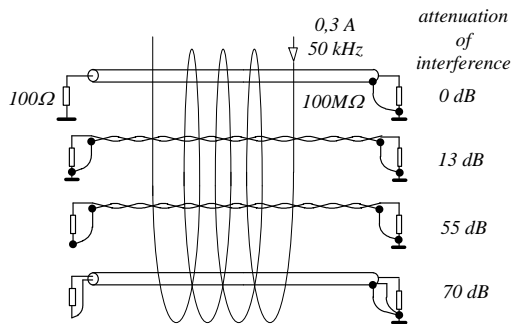


FIGURE 3.172
The attenuation of the magnetic interference signal depending on the method of the connection of the cables (Ott 1976).

The simple single wire in the coaxial shield grounded at the end practically did not attenuate the interference. Similarly the twisted wire grounded at both ends exhibited poor attenuation of interferences. The same twisted pair cable but grounded at the receiver end attenuated the interferences much better. Satisfying attenuation of interferences exhibited double wire cable with a coaxial shield grounded at the receiver end.

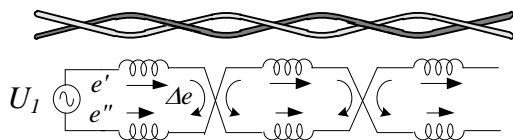


FIGURE 3.173
The twisted pair of wires and the principle of reduction of interferences in such connection.

Many of the interferences penetrate the measuring circuits through the connecting cables. Generally, the measuring signals should be connected using shielded wires. As it is demonstrated in Figure 3.172 the simple twisted wire in certain cases can be more effective than coaxial cable. In the twisted pair the interferences are reduced because the voltages e' and e'' induced in adjacent wires compensate each other and potential remaining of induced voltages Δe exhibits opposite direction in the neighbouring loops of the twisted wires.

For transmission of the digital data more and more important are fiber-optic cables. The optical system is immune to the electromagnetic interferences. The transmission of the data is extremely fast, theoretically the speed of frequency THz is possible and in practice the transmission of hundreds MHz is achieved.

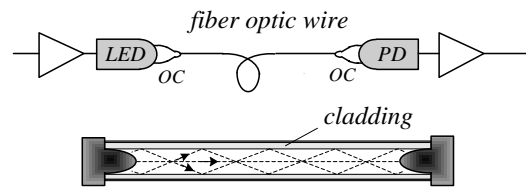


FIGURE 3.174
The fiber-optic cable as the communication wire for transmission of the measuring data.

The principle of data transmission using the fiber-optic connection is presented in Figure 3.174. The electrical signal is converted to the light by means of the LED or laser diode, then the optical system *OC* – *optical coupler* is formed. Typical length of the light wave is about 1300 nm. The optical signal should be converted again to the electrical form by means of a photo-detector device PD, before it is fed to the receiver. The effect of internal reflection of the light (the multimode transmission) is utilized for transmission of the signal through the fiber-optic wire. The core of the fiber-optic cable is surrounded by a special glass material called *cladding*. This part of fiber-optic cable exhibits the reflection coefficient ensuring that the light does not leave the wire.

In Internet communication commonly are used optical cables known as 100BASE-FX with speed up to 100 Mb/s and distance to 2 km, and 1000BASE-SX with speed up to 1 Gb/s and distance 200 – 500 m.

There is no one simple receipt for the grounding, shielding and cabling. Practically, it is always recommended to perform a series of experiments to find the best solution – sometimes a simple and cheap twisted pair of wires can exhibit better performances than expensive shielded wire.

Generally we should avoid the connection of the signal source and the receiver in such a way that the shield of the cable is a current-carrying part of the circuit (Figure 3.175) (Do not allow shield current to exist and do not allow the shield to be at a voltage with respect to the reference potential) (Rich 2005).

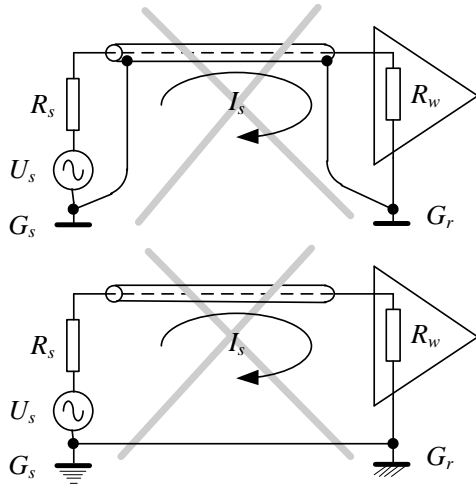


FIGURE 3.175 Not recommendable connection of the signal source and the receiver.

Similarly, it is not recommended to connect the signal source to the amplifier of different grounding potentials (Figure 3.175). In such case this potential difference U_g implies that in the R_2 resistance exists the equalizing current I_s . This current generates the conductive interference as the voltage U_z at the terminals of the amplifier.

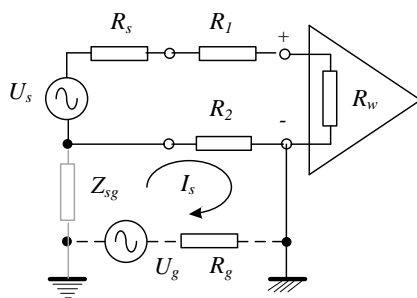


FIGURE 3.176 The connection of the signal to the amplifier with floating ground of the source.

Figure 3.176 presents the connection of the signal source with isolated ground (floating ground). The source is connected to the ground by large ($10^8 - 10^{10}$

Ω) impedance of leakage Z_{sg} . In the input of amplifier the interference signal is:

$$U_z = U_g \frac{R_2}{R_g + R_2 + R_{sg}} \approx U_g \frac{R_2}{R_{sg}} \quad (3.190)$$

The interference signal is significantly attenuated because the impedance Z_{sg} is large. If it is not possible to separate the signal source from the ground we can use the amplifier with floating point. Modern digital voltmeters generally have the floating ground terminal – practically the ground terminal is not introduced at the front panel of the instrument.

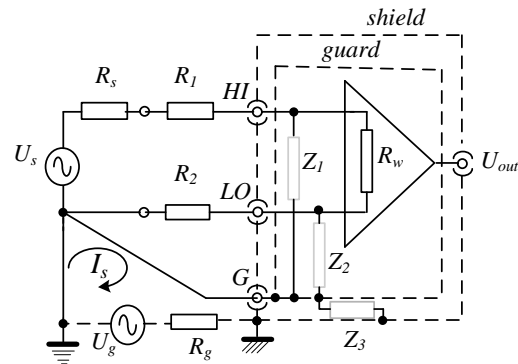


FIGURE 3.177 The connection of the grounded signal source to the amplifier with additional shield “guard”.

In modern amplifiers or voltmeters a special kind of shielding is used – a double shield. The first shield “ground shield” is connected to the ground, but the second shield “guard shield” is with floating ground – it is connected to the ground and to the “minus” terminal by large leakage impedances Z_2 and Z_3 (Figure 3.177). The equalizing current I_s is now in a closed loop outside the input signal connection.

Usually in the measuring instruments the grounds of the digital part, supply voltage and analogue part are separated. The first one (digital part and supply voltage) is called *power GND* (power ground) while the second is called *LL GND* (low level ground). The input terminals are usually with floating ground and are called *HI* (high) and *LO* (low). In high accuracy instruments the terminal *GUARD* is additionally introduced.

When small resistance R_x is connected to the measuring device as the rule the *four-wire connection* is used – with separate current and voltage terminals (Figure 3.178). The current terminals are usually larger and more massive and the connections wires R_{p2} are outside the measuring circuit. Because the voltage drop

is practically measured without current (large input resistance of the amplifier) the resistances of connection R_{p1} can be neglected. In digital multimeters the voltage terminals are indicated as “Sense HI” and “Sense LO” while the current terminals are indicated as “Input HI” and “Input LO”.

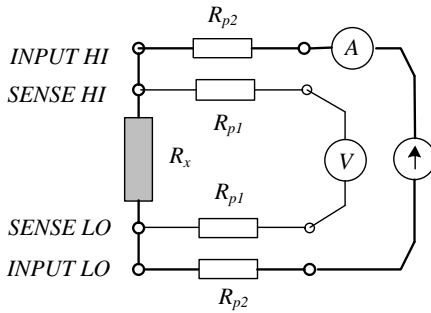


FIGURE 3.178
The connection of the measured low resistance to the four-terminal multimeter.

Figure 3.179 presents the application of the toroid choke for attenuation of the interferences. This method is used in computer connections and it is realized in such a way, that the signal cable is wound on the toroidal ferrite yoke.

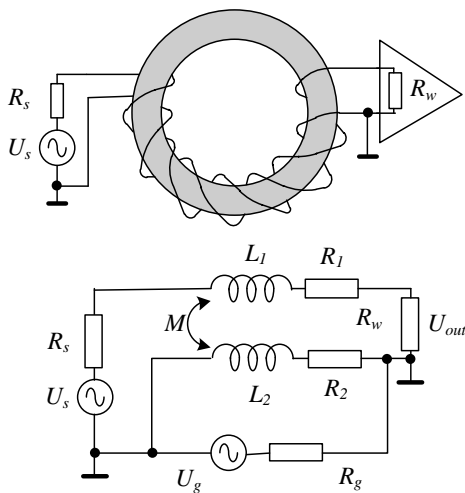


FIGURE 3.179
A toroidal longitudinal choke used for attenuation of the interferences (Northrop 1997).

The interferences are represented by the source U_g . The ratio of the signals to the interference is

$$\frac{U_{out}}{U_g} = \frac{R_2}{R_2 + R_g} \frac{1}{1 + \frac{\omega L_2}{R_g + R_2}} \quad (3.191)$$

The interference is attenuated and additionally a low-pass filter $L_2/(R_g + R_2)$ is formed. For higher frequencies (above 1 MHz) instead of toroid yoke sometimes the ferrite ring (ferrite bead) thread on the cable is used.

More difficult to attenuate are the low frequency interferences (industrial frequency interferences). Usually, various kinds of filters are used in order to suppress interferences. Practically all devices of power electronics are equipped with special filters to fulfill requirements of EMI standards – known as EMI filters. An example of EMI filter is presented in Figure 3.180.

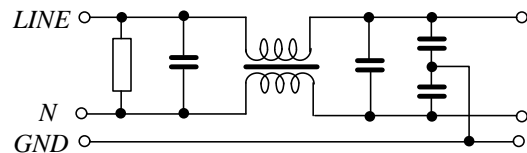


FIGURE 3.180
An example of EMI filter for rejection of high frequency interferences.

It can be important to match the noise to the amplifier. The noises of the amplifier are represented by the voltage e_n and current i_n noises. The noise factor F is the ratio of the amplifier noises to the thermal noises

$$F = \frac{e_n^2 + i_n^2 R_s^2}{e_T^2} = \frac{e_n^2 - i_n^2 R_s^2}{4kTR_s} \quad (3.192)$$

The optimal value of R_s which makes F minimal can be calculated as

$$\frac{\partial F}{\partial R_s} = 0 \quad (3.193)$$

From (3.192) and (3.193) the optimal source resistance is

$$R_{sopt} = \frac{e_n}{i_n} \quad (3.194)$$

Usually the R_{sopt} is relatively large, even up to several $M\Omega$, while the typical voltage sources exhibit rather small resistance. Therefore, matching the

resistance by using a transformer can result in reduction of the noises.

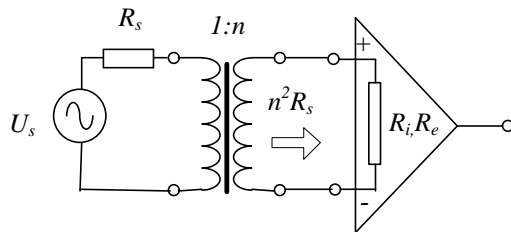


FIGURE 3.181

The noise matching by transformer coupling.

If the ratio of turns of the transformer is n the primary resistance R_s is reflected at the secondary winding as:

$$R'_s = n^2 R_s \quad (3.195)$$

Thus the optimal transformer turns ratio is:

$$n_{opt} = \sqrt{\frac{R_{sopt}}{R_s}} = \sqrt{\frac{1}{R_s} \frac{e_n}{i_n}} \quad (3.196)$$

The transformer inserted between the source and the amplifier matches the resistances, but also plays the role of isolation device (and sometimes as the symmetrization device – converting the single-ended source to the differential input).

References

- AD8551 – The data sheet of the AN 8551 amplifier of Analog Devices
- Bauch A., 2003, Caesium atomic clocks: functions, performances and applications, *Meas. Sc. Technol.*, 14, 1159-1173
- Bez S.P., Hamilton C.A., 2004, Application of the Josephson effect to voltage metrology, *Proc IEEE*, 92, 1617-1629
- Chevtchenko O.A., et al, 2005, Realization of a quantum standard for AC voltage: overview of a European Research Project, *IEEE Trans. Instr. Meas.*, 54, No.2, 628-631
- Coughlin R.F., Driscoll F.F. 2000 *Operational Amplifiers and Linear Integrated Circuits*, Prentice Hall
- Duff M., Towey J., 2010, Two ways to measure temperature using thermocouples feature simplicity, accuracy and flexibility, *Analog Dialogue*, 44-10, 1-6
- Gilber B., 1975, Translinear circuits: a proposed classification, *Electron. Lett.*, 11, 14-16
- Fraden J., 2003, *Handbook of modern sensors*, Springer
- Franco S. 2001 *Design with Operational Amplifiers and Analog Integrated Circuits*, McGraw-Hill
- Hagel R., Zakrzewski J., 1984, *Dynamic measurements* (in Polish), WNT
- Hamilton C.A., Burroughs J., Benz S.P., 1997, Josephson voltage standard – a review, *IEEE Trans. Appl. Superconductivity*, 7, 3756-3761
- Huelsman L.P. 1993 *Active and Passive Filter Design*, McGraw-Hill
- Jamal R., Steer R. 2003 *Filters*, Chapter 22 in *Electrical Measurements, Signal Processing and Displays*, CRC Press
- Jeckelmann B., Jeanneret B., 2001, The quantum Hall effect as an electrical resistance standard, *Rep. Prog. Phys.*, 64, 1603-1655
- Jung W.G. 2004 *Op Amp Application handbook*, Newnes
- Kester W., 2005, *The data conversion handbook*, Newnes
- King G., Fukushima T., 2004, RTD interfacing and linearization using an ADuC8xx microconverter, *Analog Devices AN-709*
- Kitchin C., Counts L., 1986, *RMS to DC conversion application guide*, Analog Devices
- Kitchin C., Counts J., 2006, *A designers guide to instrumentation amplifiers*, Analog Devices
- Kohlmann J., Behr R., Funck T., 2003, Josephson voltage standards, *Meas. Sc. Technol.*, 14, 1216-1228
- Levensen M.T., Chiao R.Y., Feldman M.J., Tucker B.A., 1977, An inverse AC Josephson effect voltage standard, *Appl. Phys., Lett.*, 31, 776
- Lutovac M.D., Tosic D.V., Evan B.L. 2000 *Filter Design for Signal Processing using MATLAB and Mathematica*, Prentice Hall
- Malik R., 2010, Thermocouple linearization when using the AD8497, AN-1087 Application Note of Analog Devices
- Maloberti F., 2007, *Data converters*, Springer
- Manabendra Bhuyan, 2011, *Intelligent instrumentation*, CTC Press
- Mancini R., 2002, *OpAmps for Everyone*, Texas Inst. Appl. Note
- Maxim 2003, *Analog Filter Design Demystified*, Maxim (Dallas Semiconductors) Technical Note No. 1795
- Moghimi R., 2011, To chop or auto-zero: that is the question, *Analog Devices Technical Note*, MS-2062
- MT-066, 2009, *In-Amp bridge circuit error budget analysis*, Analog Devices Tutorial
- Nash E., Greichen J., 1999, Revolutionary RF IC performs rms to DC conversion, *Microwaves & RF*, 38, 140-149
- NIST 1458 2003 NIST Measurement Service for DC Standard Resistors, NIST Technical Note 1458
- Northrop R.B. 1997 *Introduction to Instrumentation and Measurements*, CRC Press
- Novoselov K.S. et al, 2007, Room temperature quantum Hall effect in graphene, *Science*, 315, No. 5817, 1739
- Nuce D.S., 2004, *Linear position sensors*, Wiley Interscience
- Okazakio Y., Yanase S., Nakamura Y., Maeno R., 2009, Magnetic shielding by grain-oriented electrical steel sheet under alternating fields up to 100 kHz, *Przeegl. Elektr.*, 85, No.1, 55-59
- Ott H.W. 1988 *Noise Reduction in Electronic System*, John Wiley & Sons
- Padmanabhan T.R., 2000, *Industrial instrumentation*, Springer

- Pallas-Areny, Webster, 1999, Analog signals processing, John Wiley & Sons
- Pallas Areny R., Webster J.G, 2001, Sensors and signal conditioning, John Wiley & Sons
- Park P.G., Kim Y.G., Shifrin V.Y., 2005, Maintenance of magnetic flux density standards on the basis of proton gyromagnetic ratio at KRISS, IEEE Trans. Instr. Meas., 54, No.2, 734-737
- Rich A. 2005 Shielding and Guarding, Analog Devices Application Note AN-347
- Schaumann R. 2001 Design of Analog Filters, Oxford University Press
- Scholes R., 1970, Application of operational amplifiers to magnetic measurements, IEEE Trans. Magn., 6, 289-291
- Schott C., Blanchard H., Popovic R., Racz R., Hrejsa J., 1997, High accuracy analog Hall probe, IEEE Trans. Instr. Meas., 46, 613-616
- Scofield J.H. 1994 A frequency domain description of a lock-in amplifier, American Journal of Physics, 62, pp. 122-133
- Seebeck T., 1822, Magnetische polarization der Metalle und Erze durch Temperature Differenz, Abh. Der Preussischen Academic der Wissenschaft
- Stanley W.D. 2001 Operational Amplifiers and Linear Integrated Circuits, Prentice Hall
- Stata R., 1967, Operational integrators, Analog Dialogue, 1, 11-16
- Thede L. 2004 Practical Analog and Digital Filter Design, Artech House
- Van Putten A.F.P., 1996, Electronic measurement systems, IOP Publishing
- Volkenburg M.E. 1995 Analog Filter Design, Oxford University Press
- Wassenar R., Seevinck E., van Leeuwen M.G., Speelman C.J., Holle E., 1988, New technologies for high frequency rms to DC conversion based on a multifunctional V to I converter, IEEE J. Solid State Circuits, 23, No.3, 802-814
- Weyand K., 2001, Magnetic field standards – trace to the maintained units, Int. J. Apl. Electromagnetism and Mechanics, 13, 195-202
- Williams J., 1988, Thermocouple measurement, AN28 Application Note of Linear Technology
- Winder S. 2002 Analog and Digital Filter Design, Newnes
- Witt T.J., 1998, Electrical resistance standards and the quantum Hall effect, Rev. Sc. Instr., 69, No.8, 2823-2843
- Wong V., 2011, Lowest noise zero drift amplifier has 5.6 nV/rtHz voltage noise density, Analog Device Application Note AN-1114
- Yamazaki K., Muramatsu K., Hirayama M., Haga A., Torita F., 2006, Optimal structure of magnetic and conductive layers of a magnetically shielded room, IEEE Trans. Magn., 42, 3524-3526
- Zhang Y., Tan Y.W., Stormer H.L., 2005, Experimental observation of the quantum Hall effect and Berry's phase in grapheme, Nature, 438, 201-204
- Zumbahlen H. (Ed), 2008, Linear circuit design handbook, Elsevier